Universidade do Minho
Escola de Medicina

João Filipe Oliveira Viana

The Role of Astrocytic Metabotropic Glutamate Receptor 5 in Cognitive Function

outubro de 2019

João Filipe Oliveira Viana **The Role of Astrocytic Metabotropic Glutamate Receptor 5 in Cognitive Function**

UMinho | 2019

Universidade do Minho
Escola de Medicina

João Filipe Oliveira Viana

The Role of Astrocytic Metabotropic Glutamate Receptor 5 in Cognitive Function

Dissertação de Mestrado
Mestrado em Ciências da Saúde

Trabalho efetuado sob a orientação do
Doutor João Filipe Oliveira

outubro de 2019

Agradecimentos

Após a chegada ao final desta etapa não podia deixar de agradecer a todas as pessoas que me ajudaram. Um simples obrigado não é suficiente, mas aqui vai!

Primeiramente, ao Doutor João Oliveira por me ter dado a oportunidade de desenvolver este trabalho e por me ter apresentado os magníficos astrócitos. Obrigado por todo o apoio, conselhos e pelo conhecimento partilhado. Sem dúvida que aprendi muito ao longo deste ano.

Ás minhas "mães científicas", Sónia Gomes e Diana Nascimento, por todo o apoio dado para a realização deste trabalho, pelos sermões e por todos os momentos passados. Sem vocês esta tese não seria possível! Aprendi muito e estarei eternamente grato ás minhas queridas e espetaculares "mães".

Aos meus amigos, Helena, Joana S., Diana, Inês L., Inês C., Rita, Ângela, Gisela, Carolina, Bruna, Joana M. e Pedro, por terem tido paciência para me aturar e por toda a ajuda que deram. Vocês são incríveis! Obrigado também a todos os meus colegas de mestrado, a todos os NeRD, em especial ao Jorge, à Sara e ao Eduardo, e à comunidade da Escola de Medina que de alguma forma contribuíram para eu terminar esta etapa. Se me esqueci de alguém, obrigado a ti também.

Por último, um grande obrigado aos meus pais, ao meu irmão, à Marília e à minha família por todas as palavras de apoio nas horas boas e de desespero e pela confiança que tiveram em mim durante a realização desta dissertação. Sem vocês não sei se estaria aqui. OBRIGADO!

The work presented in this thesis was performed in the Life and Health Sciences Research Institute (ICVS), at the School of Medicine, University of Minho. Financial support was provided by a FCT Investigator grants (IF/00328/2015 to JO) and PTDC/MED-NEU/31417/2017 from the FCT – Foundation for Science and Technology, by BIAL Foundation grants (207/14 to JO), by Northern Portugal Regional Operational Programme (NORTE 2020), under the Portugal 2020 Partnership Agreement, through the European Regional Development Fund (FEDER) (NORTE-01-0145-FEDER- 000013); FEDER Funds, through the Competitiveness Factors Operational Programme (COMPETE), and The National Fund, through the FCT (POCI-01-0145-FEDER-007038).

STATEMENT OF INTEGRITY

I hereby declare having conducted this academic work with integrity. I confirm that I have not used plagiarism or any form of undue use of information or falsification of results along the process leading to its elaboration.

I further declare that I have fully acknowledged the Code of Ethical Conduct of the University of Minho.

O Envolvimento dos Recetores Metabotrópicos 5 de Glutamato de Astrócitos na Função Cognitiva

Resumo

Ao longo dos anos, vários estudos têm vindo a demonstrar que os astrócitos desempenham funções fundamentais no cérebro, nomeadamente na modulação de sinapses, redes neuronais e comportamento. De facto, os astrócitos têm vindo a ganhar reconhecimento como o terceiro elemento ativo nas sinapses, formando sinapses tripartidas. Neste conceito, estas células interagem diretamente com os neurónios modulando a sua atividade através da deteção e integração de transmissão sináptica. Os astrócitos são ativados por glutamato, o neurotransmissor excitatório mais abundante no cérebro e o primeiro a ser relacionado com ativação de astrócitos, através do recetor metabotrópico 5 de glutamato (mGluR5). Uma vez ativado, este recetor induz elevações intracelulares de Ca^{2+} em astrócitos com consequências para a atividade sináptica nas regiões cortico-límbicas, importantes para a função cognitiva. No entanto, a maioria dos estudos utilizou roedores jovens geralmente usando abordagens *in vitro* e *ex vivo*, sendo necessária a confirmação destas observações em murganhos adultos.

Nesta dissertação, nós geramos dois modelos de murganho adulto com a deleção mGluR5 em astrócitos, usando uma linha de murganhos que possui o gene mGluR5 flanqueado por sequências loxP. Primeiro, usando um sistema Cre-lox dependente de tamoxifeno para deleção condicional em astrócitos em todo o cérebro (GLAST-mGluR5KO). Em segundo lugar, através da injeção do vírus rAAV5:GFAP-mCherry-Cre para deletar o gene apenas em astrócitos do hipocampo (dHIP-GFAP-mGluR5KO). Uma caracterização detalhada do seu comportamento mostrou que nenhum dos modelos apresenta fenótipos do tipo ansioso ou depressivo, ou mesmo atividade motora anormal. Além disso, a avaliação da função cognitiva mostrou que os murganhos GLAST-mGluR5KO apresentam memória de referência espacial normal, mas maior flexibilidade comportamental no Morris Water Maze (MWM) e défices na memória associada a medo no Contextual Fear Conditioning (CFC). No entanto, os dHIP-GFAP-mGluR5KO possuem memória associada ao medo e memória de referências espaciais normal, mas menor flexibilidade comportamental. Uma posterior análise molecular dos cérebros dos GLAST-mGluR5KO revelou níveis de expressão do gene GFAP diminuídos. Em suma, ao usar duas abordagens para modular a expressão do mGluR5 em astrócitos na idade adulta, observamos fenótipos cognitivos dependentes de áreas especificas do cérebro. Estas descobertas contribuíram para identificar o envolvimento do mGluR5 na cognição, abrindo também portas para novos estudos nesta área.

Palavras-Chave: astrócito, cognição, córtex pré-frontal, hipocampo, mGluR5

The Role of Astrocytic Metabotropic Glutamate Receptor 5 in Cognitive Function

Abstract

Over the years, increasing evidence has been demonstrating the key role of astrocytes in the brain, namely in modulations of synapses, neuronal networks and behavior, proving that these are more than mere supportive cells. Indeed, astrocytes gained recognition as the third active element of a synapse. In this tripartite synapse concept, while interacting closely with neurons, these cells can modulate neuronal activity by sensing, processing, integrating and responding to synaptic transmission. Astrocytes were firstly shown to sense glutamate, the most abundant excitatory neurotransmitter in the brain, which occurs mostly by activation of metabotropic glutamate receptor 5 (mGluR5). Activation of mGluR5 triggers Ca^{2+} elevations in astrocytes with consequences for synaptic function in cortico-limbic areas that are critical for cognitive processing. However, the majority of these studies were focused on the biological role of mGluR5 in young rodents, often using *in vitro* or *ex vivo* approaches. Thus, further studies are needed to better understand the impact of astrocytic mGluR5 in cognitive processing of adult mice.

In this dissertation, we have generated two mouse models with temporally controlled deletion of mGluR5 in astrocytes, taking advantage of a mouse line carrying the mGluR5 flanked by loxP sites. Firstly, by inducing genetic recombination through a tamoxifen-inducible Cre–loxP system in astrocytes from the whole brain (GLAST-mGluR5KO mouse) and secondly by inducing ablation of the gene specifically in astrocytes from the hippocampus, following an injection of a rAAV5-GFAP-mCherry-Cre virus (dHIP-GFAP-mGluR5KO mouse). A detailed behavior characterization of these mouse models showed that GLAST-mGluR5KO and dHIP-GFAP-mGluR5KO mice do not present any anxious- or depressive -like phenotype or abnormal locomotor activity. Furthermore, cognitive assessment of these mice showed that GLAST-mGluR5KO mice display normal spatial reference memory but enhanced behavior flexibility in Morris Water Maze (MWM). However, in the Contextual Fear Conditioning (CFC) these mice presented impaired fear memory. The behavioral assessment of dHIP-GFAP-mGluR5KO mice also revealed normal spatial reference memory, but impaired behavior flexibility, as shown in the reversal learning task of the MWM. In addition to behavior characterization, molecular analysis of GLAST-mGluR5KO mice showed a decreased expression levels of GFAP gene upon mGluR5 deletion. Overall, by using these different approaches to modulate astrocytic mGluR5 in adulthood we observed region-specific cognitive phenotypes. These evidences confirm the involvement of astrocytic mGluR5 in cognition and opens future perspectives in the field that urge to be addressed.

Keywords: astrocyte, cognition, hippocampus, mGluR5, prefrontal cortex

Table of Contents

Abbreviations list

2TPR	-	Two -trial place recognition
AD	-	Alzheimer's disease
ALDH1L1	-	Aldehyde dehydrogenase 1 familiar member L1
AMPA	-	α-amino-3-hydroxy-5-methyl-4-isoxazolepropionic acid
BBB	-	Blood-brain barrier
CA1	-	Cornu ammonis 1
Ca^{2+}	-	Calcium ion
CA3	-	Cornu ammonis 3
cAMP	-	Cyclic adenosine monophosphate
CFC	-	Contextual fear conditioning
Cl^-	-	Chloride ion
CNS	-	Central nervous system
Cxs	-	Connexins
D.I.	-	Discrimination Index
DAG	-	Diacylglycerol
DAPI	-	4′,6-diamidino-2-phenylindole
DG	-	Dentate Gyrus
dnSNARE	-	Dominant negative domain of vesicular SNARE protein synaptobrevin II
EC	-	Entorhinal cortex
ECM	-	Extracellular matrix
EPM	-	Elevated plus maze
ER	-	Endoplasmic reticulum
FBS	-	Fetal bovine serum
GABA	-	Gamma-aminobutyric acid
GDP	-	Guanosine 5-diphosphate
GFAP	-	Glial fibrillary acidic protein
GFP	-	Green Fluorescent Protein
GLAST	-	Glutamate aspartate transporter
GLT-1	-	Glutamate transporter 1
GS	-	Glutamine Synthase

GTP	-	Guanosine 5-triphosphate
i.p.	-	Intraperitoneal
iGluRs	-	Ionotropic glutamate receptors
IHC	-	Immunohistochemistry
IP_3	-	Inositol-1,4,5-trisphosphate
IP_3R2	-	Inositol-1,4,5-trisphosphate receptor type 2
K^+	-	Potassium ion
Kir	-	Inward-rectifier potassium channel
KO	-	Knockout
LTD	-	Long-term depression
LTP	-	Long-term potentiation
mGluRs	-	Metabotropic glutamate receptors
mPFC	-	Medial prefrontal cortex
MWM	-	Morris water maze
Na^+	-	Sodium ion
NaOH	-	Sodium hydroxide
NMDA	-	N-methyl-D-aspartate
OF	-	Open field
P	-	Post-natal days
PBS	-	Phosphate-buffered saline
PCR	-	Polymerase Chain Reaction
PFA	-	Paraformaldehyde
PFC	-	Prefrontal cortex
PIP_2	-	Phosphatidylinositol 4,5-biphosphate
PLC	-	Phospholipase C protein
qRT-PCR	-	Quantitative real-time polymerase chain reaction
rAAV5	-	Recombinant adeno-associated virus 5
RG	-	Radial glia
RT	-	Room temperature
SEM	-	Standard error of the mean
TST	-	Tail suspension test
WT	-	Wild-type

List of figures

List of tables

1. Introduction

Our knowledge of the brain has been drastically changing over the past decades. When investigating brain activity these days, being restricted to the study of neurons alone will give an incomplete understanding of the underlying mechanisms. Indeed, besides neurons, the human brain is also composed by a major class of cells called glia such as astrocytes, oligodendrocytes and microglia (Allen and Barres 2009; Verkhratsky and Parpura 2014).

Contrarily to glial cells, neurons are characterized by their distinct ability to transmit and process information through electrical signals known as action potentials. These potentials may trigger the release of neurotransmitters which are important mediators involved in cell-to-cell communication. Both an electrical or chemical signal can be transmitted to a second neuron through specialized junctions/structures called synapses (Allen and Barres 2009; Allen 2014). Additionally, interconnected neurons establish fine circuits, forming large scale networks that support higher brain functions such as learning and memory (Mayford et al. 2012). In 1858 Rudolf Virchow introduced the term 'neuroglia' to describe glial cells as a type of 'nerve-cement' occupying the space between neurons and maintaining the architecture of the nervous system. Glial cells were initially classified as supportive cells assumed to have only a passive role and consequently, for a long time, neurons were accepted as the main cells in the brain (Kettenmann and Verkhratsky 2008; McIver et al. 2013).

However, since then, an increasing number of studies have been showing that these cells are not just bystanders conferring mechanical and nutritional support, but they are also active partners of neurons (Cornell-Bell et al. 1990; Araque et al. 1999; Perea et al. 2009). Even though smaller in size, glial cells are the major cellular fraction of the Central Nervous System (CNS) known today to have a substantial impact in the neuronal circuits/activity, and therefore to have an equally relevant role in brain functions of higher complexity. Indeed, oligodendrocytes are responsible for the axonal myelinization in CNS, increasing velocity in signal conduction, while microglia have immune and phagocytic functions in the brain. On their turn, astrocytes, the main focus of this dissertation, display important homeostatic and modulatory functions (Jäkel and Dimou 2017). In fact, astrocytes have recently emerged as key players in synaptic modulation, due to their ability to sense, integrate, process and respond to neuronal activity. By maintaining close contact with neighbor neurons, covering and modulating their communication, astrocytes form unique functional units with the neuronal counterparts (further explored in 1.1.2) (Araque et al. 1999, 2014; Perea et al. 2009; Petrelli and Bezzi 2016). Also, an increasing body of evidence has

been helping characterize astrocytes as a heterogeneous cell population that adapts to the immediate environment by changing their physiological properties and thus responding differently according to the cellular context. These cells may also display different morphologies and/or molecular signatures (Kettenmann and Verkhratsky 2008; Verkhratsky and Nedergaard 2018). Such homeostatic and synaptic modulation, placed astrocytes in a more central position regarding relevant brain functions such as learning and memory (Gibbs et al. 2008; Fields et al. 2014; Santello et al. 2019) while their abnormal activity was associated to brain disorders, as Alzheimer's disease (AD), Parkinson's disease or amyotrophic lateral sclerosis (Li et al. 2019). Notably, despite all the recent advances in our knowledge concerning the role glial cells in the brain, their full potential remains largely unexplored both in the healthy and pathological conditions.

1.1. Astrocytes: the stars of the brain

Described by Michael von Lenhossék in 1893, astrocytes are the most numerous glial cells in the brain (Kettenmann and Verkhratsky 2008). The number and structure of astrocytes varies among species and increases with the complexity of the neuronal network (McIver et al. 2013; Allen 2014). When compared to rodent, human astrocytes are three-fold larger and 10-times more complex and structurally diverse (Oberheim et al. 2009). These glial cells are characterized by their complex star-shaped morphology that instead of axons and dendrites is composed by multiple primary processes and fine branches (Kettenmann and Verkhratsky 2008; Oberheim et al. 2009, 2012). Different from neurons, astrocytes do not exhibit electrical excitability since they are not able to generate action potentials. Indeed, even though they express several receptors and a whole range of cell surface molecules, they have low expression of voltage-gated ion channels which are crucial for the flux of ions through the membrane and generation of electrical excitability. In addition, astrocytes have high density of potassium (K^+) channels that prevents the depolarization of the astrocytic membrane, specifically the inward-rectifying K^+ channel 4.1 (Kir4.1). This channel is responsible for the control of the extracellular K^+ concentration (Wang and Bordey 2008; Mederos et al. 2018; Seifert et al. 2018). Therefore, astrocytes communicate through intracellular signaling pathways, where local gradients of ions, such as calcium (Ca^{2+}) and sodium (Na^+), interact with intracellular targets, triggering physiological responses (Parpura and Verkhratsky 2012). In fact, intracellular elevations of Ca^{2+}, released from internal stores, is the mostly studied form of excitability in astrocytes, occurring in response to synaptic activity. Astrocytes display dynamic Ca^{2+} elevations in several brain regions with particular spatial and temporal properties, which appears to be linked to their morphological and molecular heterogeneity (Volterra et al. 2014; Bazargani and Attwell 2016). Indeed,

astrocytes can have distinct morphologies and molecular profiles depending on their location, cellular context and embryonic origin (Zhang and Barres 2010; Oberheim et al. 2012; Ben Haim and Rowitch 2017). The particular properties of these cells and their implication for the normal brain function will be reviewed in more detail in the following sections.

1.1.1. Morphology and molecular profiles: a heterogeneous population

Astrocytes have highly complex bushy morphologies being constituted by fine processes that occupy a substantial surface area. This peculiar structure allows them to cover an incredible number of synapses and still contact with blood vessels and other glial cells (Allen 2014). The heterogeneity of astrocytes can be associated with the site of their origin in the ventricular zone during embryogenesis (Figure 1). During the CNS development, neuroepithelial cells from the neuroepithelium give rise to two types of radial glia (RG). At the early stages of embryogenesis, radial glia has a neurogenic nature, forming several types of neurons in a sequential manner. However, at later stages these cells become gliogenic, generating immature subtypes of astrocytes. The progenitor domains of the neuroepithelial and RG cells are regionally specialized to the production of distinct cells types and are determined by different cell-extrinsic

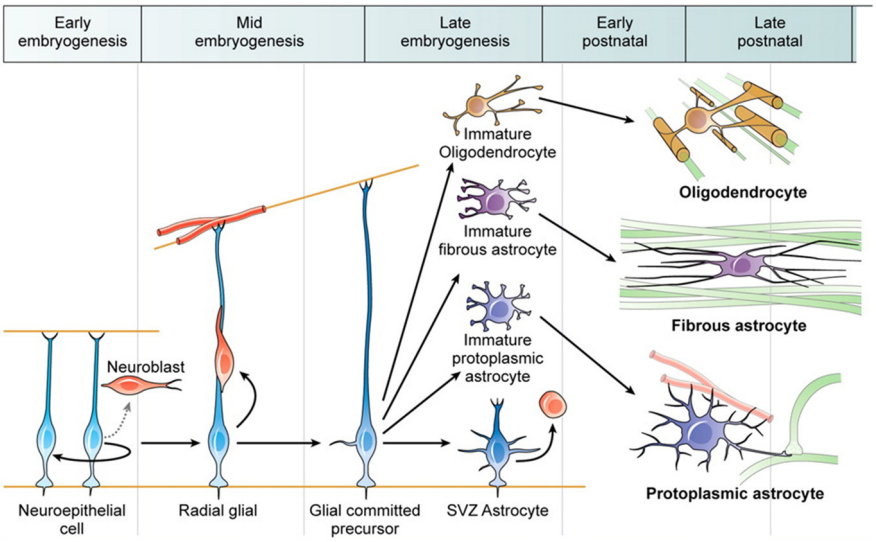

Figure 1 - The appearance of astrocytes during development

At the early stages of embryogenesis, neuroepithelial cells give rise to radial glia (RG) that in mid embryogenesis has a neurogenic nature and originate several types of neurons. At later stages of embryogenesis neurogenic RG becomes glial committed precursor cells generating immature subtypes of astrocytes and immature oligodendrocytes. Then, these glial committed cells retract their processes originating astrocytes in the subventricular zone. After birth, astrocytes undergo maturation originating fibrous and protoplasmic astrocytes (Molofsky et al. 2012).

signals that indicate positional information in the dorsal-ventral axes. Moreover, it has been shown that astrocytes heterogeneity might be due to the regional pattern of gliogenic RG. During postnatal development, the immature astrocytes undergo maturation giving rise to distinct classes of cells, such as protoplasmic and fibrous astrocytes (Molofsky et al. 2012; Bayraktar et al. 2015; Verkhratsky and Nedergaard 2018)..

Thus, due to their distinct embryonic origin and morphologies (Figure 1), astrocytes were classically divided into two main subpopulations, fibrous astrocytes from the white matter and protoplasmic astrocytes from the grey matter. Protoplasmic astrocytes have highly branched bushy processes, whereas the fibrous astrocytes mainly present straight and long processes (Kettenmann and Verkhratsky 2008). However, since then, other specialized cells with astrocytic properties have been identified, such as Müller cells from the retina, Bergmann glia and velate astrocytes from the Cerebellum, tanycytes from perivascular organs, pituicytes from the posterior pituitary, perivascular and marginal astrocytes close to the pia mater and ependymocytes from the ventricles and subretinal space (Emsley and Macklis 2006; Matyash and Kettenmann 2010; Oberheim et al. 2012; Ben Haim and Rowitch 2017; Mederos et al. 2018). Indeed, recent findings have been increasing our knowledge on their morphology, regional and spatial distribution, challenging the idea that these cells are a homogenous population. Consistent body of evidence has been demonstrating that astrocytes in the brain are not only regional but also layer specific, therefore further expanding this concept of populational heterogeneity (Ben Haim and Rowitch 2017; Lanjakornsiripan et al. 2018).

Interestingly, regardless of their higher or lower morphological complexity and spatial distribution, their numerous bushy processes form specific and individual territories that barely overlap with neighbor astrocytes. Thus, one synapse can be modulated only by one astrocyte while a single astrocyte is able to establish contact with thousands of synapses at the same time (Bushong et al. 2004; Halassa et al. 2007; Allen 2014). Moreover, astrocytes also interact with blood vessels enwrapping endothelial cells and pericytes with specialized structures called endfeet (McIver et al. 2013). Indeed, this strategic positioning is another crucial feature not only for the modulation of the synaptic transmission, but also for the monitorization/control of the Blood-Brain Barrier (BBB) and uptake of nutrients from the bloodstream (critical for the brain homeostasis) (Allen 2014). Noteworthy, these cells also communicate intercellularly with neighboring astrocytes through gap junctions formed by connexins (Cxs), establishing astrocytic networks. For instance, gap junctions formed by Cx43 and Cx30 allow the intercellular diffusion of ions as Ca^{2+}, second messengers as cyclic adenosine monophosphate (cAMP) and inositol-1.4.5-

trisphosphate (IP_3), and small molecules up to 1.8 KDa as glutamate and glucose. Interestingly, connexins have been identified as strong candidates involved in the morphological heterogeneity found in astrocytes (Nagy et al. 1999; Giaume et al. 2010; Pannasch et al. 2011; Pannasch and Rouach 2013; Mederos et al. 2018). Despite these advances, the exact mechanisms responsible for this morphological diversity are still not fully understood. Studies suggest that neuronal cues are needed in astrocytic morphogenesis, however other proteins just like connexins may play key roles (Pannasch et al. 2014; Khakh and Sofroniew 2015). Recently, transcriptomic analysis has been used to identify the molecular profiles of distinct astrocytic populations, which could help elucidate region and layer-specificity (Khakh and Sofroniew 2015; Batiuk et al. 2018).

Indeed, also at the molecular level, astrocytes seem to be quite diverse. The glial fibrillary acidic protein (GFAP), an intermediate filament protein from the cytoskeleton, is one common molecular marker used not only to identify astrocytic cell populations but also for the study of their morphology (Khakh and Sofroniew 2015). Indeed, staining of GFAP by immunohistochemistry labels the main processes of astrocytes (around 15% of their total area though) allowing a practical screening of their main structure (Tavares et al. 2017). However, the use of markers like GFAP should be cautious as several studies have shown that astrocytes express different levels of GFAP throughout the brain. Almost all hippocampal astrocytes express detectable levels of GFAP, while thalamic astrocytes exhibit low levels. In addition, in the cerebral cortex, astrocytes in superficial and deep layers are GFAP-positive ($GFAP^+$) cells while few astrocytes from the middle layers express this marker (Khakh and Sofroniew 2015). Hence, non-detectable GFAP levels does not imply the absence of astrocytes since they can still be detected by other specific molecular markers. Moreover, ten different isoforms and splice variants of GFAP (α, β, γ, GFAPΔexon6, GFAPΔ164, GFAPΔexon7, GFAPΔ135, δ, κ, and ζ) are described which may also account for the distinct GFAP patterns of expression in astrocytes (Kamphuis et al. 2012; Hol and Pekny 2015).

Consistently, throughout the years several astrocytic markers were characterized. For example, glutamate transporters, such as glutamate transporter 1 (GLT-1) and glutamate aspartate transporter (GLAST), are expressed throughout the brain with different expression patterns. Astrocytes from the hippocampus, cerebral cortex and striatum have higher expression of GLT-1 while GLAST is also highly expressed in the cerebellum (Khakh and Sofroniew 2015). The Glutamine Synthase (GS), important for the conversion of glutamate in glutamine in astrocytes, has been used as well to identify these cells, since it appears to stain practically all astrocytes (Anlauf and Derouiche 2013; Verkhratsky and Nedergaard 2018). In fact, a study showed that from all cells that were GS-positive in the hippocampus only 60% were also $GFAP^+$

(Walz and Lang 1998). Both glutamate transporters and GS are key players in the glutamate turnover in CNS, which is another important function of astrocytes (further explained in section 1.1.2) (Verkhratsky and Nedergaard 2018).

Besides GS, GLT-1 and GLAST, also the glycoprotein S100β, aldehyde dehydrogenase 1 family member L1 (ALDH1L1), water channel aquaporin 4 and vimentin are commonly used to identify astrocytes (Khakh and Sofroniew 2015; Verkhratsky and Nedergaard 2018). The S100β is a Ca^{2+} binding protein that acts as Ca^{2+} buffer or sensor (Donato et al. 2013). This astrocytic marker has been used to identify mature astrocytes because of its high expression in the brain. In opposition to the GFAP, this protein is more present in astrocytes from the grey matter when compared to astrocytes from the white matter (Verkhratsky and Nedergaard 2018). However, in the rat brain, S100β is expressed in almost three times more astrocytes than GFAP (Savchenko et al. 2000). Accordingly, the ALDH1L1, a key enzyme in the folate metabolism, is also used to identify mature astrocytes (Cahoy et al. 2008). This enzyme was shown to mark mainly cortical astrocytes, with little expression in astrocytes from the white matter (Verkhratsky and Nedergaard 2018). In the CNS, the water channel aquaporin 4 was shown to be expressed by astrocytes and ependymocytes. This channel exhibits a high expression in the endfeet of astrocytes, being used to identify these structures (Nielsen et al. 1997; Nagelhus and Ottersen 2013; Verkhratsky and Nedergaard 2018).

In contrast to these markers for mature astrocytes, vimentin, an intermediate filament, is mainly expressed by immature astrocytes. After birth the expression levels of these filaments decreases, although it is still present in some astrocytic populations (Verkhratsky and Nedergaard 2018). Besides, upon an insult, expression of structural filaments as vimentin and GFAP may increase contributing to astrocytic hypertrophy (Pekny et al. 1999; Sofroniew 2015). Indeed, in a process called astrogliosis, adult and well-established astrocytes undergo morphological and cellular changes becoming reactive and acquiring a distinct phenotype (Sofroniew 2015). Therefore, besides the described changes that astrocytes from different brain regions may present, or modifications happening throughout development and aging, it is today known that astrocytic plasticity also occurs in specific conditions, as astrogliosis (Sofroniew 2015; Verkhratsky and Nedergaard 2018).

Due to this remarkable heterogeneity and plasticity, to date a universal marker allowing the identification of all astrocytes in the CNS does not exist. Nevertheless, studies indicate that most of these proteins coexist in a majority of astrocytes. It is also important to note that, although these markers are widely expressed in astrocytes, some can also be detected in other cell types in the nervous system (Khakh and

Sofroniew 2015; Verkhratsky and Nedergaard 2018). For example, in the CNS, GFAP and GLAST expression is also detected in progenitor cells derived from RG throughout life, which later on may give rise to either neurons or glial cells (Dimou and Götz 2014). In addition, ALDH1L1 and S100β may be also present in some subpopulations of oligodendrocytes (Steiner et al. 2007; Yang et al. 2011). Therefore, researchers have been selecting and using these markers carefully, taking into consideration the developmental stage, the brain region being studied, and also the methodological approaches. Indeed, many of these proteins are also used as promoters for gene manipulation in astrocyte-targeted strategies, and thus it is important to have all this in mind when designing experiments and generating mouse models to specifically tackle astrocytes.

Overall, these morphological and molecular heterogeneity of astrocytes as well as the highly dynamic networks they form, are closely related with the roles that they play in the nervous system. Regarding their functions, they generally can be divided into two major subtypes: homeostatic functions, that provide housekeeping needed to maintain normal neuronal activity and modulatory functions, related to the modulation of the synaptic activity (Wang and Bordey 2008). These functions will be detailed in the next sub-sections.

1.1.2. Homeostatic functions

Astrocytes in the CNS are critical for the maintenance of the normal functioning of brain networks. In this context, one important structure of the CNS and in general all connective tissues, is the extracellular matrix (ECM) where cells are embedded. In CNS though, this matrix is peculiar as it lacks the typical fibrous collagen backbone, being rich in proteoglycans and glycoproteins instead. Besides conferring structural support, the ECM is extremely important as it provides cues that signal and modulate cell fate, development, shape, polarity, and behavior (Barros et al. 2011). Interestingly, astrocytes express several types of ECM proteins and adhesion molecules, which are pivotal for the maintenance of the matrix. They are also involved in ECM degradation and remodeling by synthetizing and secreting matrix metalloproteinases. By expressing specific proteoglycans for instance, during development, astrocytes can even control neurite growth and guide axons. Indeed, being so actively involved in ECM homeostasis, astrocytes help promoting cellular stability in the brain, and are particularly relevant for many vital functions in neurons (Wang and Bordey 2008).

Astrocytes can also secrete multiple growth factors such as nerve growth factor, brain-derived neurotrophic factor, neurotrophin-3, fibroblast growth factor and ciliary neurotrophic factor which are

directly involved in neuronal survival, differentiation and maturation (Wang and Bordey 2008; Cabezas et al. 2016). Also important for neuronal survival is the tight control over extracellular ion concentrations, since minor changes may be critical. Indeed, during neuronal activity, K^+ accumulates in the extracellular space as a consequence of the release of K^+ by depolarized neurons. If basal levels of intracellular K^+ are not restored, it may result in the depolarization and hyperexcitability of neighboring neurons, which could ultimately lead to seizures. The basal levels of K^+ in the extracellular space are restored by astrocytes that take up the excess extracellular K^+ ions, transmitting the ions to neighboring astrocytes through gap junctions and releasing them at spaces with low concentration of extracellular K^+ (Wang and Bordey 2008; Allen 2014). Extracellular K^+ buffering is accomplished mainly by Kir channels expressed in the astrocytic membrane, more specifically Kir4.1 (Djukic et al. 2007). In addition, astrocytes have low expression of Na^+/K^+ ATPase, an active transporter of K^+ (Wang and Bordey 2008; Allen 2014).

Besides ions buffering, astrocytes also take up neurotransmitters from the synaptic cleft. At their processes close to the synaptic cleft, astrocytes express transporters for several neurotransmitters, as glutamate, gamma-aminobutyric acid (GABA) and glycine (Allen 2014). In astrocytes, glutamate is taken up by GLT-1 and GLAST transporters, GABA by GABA transporter 1 and 3 and glycine by glycine transporter 1 (Wang and Bordey 2008; Allen 2014; Ghirardini et al. 2018). After the uptake of neurotransmitters, these cells can metabolize neurotransmitters and then redistribute them to presynaptic neurons. Recycling of neurotransmitters by astrocytes reduce the synthesis of new transmitters from precursors of the periphery and avoid neuronal excitotoxicity. A good example is the case of glutamate and the glutamate-glutamine cycle. This neurotransmitter is taken up by astrocytes and is then converted to glutamine by GS. Astrocytes then release glutamine to the extracellular space, which is used afterwards by glutamatergic and GABAergic neurons for the *de novo* synthesis of glutamate (Wang and Bordey 2008; Allen 2014; Rose et al. 2018). Interestingly, besides these buffering and recycling properties at the synaptic cleft, astrocytes were shown to be involved in the development and remodeling of synapses (Allen and Eroglu 2017).

Being so strategically placed, astrocytes can not only easily reach and interact with nearby synapses, but also be in close contact with blood vessels. Even though astrocytes do not structurally contribute to the BBB, this close interaction with endothelial cells is thought to help maintaining the BBB integrity. During development, astrocytes regulate the formation of the BBB being involved in distinct transport mechanisms and establishment of tight junctions between microvascular endothelial cells. Furthermore, astrocytes are also involved in angiogenesis, controlling blood vessels formation (Wang and Bordey 2008;

Alvarez et al. 2013). Additionally, by expressing specific transporters at their endfeet, specialized structures that enwrap vasculature, they are also able to uptake nutrients from the bloodstream and, thus give metabolic support to neighboring neurons. Glucose transporters, specifically type 1, allow astrocytes to uptake glucose from the bloodstream (Wang and Bordey 2008). These glucose molecules can be immediately used by astrocytes to produce energy through glycolysis. During synaptic activity, the uptake of glutamate by astrocytes and conversion into glutamine (already mentioned above) requires energy that is provided by glycolysis. Besides, astrocytes use the pyruvate resulting from glycolysis to produce lactate. To maintain synaptic transmission, lactate is then shuttled to neurons to produce ATP by oxidative phosphorylation (Allen 2014; Calì et al. 2019). In fact, several studies have shown that under intense neuronal activity, the energy provided by glycolysis is not sufficient to maintain synaptic transmission. In these cases, lactate is more effective as an energy substrate in maintaining synaptic transmission rather than glucose. In the hippocampus, astrocytic lactate is essential in processes as memory formation (Suzuki et al. 2011; Boury-Jamot et al. 2016; Gao et al. 2016). Moreover, astrocytes can also produce lactate by glycogenolysis using their internal storages of glycogen. In the CNS, astrocytes are the main stores of glycogen since they express and activate enzymes involved in glycogen synthesis and metabolization (Calì et al. 2019). Ultimately, these glial cells can also synthetize lipids, as cholesterol, to enhance neuronal synaptic function (as also mentioned above) (Allen 2014). Altogether, these findings stress the importance of astrocytes in many vital brain functions, with particular relevance for the physiological activity of neurons.

1.1.3. Modulation of synaptic activity

The acceptance that astrocytes were only involved in the maintenance of normal neuronal function by promoting and eliminating synapses, and being involved in neurotransmitters uptake and recycling, was challenge by the discovery that these cells also respond to these neurotransmitters. Cornell-Bell and colleagues (1990) reported that cultured astrocytes responded to glutamate, the main excitatory neurotransmitter, through specific glutamate receptors. They showed that astrocytic activation by glutamate originate intracellular Ca^{2+} elevations, creating calcium waves that could propagate to neighboring astrocytes (Cornell-Bell et al. 1990). Increasing evidence showing that the astrocyte-neuron communication is a bidirectional process, instead of a unidirectional interaction, gave rise to a new concept known as the Tripartite Synapse hypothesis (Araque et al. 1999; Perea et al. 2009). In this concept, neurotransmitters released by presynaptic neurons can bind to astrocytic receptors (1) activating signaling cascades that lead to intracellular Ca^{2+} elevations (2) which consequently triggers the release of

neuroactive substances into the synaptic cleft that signal back to presynaptic and postsynaptic neurons (3) (Figure 2) (Araque et al. 1999; Perea et al. 2009). In the context of this dissertation we will focus in how astrocytes sense neurotransmitters during synaptic transmission.

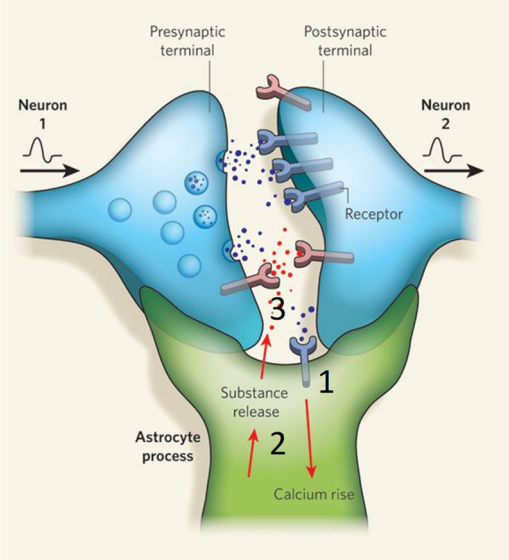

Figure 2 - The tripartite synapse

Astrocytes express several neurotransmitter receptors. When neurotransmitters are released to the synaptic cleft by neurons, they can bind to postsynaptic neuronal receptors or to astrocytic receptors. Activation of astrocytic receptors evokes intracellular Ca^{2+} elevations that induces the release of active substances, as glutamate, ATP and D-Serine, to the synaptic cleft (2). These active molecules will then act on presynaptic and/or postsynaptic neuronal receptors, modulating synaptic activity (3). Adapted from (Allen and Barres 2009).

Astrocytes are reactive to a wide range of neurotransmitters such as glutamate, GABA, norepinephrine, adenosine, acetylcholine and endocannabinoids which is only possible because they express receptors for these molecules (point 1 in Figure 2) (Pannasch and Rouach 2013; Verkhratsky and Parpura 2014; De Pittà et al. 2016). These receptors can be included generally in two main classes; metabotropic and ionotropic receptors (Figure 3) (Verkhratsky 2008). On the one hand, ionotropic receptors are associated with ion channels and their activation induces the flux of ions, such as Na^+, K^+, Ca^{2+} or chloride (Cl^-), resulting in membrane depolarization. Astrocytes were described to express ionotropic receptors such as α-amino-3-hydroxy-5-methyl-4-isoxazolepropionic acid (AMPA) and N-methyl-D-aspartate (NMDA) for glutamate, GABA type A receptors, P2X purinoreceptors for ATP, glycine receptors and nicotinic acetylcholine receptors (Verkhratsky 2008). On the other hand, the majority of astrocytic receptors are metabotropic, which are G protein-associated. These are a family of transmembrane receptors, composed by a heterotrimeric complex of α, β and γ subunits that sense transmitters outside the cells and induce

internal signaling cascades. Depending on the transmitter they respond to, these receptors can be metabotropic glutamate receptors (mGluRs type 3 and type 5), GABA type B receptors, adenosine receptors type 1, 2 and 3, P2Y receptors for ATP, adrenergic receptors, muscarinic acetylcholine receptors and dopamine receptors type 1 and 2 (Verkhratsky 2008). More recently, the cannabinoid type 1 receptor (CB1R), a metabotropic receptor, was also characterized (Navarrete and Araque 2008, 2010; Robin et al. 2018).

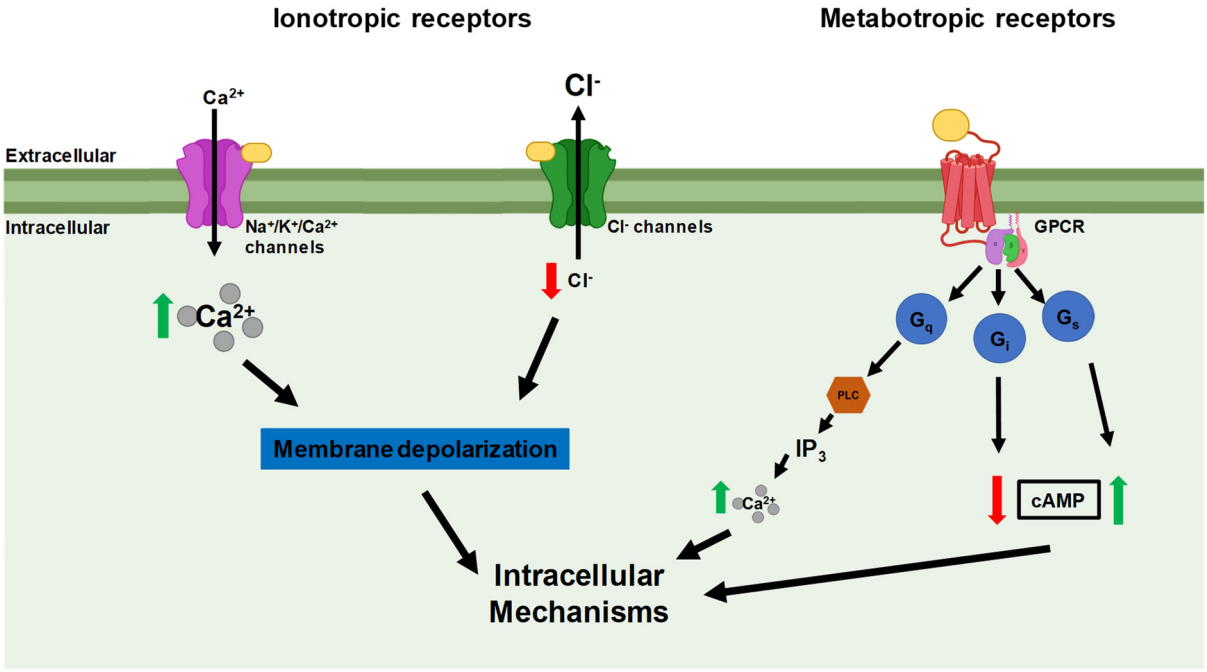

Figure 3 – Representative signaling pathways for ionotropic and metabotropic receptors in astrocytes

Astrocytes are activated by several neurotransmitters such as glutamate, GABA, norepinephrine, adenosine, acetylcholine and endocannabinoids which is only possible because astrocytes express receptors for these molecules. Astrocytic receptors can be ionotropic or metabotropic. Ionotropic receptors are ion channels, $Na^+/K^+/Ca^{2+}$ channels or Cl^- channels, that cause membrane depolarizing. Metabotropic receptors are G protein-coupled receptors (GPCR), that depending on the coupled G protein could trigger different signaling pathways. G_q protein-coupled receptors signal through the phospholipase C protein (PLC)/inositol 1,4,5-triphosphate (IP_3) pathway. G_i and G_s coupled receptors signal by decreasing or increasing the levels of second messenger cyclic adenosine monophosphate (cAMP), respectively.

When a neurotransmitter binds to GPCR, the receptor suffers a conformational change which activates the G protein. Prior to activation, the inactive G protein is bound to guanosine 5-diphosphate (GDP). Thus, to activate the receptor, GDP is phosphorylated into guanosine 5-triphosphate (GTP) by an ATPase, within

the α subunit. Once activated, G protein subunits trigger different signaling mechanisms that are dependent on the sub-class of the coupled G protein (G_q, G_i or G_s). Receptors coupled to the a G_q protein have control in the activation phospholipase C protein (PLC) enzyme which converts phosphatidylinositol 4,5-biphosphate (PIP_2) into diacylglycerol (DAG) and inositol 1,4,5-triphosphate (IP_3). The second messenger IP_3 will then bind and activate the IP_3 receptors at the endoplasmic reticulum (ER) membrane triggering the release of Ca^{2+} (Figure 3). Astrocytes express mainly the IP_3 receptor type 2 (IP_3R2) which is the main internal source of global Ca^{2+} elevations in these cells. On the other hand, receptors coupled to G_i and G_s sub-classes are responsible for the decrease or increase of the secondary messenger cAMP, respectively (Figure 3) (Verkhratsky 2008; Niswender and Conn 2010; Bradley and Challiss 2012). Interestingly, the activation of all these G protein-coupled receptors in astrocytes, even G_i-proteins assumed as inhibitory in neurons, always lead to intracellular Ca^{2+} elevation, which is the main form of astrocytic excitability (as previously mentioned; point 2 in Figure 2) (reviewed in Guerra-Gomes, Sousa, et al. 2018).

Ultimately, these Ca^{2+} elevations modulate downstream cascades that could lead, among other outcomes, to the release of chemical transmitters known as gliotransmitters that bind to neuronal receptors and modulate synaptic activity through a process called gliotransmission (point 3 in Figure 2). The released gliotransmitters may include glutamate, ATP, D-serine, GABA, tumor necrosis factor alpha, prostaglandins and peptides. Their release can be mediated by exocytosis, lysosomes, anion channels, transporter reversal and hemichannels (Allen 2014; Araque et al. 2014; De Pittà et al. 2016; Harada et al. 2016; Petrelli and Bezzi 2016). Through gliotransmission astrocytes can coordinate and modulate functional neuronal networks (Araque et al. 2014; Mederos et al. 2018). In fact, under high frequency synaptic activity, Ca^{2+} signaling can expand intracellularly towards different cell locations and trigger the release of gliotransmitters influencing distant synapses. Thus, through gliotransmission astrocytes can exert a spatial-temporal modulation of neuronal networks sustaining physiological brain function (Araque et al. 2014).

1.2. Astrocytic modulation by glutamatergic neurotransmission

Glutamate is the primary excitatory neurotransmitter in the brain. Glutamatergic synapses are responsible for fast excitatory neurotransmission in cortico-limbic areas of the CNS such as prefrontal cortex (PFC) and hippocampus which are crucial for information processing and cognitive function (McIver et al. 2013; Rose et al. 2018). At glutamatergic synapses, astrocytes can sense the glutamate released by presynaptic

neurons because they are equipped with specific glutamate receptors that can be either ionotropic glutamate receptors (iGluRs) or metabotropic glutamate receptors (mGluRs) (Rose et al. 2018).

The expression of iGluRs, as AMPA and NMDA receptors in astrocytes, is highly heterogeneous and differs between brain regions. AMPA receptors are expressed by Bergmann glia of the cerebellar cortex, being involved in the close interaction between calcium signaling, ensheathment of synapses by glial processes and clearance of glutamate (Matsui et al. 2005; Rose et al. 2018). Some studies have shown that deletion of AMPA receptors in Bergmann glia delayed the glutamate clearance from the synaptic cleft, slowing the decay of excitatory postsynaptic potentials in Purkinje cells and consequently impairing fine motor coordination (Iino et al. 2001; Saab et al. 2012; Rose et al. 2018). Furthermore, these receptors are also present in astrocytes from the neocortex and in radial-like glial cells in the dentate gyrus (Lalo et al. 2006; Renzel et al. 2013; Hadzic et al. 2017). Functional NMDA receptors have been identified in cortical astrocytes as players in astrocyte-neurons signaling (Conti et al. 1996; Schipke et al. 2001; Lalo et al. 2006). In addition, these receptors were also identified in hippocampal astrocytes (Porter and McCarthy 1995; Serrano et al. 2008; Letellier et al. 2016). A study showed that astrocytic NMDA receptors is involved in the modulation of synaptic strength in the hippocampus (Letellier et al. 2016). However, the functions of AMPA and NMDA receptors in astrocytes are still under debate (Rose et al. 2018).

Regarding the mGluRs, they are a family of GPCRs composed by eight subtypes of receptors, from mGluR1 to mGluR8. Their main structure consists in a large extracellular N-terminal domain, the Venus flytrap domain, where the glutamate binding site is located. The Venus flytrap domain is attached to seven transmembrane-spanning domains and to an intracellular C-terminus. This C-terminus is important for the modulation of G protein coupling (Niswender and Conn 2010; Panatier and Robitaille 2016). These receptors are divided in three main groups, Group I (mGluR1 and 5), Group II (mGluR2 and 3) and Group III (mGluR4, 6, 7 and 8), based on the aminoacidic sequence, type of G protein-coupled and physiological profile of each receptor (Niswender and Conn 2010; Spampinato et al. 2018). Expressed mainly at postsynaptic levels, Group I receptors are associated with a G_q protein and are responsible for cell depolarization and excitability. In contrast, Group II and III are G_i protein-coupled receptors, being more expressed at presynaptic structures, controlling the release of neurotransmitters (Spampinato et al. 2018). Although eight types of mGluRs were identified, astrocytes were only reported so far to express mGluR5 and mGluR3 in the brain (Sun et al. 2013; Morel et al. 2014). The activation of mGluR5 is particularly important for astrocyte-neuron interactions, regulating glutamate transporter activity and

gliotransmission. (Bradley and Challiss 2012; Panatier and Robitaille 2016). For the purposes of this work and dissertation, mGluR5 properties and functions will be further explored in the following sections.

1.2.1. Metabotropic glutamate receptor 5 in astrocytes

In astrocytes, glutamate can be sensed by mGluR5 (a G_q protein-coupled receptor) and mGluR3 (a G_i protein-coupled receptor) receptors. Amongst these two, mGluR5 is associated with the activation of the intracellular signaling cascades while mGluR3 is considered inhibitory by decreasing the expression of downstream molecules (Bradley and Challiss 2012). Several studies, majorly using pharmacological and electrophysiological approaches, have already demonstrated that activation of astrocytic mGluRs leads to Ca^{2+} elevations, the major form of astrocytic excitability (Porter and McCarthy 1995, 1996; Latour et al. 2001; Wang et al. 2006; Panatier et al. 2011; Honsek et al. 2012). However, although the functional implications of astrocytic mGluR5 in synaptic transmission seems to be undeniable, studies are still somehow controversial mostly because of a reported decrease in mGluR5 expression during lifetime (Sun et al. 2013; Morel et al. 2014). These findings are most likely the reason why the majority of the studies mentioned above were performed in young mice and tissues (brain slice or culture). Hence, it is urgent to investigate roles for astrocytic mGluR5 activation in adult mice, specially using *in vivo* approaches, in order to better understand the functional implications of these receptors in astrocytes. It is noteworthy that despite the lower expression of mGluR5 during adulthood, evidence still points to an important physiological and pathological role of this receptor in mature astrocytes (Panatier and Robitaille 2016).

Expression levels of mGluR5 in astrocytes

Throughout the brain, mGluR5 is highly expressed in mature neurons, located mainly at postsynaptic structures (Berthele et al. 1999; Aronica et al. 2001; López-Bendito et al. 2002; Sun et al. 2013), functioning as one of the major sensors for glutamate in synapses. In contrast, expression of mGluR5 in astrocytes has a distinct pattern, being highly expressed mostly during development at early postnatal stage while poorly expressed during adulthood. Several studies showed that acutely isolated astrocytes have distinct levels of mGluR5 mRNA during development (Schools and Kimelberg 1999; Cai et al. 2000; Sun et al. 2013; Morel et al. 2014). Kimelberg's lab showed that only 58% of $GFAP^+$ cells, isolated from the hippocampus of rats with 1-10 post-natal (P) days, expressed mGluR5 mRNAs (Schools and Kimelberg 1999). An increase to 77% and a further decrease to 36% in mGluR5 mRNAs expression levels was observed in $GFAP^+$ cells from P11-20 and P25-35 rats, respectively. This decrease in mGluR5 expression was directly related with the number of cells responding to glutamate stimulation (Cai et al. 2000). More

recently, another study reported highly mGluR5 mRNAs expression levels in cortical and hippocampal astrocytes from 1-week old mice, with a decrease in mGluR5 expression in mice with 2 weeks until adulthood, when mGluR5 expression by astrocytes was reduced (Sun et al. 2013). Moreover, these lower levels of mGluR5 expression in mature astrocytes was also observed in cortical astrocytes from adult human samples (Sun et al. 2013). In addition, Morel and colleagues (2014) showed that cortical astrocytic mGluR5 mRNA associated with ribosomes increased from P7 to P21 mice, but it agrees with Sun and colleagues (2013) in the fact that mRNA levels decreased significantly in P40 mice. Interestingly, despite the low expression of mGluR5 in astrocytes reported both in rodents and humans, evidence points to an important functional role of this receptor in what seems to be a fine-tuning of glutamate system in physiological conditions (further explored in this section). Besides, it is also intriguing how the same cells, when shifting to a reactive state, may respond to stressful stimuli or insults by up-regulating mGluR5 expression. Indeed, mGluR5 expression levels are increased in mouse models of neurogenerative or neuropsychiatric disorders, as epilepsy (Szokol et al. 2015; Umpierre et al. 2019). In accordance, in humans astrocytes have high levels of mGluR5 expression under pathological conditions, such as amyotrophic lateral sclerosis and multiple sclerosis (Aronica et al. 2001; Geurts et al. 2003). Hence, promising data suggests that astrocytic mGluR5 is a key player in both healthy and pathological events (Niswender and Conn 2010; Panatier and Robitaille 2016; Spampinato et al. 2018).

Signaling mechanism

When glutamate released by presynaptic neurons binds to mGluR5s in astrocytes, it induces conformational changes promoted by the conversion of GDP into GTP within the α subunit, activating the G_q protein which in turn recruits PLC to hydrolyze membrane lipid PIP_2 into IP_3 and DAG. The secondary messenger IP_3 will then bind to IP_3R2s in the ER leading to the cytosolic Ca^{2+} elevations. These elevations of Ca^{2+} will activate Ca^{2+}-dependent mechanisms that can have implications at the level of the neuronal circuits and behavior (Figure 4) (Niswender and Conn 2010; Panatier and Robitaille 2016).

The spatiotemporal characteristics of Ca^{2+} elevations mediated by mGluR5 seem to require some type of interaction between the receptor and the molecular elements of their signaling machinery. In neurons, mGluR5-dependent Ca^{2+} signaling requires two scaffold proteins, Shank1B and Homer1b (Sala et al. 2005). In addition, Homer is also related with the localization of the receptor (Niswender and Conn 2010), Ca^{2+} homeostasis (Ango et al. 2001), protein kinase signaling and behavior (Ménard and Quirion 2012). In astrocytes, it was recently reported that mGluR5 signaling is functionally controlled by Homer1 scaffold proteins, more specifically Homer1b/c. This variant of Homer is involved in the attachment of the ER

tubules to submembrane microdomains (Figure 4). The anchoring of these two structures optimizes temporal correlation between Ca^{2+} events, mediated by the activation of mGluR5, and exocytosis. In contrast, expression of Homer1a disrupts this mechanism in astrocytes by preventing the interaction between the ER and submembrane microdomains (Buscemi et al. 2017). The intracellular Ca^{2+} elevations evoked by the activation of mGluR5, will induce Ca^{2+}-dependent mechanism like the release of gliotransmitters that is intimately related to functional outcomes, as described below (Niswender and Conn 2010; Panatier and Robitaille 2016).

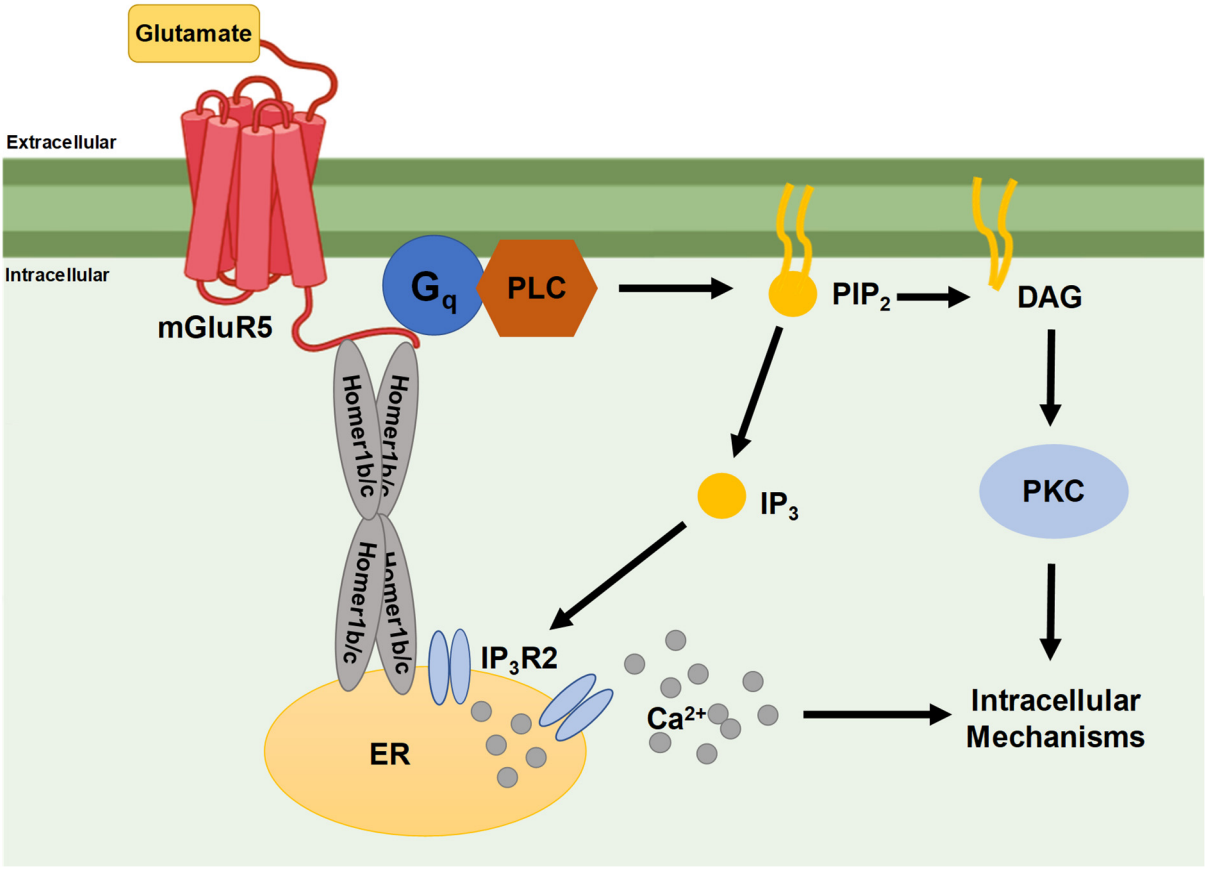

Figure 4 - Activation of mGluR5 in astrocytes induces intracellular calcium elevations

Activation of mGluR5 by glutamate activates the G_q protein signaling that recruits a phospholipase C (PLC). Once activated, PLC converts phosphatidylinositol 4,5-biphosphate (PIP_2) in diacylglycerol (DAG) and inositol 1,4,5-triphosphate (IP_3). DAG will activate a protein kinase C (PKC), which is involved in various signaling cascades. In contrast, IP_3 will bind to the IP_3 receptor type 2 (IP_3R2) in the endoplasmic reticulum (ER) membrane leading to the release of Ca^{2+} to the cytosol. Intracellular Ca^{2+} elevations will then initiate several cellular responses. In astrocytes, homer1b/c scaffold proteins are responsible for the attachment of ER tubules to submembrane microdomains.

Functional implications of astrocytic mGluR5

For the past decades, astrocytes excitability induced by glutamate have been associated with the activation of the astrocytic mGluR5. As mentioned above, the activation of these receptors leads to oscillatory Ca^{2+} events that can propagate throughout the cell or in the astrocytic microdomains (Panatier and Robitaille 2016). Porter and McCarthy (1995) showed that CA1 astrocytes from hippocampal slices acutely isolated from P9-13 animals, exhibit Ca^{2+} elevations when stimulated with mGluRs agonists. One year later, the same authors electrically stimulated the Schaffer collaterals (group of CA3 projections synapsing with CA1 neurons) which induced intracellular Ca^{2+} elevations in CA1 astrocytes (Porter and McCarthy 1996). In addition, Pasti and co-authors (1997) showed that repetitive electrical stimulation of neurons or repetitive pharmacological stimulation with an agonist of mGluRs, induces a long-lasting increase in Ca^{2+} oscillation frequency in astrocytes. Therefore, detection of synaptic activity by astrocytes is dependent on the pattern of neuronal activity (Pasti et al. 1997; Panatier and Robitaille 2016). Accordingly, astrocytes activation by both glutamate application or electrical stimulation of the Schaffer collaterals was shown to induce Ca^{2+} elevations in astrocytes mainly through mGluRs (Latour et al. 2001). It is important to note that at Schaffer collateral synapses, glutamate is the main neurotransmitter released by presynaptic neurons (Collingridge et al. 1983). Moreover, all studies mentioned above used the same mGluRs antagonist, to assure that astrocytic Ca^{2+} oscillations observed during pharmacological or electrical stimulation were mediated by this type of receptors (Porter and McCarthy 1995, 1995; Pasti et al. 1997; Latour et al. 2001). More recently, several studies using a specific antagonist for mGluR5 in hippocampal slices of young animals, showed an astrocytic mGluR5-dependent increase in internal astrocytic concentrations of Ca^{2+} during synaptic activity (Panatier et al. 2011; Honsek et al. 2012; Sun et al. 2014). Overall, astrocytes are not only important modulators of neuronal networks activity during sustained and intense synaptic transmission but they are also involved in the modulation of basal synaptic activity (Panatier et al. 2011). Indeed, astrocytes detect basal neuronal activity at the level of a single synapse from Schaffer collateral in hippocampal slices from juvenile rats. The same authors also observed small and fast spontaneous Ca^{2+} elevations in astrocytic microdomains close to postsynaptic elements, as dendritic spines (Panatier et al. 2011; Panatier and Robitaille 2016). Despite their role in the hippocampus, mGluR5 was also reported to be crucial for synaptic transmission detection by astrocytes in the cortex of adult mice (Wang et al. 2006). Increases in Ca^{2+} levels in astrocytes from the cortex of mice after whisker stimulation seems to be mGluR5-dependent. In fact, after whisker stimulation astrocytic Ca^{2+} events were inhibited by administration of a specific mGluR5 antagonist. In addition, they

observed robust Ca^{2+} elevations in astrocytes from the layer II of the barrel cortex after administration of a mGluRs agonist (Wang et al. 2006).

Based on the above, astrocytic mGluR5 appears be crucial for glutamatergic modulation of astrocytes in the several brain regions, namely the hippocampus, with potential impact for circuits and behavior (further explored in 1.3.3) (Panatier and Robitaille 2016).

1.3. Astrocytes in cognitive function

As described above, over the years, astrocytes have been considered key players in brain homeostasis and synaptic plasticity. More recently, their ability to sense and respond to neuronal activity has been shown to be important for processes involved for instance in learning and memory (Gibbs et al. 2008; Fields et al. 2014; Oliveira et al. 2015; Dallérac and Rouach 2016; Santello et al. 2019). Most studies reporting the involvement of astrocytes in information processing and cognitive function were performed in the PFC and hippocampus, brain regions highly related to memory processing (Mayford et al. 2012; Santello et al. 2019). Still, exploring the exact functional impact of astrocytes in cognitive behavior (as learning and memory) is one of the major challenges of the field. For the past decades, distinct types of animal models of astrocytic dysfunction were proposed and used to address how astrocytic modulation of neuronal networks affects cognitive outputs *in vivo* (Oliveira et al. 2015). Taking advantage of top-edge pharmacological and genetic tools, researchers are now being able to target specific astrocytic features, as sensing, signaling and gliotransmission, and to better infer on its behavioral consequences.

1.3.1. Learning and memory as astrocyte-mediated tasks

Cognition includes specific domains of the human intellect as perception, action, motivation, attention, learning and memory. In the scope of this dissertation, this section will focus on learning and memory. These two cognitive functions are closely related, since learning is how we acquire new knowledge and memory is how we retain and recall the acquired knowledge over time (Kandel et al. 2012, 2014). Throughout life, we are always learning, whenever the brain is processing information. Learning processes induce changes in synaptic activity that are important for mechanisms involved in memory storage. In fact, our brain has the capacity to recall previously acquired knowledge for guidance in future behaviors (Mayford et al. 2012; Kandel et al. 2014). Memory can be classified into short-term memory and long-term memory based on the time course of storage and the nature of the stored information. Short-term memory is associated with goal-relevant knowledge and requires modification of preexisting proteins and temporary changes in synaptic strength, lasting minutes to hours. In contrast, long-term memory involves

synthesis of new proteins, synaptogenesis and changes in synaptic strength that could last hours or weeks. Furthermore, conversion of short-term into long-term memory is achieved through protein kinase A, mitogen-activated protein kinase and cAMP response element-binding protein type 1 and 2 signaling pathway (Bailey et al. 2008; Mayford et al. 2012; Kandel et al. 2014). In addition, long-term memory can be divided into explicit (declarative) and implicit (nondeclarative) memory. Associated with events (episodic memory) and facts (semantic memory), explicit memory is dependent on the medial temporal lobe, mainly the hippocampus. Moreover, implicit memory is dependent on the cerebellum, striatum and amygdala, being related with perceptual and motor skills (Kandel et al. 2012, 2014; Mayford et al. 2012).

Recently, several *in vivo* studies showed that astrocytic modulation can impair or enhance cognitive performance of adult rodents in different behavioral tasks (Sardinha et al. 2017; Adamsky et al. 2018; Robin et al. 2018; Mederos et al. 2019). In our lab, by partially blocking gliotransmission using a mouse model that express a dominant negative domain of vesicular SNARE protein synaptobrevin II (dnSNARE) that interferes with the formation of the SNARE complex, which impairs vesicular release of gliotransmitters in astrocytes, we observed deficits in spatial memory related to hippocampal-dependent tests (Sardinha et al. 2017). Furthermore, Robin and colleagues (2018) have shown that the knockdown of the CB1R in astrocytes impaired object recognition memory. Interestingly, in both studies memory deficits were rescued by the administration of D-serine, a gliotransmitter known to be released by astrocytes (Sardinha et al. 2017; Robin et al. 2018). Another study showed that the expression of a modified muscarinic receptor in astrocytes modulates mice performance in the T-maze task and Contextual Fear Conditioning (CFC), enhancing episodic-like memory and fear memory, respectively (Adamsky et al. 2018). In the same line of study, Mederos and colleagues (2019) reported that the expression of a photopigment coupled to a G protein in astrocytes was responsible for enhancements in episodic-like memory, during the object recognition task. In addition, several authors have been studying astrocytes dysfunction, using similar techniques, in brain disorders associated with cognitive deficits like AD (Orr et al. 2015; Reichenbach et al. 2018). For example, Reichenbach and colleagues (2018) showed that pharmacological inhibition of P2Y purinoreceptors or the genetic deletion of IP_3R2 in astrocytes in an AD mouse model restored spatial learning memory. In the same line, the other study reported that the deletion of astrocytic A2A receptors in an AD mouse model restored spatial memory in the Morris Water Maze (MWM). The expression of A2A receptor was increased in AD and was associated with cognitive deficits. In the same study, authors showed that deletion enhanced spatial memory and this enhancement was maintained in aged mice (Orr et al. 2015). Likewise, our lab showed that interfering with IP_3R2-dependent Ca^{2+} signaling in astrocytes prevents cognitive decline, namely in episodic-like memory, along

aging (Guerra-Gomes, Viana, et al. 2018). All together, these studies have shown that affecting astrocyte functions in specific brain regions as the PFC and hippocampus induces changes in learning and memory and can prevent age or disease-related cognitive decline, elucidating the impact of these cells in cognitive processing.

1.3.2. The prefrontal cortex and the hippocampus in learning and memory

For the past decades, studies on cognition have been focusing mainly in the PFC and hippocampus, two important brain regions for cognitive processing in humans and rodents. Located in the anterior portion of the frontal lobe, the PFC is an interconnection of subcortical structures and cortical systems, as sensory and motor. This arrangement of neural activity in the PFC enables this region to be involved in several complex cognitive functions such as, executive function, behavioral inhibition and intelligence (Miller and Cohen 2001; Wilson et al. 2010). In fact, PFC plays a key role in working memory, behavioral flexibility, attention, planning and decision making (Miller and Cohen 2001; Cerqueira et al. 2005). This brain area is crucial for behavior based on internal states or intentions, for example, when one plays a video-game where the paradigms and instructions are not constant and change frequently (Miller and Cohen 2001). In humans, the PFC can be divided mainly into two sub-regions, the dorsolateral, involved in cognitive function, and the ventromedial or orbitomedial, important in emotion and motivation regulation (Fuster 2009). However, in rodents the PFC is subdivided into three main regions: the medial prefrontal cortex (mPFC), the orbital prefrontal cortex and the agranular insular cortex. Specifically, mPFC is organized into four distinct layers: the medial precentral, anterior cingulate, prelimbic, and infralimbic cortex (Heidbreder and Groenewegen 2003). In addition, the mPFC is connected to other components of the limbic system, which allows the control of cognitive, mnesic and emotional processing (Heidbreder and Groenewegen 2003; Hoover and Vertes 2007), being functionally related to the human dorsolateral PFC.

The hippocampal formation is a portion of the medial temporal lobe of the mammalian brain. It is composed by the hippocampus, dentate gyrus (DG) and subiculum. While these structures are important for the formation of long-term memories, specifically episodic memories related with daily experiences, their storage appears to be located elsewhere. Lesions in the hippocampal formation were shown to impair the formation of new memories without affecting the ability to recall old memories, before the lesion. The first and well-studied case was the Henry Molaison's, a man who suffer from epilepsy. Molaison had is hippocampal formation surgically removed in an attempt to control seizures related with the disease. After surgery, he had a better controlled clinical condition, regarding epilepsy, but he had memory deficits. Maloison had normal working and episodic memory, during seconds or minutes,

nonetheless he could not retain it. Curiously, he was able to recall long-term memories of events that happened before the surgery (Kandel et al. 2012). The hippocampus can be classified as dorsal, important for spatial navigation and episodic memory, and ventral hippocampus, involved in affective and motivational behavior, and subdivided in two main *cornu ammonis* areas (CA1 and CA3). Thus, the hippocampus is responsible for processing information involved in spatial memory, anxiety and motivation (Kandel et al. 2012; Ciocchi et al. 2015). The link between spatial navigation and the hippocampus was made with a discovery of place cells, neurons with specific firing patterns related with spatial location (O'Keefe and Dostrovsky 1971; Ciocchi et al. 2015). Furthermore, long-term potentiation (LTP) in the hippocampus arose as a key player in memory consolidation mechanism in the mammalian brain (Malenka and Bear 2004; Kandel et al. 2012, 2014; Nabavi et al. 2014). Bliss and Lomo reported that high-frequency stimulation of the hippocampal perforant path induces LTP, which increases synaptic strength (Bliss and Collingridge 1993). In contrast, long-term depression (LTD) modulates synaptic plasticity, weakening previous stablished synapses, what is important for elimination of weaker synapses (Malenka and Bear 2004; Kandel et al. 2012, 2014; Nabavi et al. 2014). In fact, the hippocampus presents a fine well-organized neural circuit that is connected with different brain regions. Hippocampal neurons, mainly CA1 pyramidal neurons, receive sensory and spatial inputs from the entorhinal cortex (EC) directly and indirectly through the perforant pathway. Layer III neurons from the EC project directly to CA1 forming synapses with distal apical dendrites of CA1 neurons. However, layer II neurons use an indirect pathway, the trisynaptic circuit, to send information to CA1 neurons. In this trisynaptic hippocampal circuit, EC neurons project to the DG through the perforant pathway establishing synapses with granular neurons from this area. These cells will then project through to CA3, forming the mossy fibers pathway and interacting with local pyramidal neurons. Then, CA3 neuronal axons projections, also known as Schaffer collaterals, interact with CA1 neurons that in turn signals back to the EC and subiculum (Figure 5) (Kandel et al. 2012). Additionally, ventral hippocampus neurons also project to the nucleus accumbens, amygdala and mPFC, the subregion of the rodent PFC involved in cognition (Ciocchi et al. 2015).

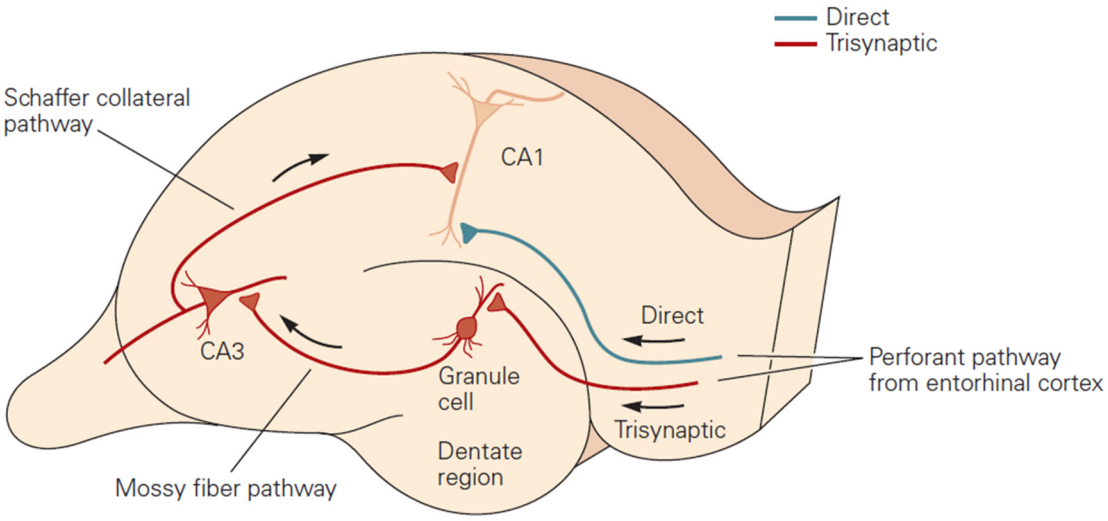

Figure 5 – The hippocampal circuit

Neurons from the entorhinal cortex (EC) communicate with CA1 neurons through the perforant pathway, in a direct (blue) or indirect (red) manner. EC neurons can project their axons directly to CA1 subfield establishing synapses with local neurons. In contrast, in the indirect pathway neurons from the EC present axonal projections to the dentate gyrus (DG) which allows them to interact with granule cells from this region. Then, granule cells will project to the CA3 subfield through the mossy fiber pathway. Ultimately, CA3 pyramidal neurons form synapses with neurons from the CA1 forming the Schaffer Collateral pathway. Adapted from (Kandel et al. 2012).

The hippocampus-mPFC interaction is mainly due to monosynaptic projections from neurons of the hippocampal subfields, CA1 and subiculum. In their turn, PFC neurons project back to the hippocampus through the EC (Tierney et al. 2004; Hoover and Vertes 2007; Parent et al. 2010). In addition, a monosynaptic glutamatergic projection from the anterior cingulate layer of the mPFC to the CA1 and CA3 of the dorsal hippocampus have also been identified (Rajasethupathy et al. 2015). The functional interaction between these two brain regions have been shown to be involved in memory processes and seems to be important in tasks dependent in both brain regions (Yoon et al. 2008; Churchwell et al. 2010; Spellman et al. 2015). For example, Spellman and colleagues (2015) have shown that the direct communication between the ventral hippocampus and the mPFC is crucial for the encoding of spatial cues in a working memory task. Therefore, these two brain regions and the communication between them seems to be crucial in cognition, mainly in learning and memory recall.

Astrocytes have also emerged as important players in cognitive function associated with these brain regions. Our lab showed that impairing astrocytic function in the PFC also impairs spatial working

memory, attention and behavioral flexibility in rats (Lima et al. 2014). In addition, studies have shown that release of D-serine by astrocytes in the hippocampus is necessary for the induction of LTP, an important phenomenon for learning and memory (Yang et al. 2003; Panatier et al. 2006; Henneberger et al. 2010). Accordingly, our lab showed that gliotransmission blockage (using the dnSNARE mouse model) impairs mice performance in hippocampal-dependent tasks involving spatial reference memory. This deficit in spatial memory was rescued with D-serine administration (Sardinha et al. 2017) strengthening the role of astrocyte-released mediators in such complex behavior.

1.3.3. Astrocytes activation mediated by mGluR5: is there a role in cognition?

The activation of mGluR5 in neurons has been shown to be crucial for neuronal excitability, which is important for several aspects of learning and memory (Niswender and Conn 2010). Different studies have shown that mGluR5 activation in distinct brain regions is important for fear memory acquisition and expression (Lu et al. 1997; Schulz et al. 2001; Rodrigues et al. 2002) and for learning and memory acquisition in the MWM (Lu et al. 1997). More recently, Xu and colleagues (2009) demonstrated that mice lacking mGluR5 displayed mild deficits in memory acquisition in the MWM and Contextual Fear Conditioning (CFC) and presented impaired reversal learning and fear extinction. Moreover, the same lab were also able to show that pharmacological activation of mGluR5 enhanced reversal learning and fear extinction (Xu et al. 2013). Altogether, these studies reported a clear role of neuronal mGluR5 in cognition. However, how astrocytic mGluR5 is contributing for processes of learning and memory is still unexplored.

Astrocytes activation by mGluR5 has been shown to modulate synaptic activity in the hippocampus mainly at the level of CA3-CA1 synapses, an important circuit for cognition. In fact, in the hippocampus, activation of astrocytic mGluR5 allows astrocytes to modulate basal synaptic activity and neuronal synchrony, acting in pre- or postsynaptic neurons at Schaffer collaterals. After mGluR5 activation by glutamate, astrocytes can also release glutamate that will activate extrasynaptic NMDA receptors (Angulo et al. 2004; Fellin et al. 2004). Curiously, astrocytic glutamate will specifically bind to these extrasynaptic receptors (Fellin et al. 2004). The activation of NMDA receptors by glutamate induces slow transient currents (Angulo et al. 2004) or slow inward currents (Fellin et al. 2004; Perea and Araque 2005), that seem to be crucial for the synchronization of activity from neighboring neurons (Angulo et al. 2004; Fellin et al. 2004). The These neuronal synchrony could be due to Ca^{2+} waves propagation through astrocyte networks which allows astrocytic release of glutamate in adjacent synapses (Angulo et al. 2004; Fellin et al. 2004).

More recently, a study presented new evidences that astrocytes in the hippocampus also release purines in a vesicular-dependent manner upon mGluR5 activation which activates A_{2A} receptors in presynaptic neurons, enhancing basal synaptic transmission (Panatier et al. 2011). Interestingly, astrocytes released purines can also bind to presynaptic A_1 receptors which are associated with inhibition of synaptic activity in the Schaffer collaterals (Pascual et al. 2005). Thus, an A_1-A_{2A} receptors interaction might be a mechanism used by astrocytes to regulate synaptic plasticity (Panatier et al. 2011; Panatier and Robitaille 2016). In addition, astrocytic mGluR5 activation was shown to be important for the potentiation of glutamate uptake and K^+ influx in astrocytes from the CA1 region through a PKC dependent mechanism (Devaraju et al. 2013). Furthermore, pharmacological inhibition or genetic deletion of the mGluR5 seems to impair developmental growth of cortical astrocytic processes and induction of functional GLT-1 expression (Morel et al. 2014).

Overall, (the few) studies on astrocytic mGluR5 show that this receptor modulates synaptic transmission at different levels. Modulation of synaptic activity by astrocytes is known to be crucial in cognitive processing. However, to date, no direct link between the role of astrocytic mGluR5 and cognition could be made mostly because the majority of studies involving mGluR5 activation in astrocytes were performed in cultured astrocytes or in acute brain slices of young rodents. Thus, further *in vivo* studies during adulthood are needed to better understand the role of this receptor in synaptic plasticity and behavior. Moreover, as mentioned above, the expression of these receptors may also vary along development and throughout different brain regions. Hence, better characterizing the heterogenous patters of these receptors and its functions will provide unprecedented insights into the astrocytic role on neural circuits that support cognitive behavior.

2. Research aims

Emerging evidences over the years have shown that astrocytic mGluR5 is crucial for synaptic sensing and its activation modulates synaptic activity. In fact, these studies have shown that intracellular Ca^{2+} elevations in astrocytes after stimulation of Schaffer collaterals (CA3-CA1 synapses important for learning and memory) in hippocampal brain slices are mediated by the activation of mGluR5. Importantly, most of these studies were performed in situ in brain slices from young mice, focusing on the developmental role of astrocytic mGluR5. Thus, the field is lacking more studies, especially *in vivo*, focusing on the roles of astrocytic mGluR5 in adulthood and its behavioral implications.

Hence, the main goal of this dissertation was to address the role of astrocytic mGluR5 in cognitive processing in adult mice. For that, this work was sub-divided in two main tasks:

1. Generation and validation of two mouse models allowing the temporal control over the deletion of mGluR5, specifically in astrocytes:
    a. Generation of a conditional mGluR5 knock-out (KO) mouse line lacking expression of this receptor in astrocytes in the whole brain.
    b. Generation of a region-specific deleted mice, lacking the expression of mGluR5 in astrocytes uniquely in the hippocampus.
2. Evaluation of the impact of whole brain or hippocampal astrocytic mGluR5 gene deletion in the motor function, mood and cognitive function.

Here, we provide unprecedented evidence on the behavioral consequences associated with deletion of mGluR5 in astrocytes. By using two different approaches to conditionally block mGluR5 expression and a battery of behavioral tests dependent on different neuronal circuits, this study also allows the dissection of region-specific events. By affecting the mGluR5-downstream cascade of events, we also demonstrate how the expression of relevant astrocytic targets are also affected. Overall, this work has contributed to a better understanding of the impact of mGluR5 activation in astrocytes for cognitive function.

3. Methods

3.1. Animal welfare and generation of mouse models

Adult male mice, with a C57BL6/J background, were used in all experiments. Mice were group-housed in standard cages (3 to 6 mice per cage) with food and water *ad libitum*. The housing room was at 22°C with controlled ventilation and was under a light/dark cycle of 12 hours (8 AM to 8 PM). All procedures involving mice were performed according to the guidelines for the welfare of laboratory mice as described in Directive 2010/63/EU. In addition, they were approved by the Local Ethics Committee (SECVS 075/2015; ORBEA 004/2018, Annex 1) and the National Authority for Animal Experimentation, DGAV (DGAV 17469/2012).

In this dissertation, in order to explore the functional roles of astrocytic mGluR5, two mouse models with temporally controlled deletion of the receptor specifically in astrocytes were generated. For that, a conditional knock-out (KO) mouse line lacking mGluR5 in astrocytes in the whole brain was obtained through genetic recombination (as explained in detail in section 3.1.1) while by local stereotaxic virus injection we were able to delete mGluR5 in astrocytes solely in the hippocampus (explained in more detail in section 3.1.2).

3.1.1. Generation of inducible, astrocyte-specific mGluR5 conditional knockouts (GLAST-CreER^{T2}-mGluR5$^{fl/fl}$)

The Cre/lox site-specific recombination system emerged as an important tool allowing the generation of conditional mutants, where cell or region-specific ablation of a gene is achieved. Mice, with loxP sequences flanking the mGluR5 gene (mGluR5$^{loxP/loxP}$ or mGluR5$^{fl/fl}$ mice) were kindly provided by Dr. Anis Contractor (USA) (Xu et al. 2009), and used to generate the conditional KO mouse line needed for this dissertation. Firstly, mGluR5$^{fl/fl}$ were crossed with mice where a mutated estrogen receptor (ER^{T2}) was fused to Cre recombinase as a transgene (CreER^{T2}) in the locus of the GLAST promoter. The GLAST-CreER^{T2}, whose transgene activation is induced by tamoxifen, were kindly provided by Prof. Magdalena Götz (Germany) (Mori et al. 2006) (Figure 6A). Mice from the first generation (F1) were all heterozygous for the flanked mGluR5 and could be either positive or negative for the GLAST-CreER^{T2} gene, namely GLAST-CreER^{T2}-mGluR5$^{fl/+}$ and mGluR5$^{fl/+}$ mice, respectively (Figure 6B). The GLAST-CreER^{T2}-mGluR5$^{fl/+}$ (from F1) were later crossed with mGluR5$^{fl/fl}$ mice in order to obtain the second generation (F2) with following possible genotypes: mGluR5$^{fl/+}$, mGluR5$^{fl/fl}$, GLAST-CreER^{T2}-mGluR5$^{fl/+}$, GLAST-CreER^{T2}-mGluR5$^{fl/fl}$

(Figure 6C). Finally, the GLAST-CreER^{T2}-mGluR5$^{fl/fl}$ mice were crossed one more time with mGluR5$^{fl/fl}$ mice to obtain littermates of the two genotypes used in our studies GLAST-CreER^{T2}-mGluR5$^{fl/fl}$ and mGluR5$^{fl/fl}$ mice (generation F3 - Figure 6D), therefore reducing the number of surplus mice. Mice from these two genotypes were then injected with tamoxifen for mGluR5 ablation. The mGluR5$^{fl/+}$ mice from F1 were also kept and used to generate another mouse colony that will be explained in section 3.1.2.

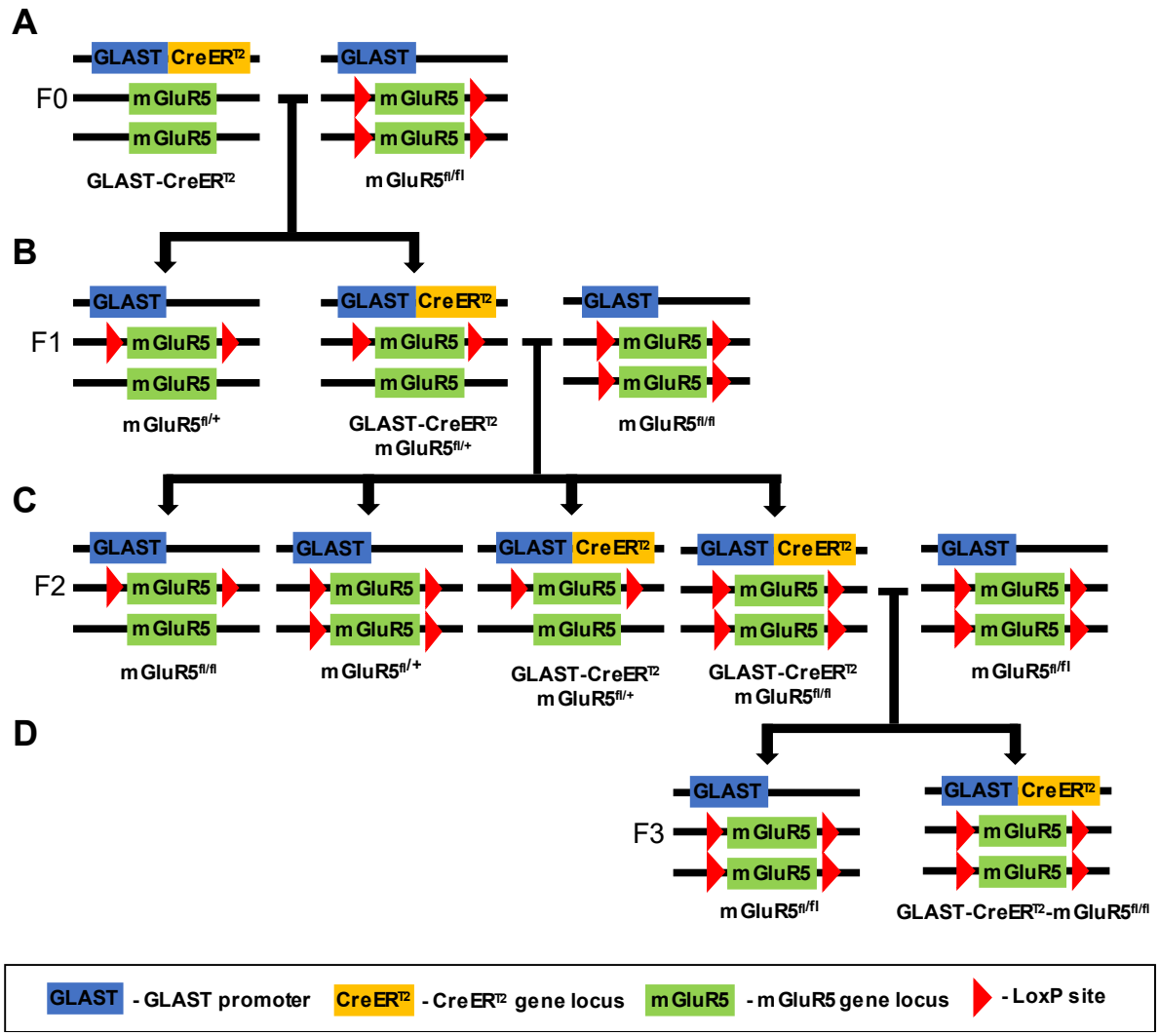

Figure 6 – Breeding scheme of the GLAST-CreER^{T2}-mGluR5$^{fl/fl}$ conditional knockout colony

In vivo tamoxifen injections

In this GLAST-CreER^{T2} inducible mouse line, tamoxifen, a selective estrogen-receptor modulator, is used to temporally control the initiation of recombination. Its metabolite 4-hydroxytamoxifen shows high affinity to the mutated-ER^{T2} present in these mice, which on the other hand is insensitive to endogenous estrogen. When binding to the receptor, the fused protein Cre recombinase is translocated to the nucleus, where it recombines the loxP sites resulting in gene deletion. Thus, in the absence of tamoxifen, the Cre-ER fusion

protein is retained in the cytoplasm and no deletion should occur prior to the injections (Feil et al. 2009), allowing the normal development of these mice in the presence of the functional receptor.

In this study, GLAST-CreER^{T2}-mGluR5$^{fl/fl}$ mice with 6 to 8 weeks, and their mGluR5$^{fl/fl}$ littermates, were injected intraperitoneally (i.p.) with tamoxifen. Genotyping protocols, used previously to identify mice for the different experimental groups, are detailed below. The day before the first injection, tamoxifen was dissolved in corn oil (Sigma; C-8267) at a final concentration of 20 mg/mL and was maintained overnight at 37°C and shaking at 200 – 250 rpm in an Orbital Shaker – Incubator ES-20/60 (Biosan, Latvian Republic). Mice were injected with 1 mg of tamoxifen, twice a day for 5 consecutive days. After a resting period of 7 days, the protocol was repeated (Mateus-Pinheiro et al. 2017). Three weeks after the last injection mGluR5$^{fl/fl}$ and now GLAST-CreER^{T2}-mGluR5$^{del/del}$ (henceforth referred as GLAST-mGluR5KO) mice were used for behavioral characterization, explained in detail in section 3.2. In a pilot experiment, mice under a Balb/c background, from a GLAST-CreER^{T2}-CAG-Green Fluorescent Protein (GFP) colony, also bred in our facility, were similarly injected with tamoxifen and used later to confirm the general distribution of GLAST expression in the brain. This mouse line, contrarily to GLAST-CreER^{T2}-mGluR5$^{fl/fl}$, presents the GFP reporter gene that allows detection of recombined cells by immunohistochemistry analysis (detailed in section 4.1.1).

Mice genotyping

Toe tip samples from all mice were collected 5-7days after birth for DNA extraction (for older mice, ear clips were used instead). Toe or ear clipping was also used for mice identification. For DNA extraction, 300 μL of sodium hydroxide (NaOH) 50 mM were added to each sample, followed by incubation at 98°C in a heating block (AccuBlock Digital Dry Bath, Labnet International, NJ, USA) during 50 min, for tissue dissociation. Next, samples were homogenized using a vortex for 15 s and the reaction was neutralized with 30 μL of Tris 1 M. For confirmation of the gene deletion in tamoxifen-induced mice, after sacrifice a part of the freshly collected brains was also used for DNA extraction. After tissue digestion was completed, samples were centrifuged at 14000 rpm for 6 min and the supernatant was transferred to a new tube and maintained at 4°C. Gene loci of interest were then amplified by Polymerase Chain Reaction (PCR) using specific pairs of primers.

In order to select mice with correct genotype for tamoxifen injections, two independent genotyping protocols, optimized in the scope of this dissertation, were used to amplify the mGluR5 gene or the CreER^{T2} gene. In the protocol for the mGluR5 gene, the *pair 1* of primers was used to amplify the two forms of mGluR5, mGluR5$^{+/+}$ present in WT mice and mGluR5$^{fl/fl}$ for the homozygous flanked mice (Table 1). The

same pair of primers origins both products, allowing the identification of both genotypes, since the 5' loxP site is located between primers binding site as represented in Figure 7A. In this case, there is no need for the use of an internal control (constitutive gene) as all genotypes would result in amplification and generate a product. In the protocol for the CreER^{T2} gene, two set of primers were used. The *pair 2* was used to amplify the CreER^{T2} gene and the *pair 3*, corresponds to the amplification of IP$_3$R2 gene, which was used as a constitutive gene (internal control), to validate the PCR protocol especially in the case of WT mice which are CreER^{T2}-negative (Table 1). Lastly, and because this is a tissue and cell-specific conditional KO, genotyping of brain samples were done after mice were sacrificed, to confirm effective deletion of the mGluR5 gene after behavioral testing. In this case, the *pair 4* of primers were used (Table 1). Forward primer binds upstream of the 5' loxP site, whereas the reversal primer binds downstream of the 3' loxP site. After exon 7 deletion the PCR product size obtained is 360 bp (Figure 7B). In this case the *pair 3* was also used as internal control to validate the PCR protocol for mice that did not undergo gene deletion. The PCRs were performed in a thermal cycler (Bio-Rad) and the conditions used to genotype these mice were optimized in the scope of this dissertation (Table 2).

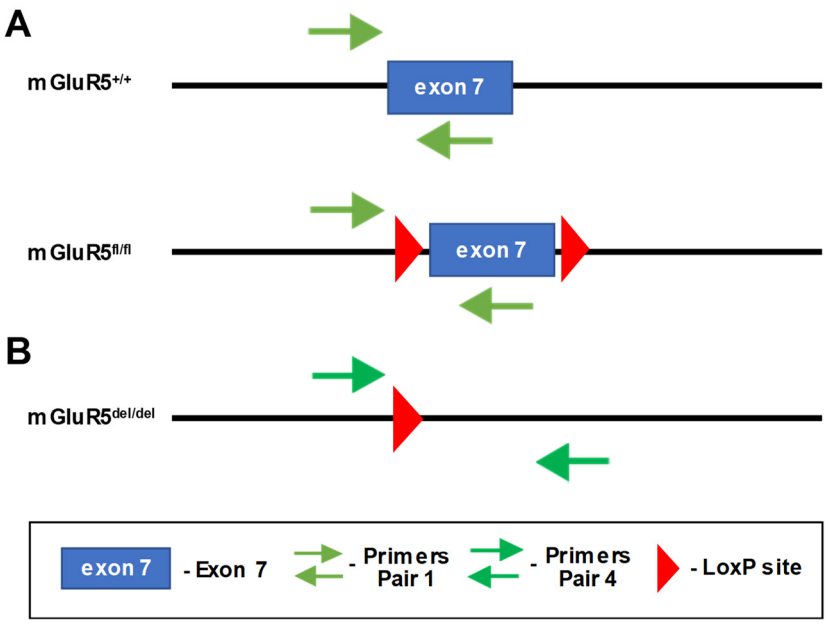

Figure 7 - Representation of the mGluR5 gene (*Grm5*) locus and binding sites for pair 1 and pair 4 primers for genotyping

Table 1 – PCR primer sequences used to amplify the mGluR5, CreER^{T2} and IP$_3$R2 genes, respective nucleotide sequences and product sizes

Primer Pair	Gene Amplified	Primer Sequence (5´- 3')	Product size (bp)
Pair 1	mGluR5	F: AGA TGT CCC ACT TAC CTG ATG T	200[1]
		R: AGT TCC GTG TCT TTA TTC TTA GC	270[2]
Pair 2	CreER^{T2}	F: GAG GCA CTT GGC TAG GCT CTG AGG A	500
		R: GGT GTA CGG TCA GTA AAT TGG ACA T	
Pair 3	IP$_3$R2	F: AAC CTG ATG AGG GAA GGT CT	250
		R: ATC GAT TCA TAG GGC ACA CC	
Pair 4	mGluR5	F: AGA TGT CCC ACT TAC CTG ATG T	360
		R: AGG CGC TTC CAA AAT AGA GG	

F – Forward; R – Reversal
[1]Product size for mGluR5$^{+/+}$
[2]Product size for mGluR5$^{fl/fl}$

Table 2 – PCR mix composition for mGluR5, CreER^{T2} or IP$_3$R2 amplification and reaction conditions

Reagents	Mix for mGluR5 gene	Mix for CreER^{T2} gene	Mix for mGluR5KO	PCR program
Taq Buffer[1]	2 µL	2 µL	2 µL	95°C – 4 min 35 cycles of: 95°C – 30 s 56°C – 1 min 72°C – 45 s 72°C – 15 min 4°C - ∞
Pair 1	0.2 µL per primer	–	–	
Pair 2	–	0.2 µL per primer	–	
Pair 3	–	0.2 µL per primer	0.2 µL per primer	
Pair 4	–	–	0.2 µL per primer	
Taq polymerase[2]	0.1 µL	0.1 µL	0.1 µL	
H_20 (Braun)	5.5 µL	5.1 µL	5.1 µL	
DNA template	2 µL	2 µL	2 µL	

[1]MyTaq Reaction buffer (Bioline)
[2]MyTaq DNA polymerase (Bioline) (5u.1µL)

After amplification the resulting products were separated in a 2% agarose gel using Greensafe Premium dye (NzyTech, Portugal) to allow DNA bands detection (corresponding to the generated products in each case). A DNA size marker (0.5 µg/µl; GeneRuler 1 Kb; Fermentas) was also used to assure a correct assessment of the bands size. The electrophoresis was performed during 30 min at 140 V. After electrophoresis, gel pictures were obtained by a Geldoc™ IZ imager (Bio-Rad) and visualized using Image LabTM Software (Alpha Innotech Corporation, Biorad).

3.1.2. Generation of the astrocyte and hippocampus-specific mGluR5 Conditional Knockout (dHIP-GFAP-mGluR5KO)

A new mGluR5 mice colony was established to obtain littermate mice that have an intact or flanked form of the mGluR5 gene. For that, mGluR5$^{fl/+}$ mice obtained as described in section 3.1.1 (Figure 6B, F1) were crossed between them to obtain Wild-type (WT) (mGluR5$^{+/+}$) and mGluR5$^{fl/fl}$ mice (Figure 8). Their genotype was identified by PCR, using the protocol to amplify the mGluR5 gene as described in section 3.1.1. Then, mGluR5$^{+/+}$ and mGluR5$^{fl/fl}$ mice were injected in the hippocampus with a viral vector carrying the Cre enzyme that allowed ablation of the mGluR5 gene in astrocytes, in a temporally- and spatially-controlled manner.

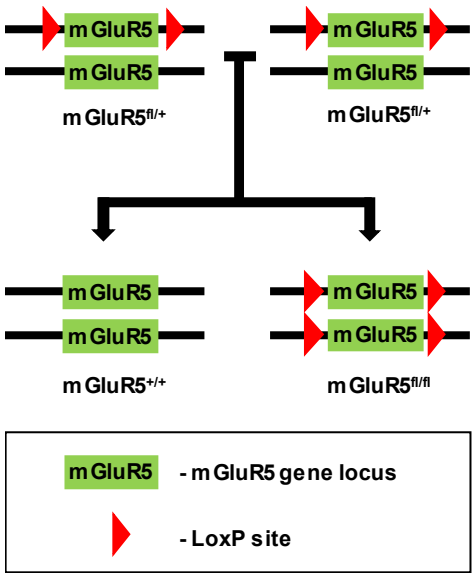

Figure 8 – Breeding scheme of the floxed mGluR5 mouse colony

Intracranial viral injection

Ablation of mGluR5 specifically in hippocampal astrocytes from mGluR5$^{fl/fl}$ mice was achieved though intracranial bilateral injection of a recombinant adeno-associated virus 5 (rAAV5), purchased from UNC Vector Core (USA). The rAAV5 was fused with a Cre recombinase vector and a reporter gene (mCherry) under the control of GFAP promoter (rAAV5/GFAP:mCherry-Cre) and dissolved in Phosphate-buffered saline (PBS) 5% D-Sorbitol with 350 nM NaCl at a final concentration of 4.3x10^12 genome copies (g.c.)/mL.

For the intracranial injection procedures, 8 to 10 weeks mGluR5$^{+/+}$ and mGluR5$^{fl/fl}$ mice were anesthetized with an i.p. injection of a mixture of ketamine (75 mg/kg; Imalgene 1000, Merial, USA) and medetomidine

(1 mg/kg, Dorbene Vet, Pdizer, USA). When fully anesthetized, mice were placed on the stereotaxic apparatus, their eyes were covered with Vaseline to prevent dryness of the corneas and 0.5% lidocaine was locally injected in the head. Using a scalpel blade, a small incision (rostral to caudal) was made to expose the surface of the skull. With the help of a semi-automatic drill, two symmetric holes (related to the skull medial line) were open in the mice skull using the following coordinates related to Bregma: 1.8 mm anteroposterior, 1.3 mm mediolateral (Franklin and Paxinos 2001). Bilateral injections were then performed, directly into the dorsal hippocampus, using a Hamilton syringe coupled to a 30-gauge needle (Hamilton, Switzerland), 1.3 mm below the brain surface (dorsoventral coordinate) (Franklin and Paxinos 2001). Mice were injected with 1 µL of rAAV5/GFAP:mCherry-Cre dissolved in 0.9% saline at the final concentration of 4.3x10^11 g.c./mL per injection at a rate of 100 nL/min. After each injection, the needle was moved 0.1 mm up and left in place for 5 min to allow proper viral vector diffusion and to avoid reflux up the needle tract. Finally, mice were sutured and given intramuscular injections with atipamezole (1 mg/Kg), to withdraw the anesthesia. Finally, they were injected subcutaneously with an opioid for analgesia (Bupac, 0.05 mg/kg), a multivitamin mixture (Duphalyte/Pfizer, USA) and an anti-inflammatory drug (Carprofeno, 0.05 mg/kg) and left in a recovery room for the rest of the day under a warming lamp. In the next day, all mice were injected again i.p. with an opioid and anti-inflammatory and multivitamin mixture were administrated if needed. Three weeks after the surgical procedure, $mGluR5^{+/+}$ mice and $mGluR5^{fl/fl}$ mice that after recombination were $mGluR5^{del/del}$ in hippocampal $GFAP^{+}$ cells (henceforth referred as dHIP-GFAP-mGluR5KO mice) (Figure 9) were used for behavior assessment, described in the following section.

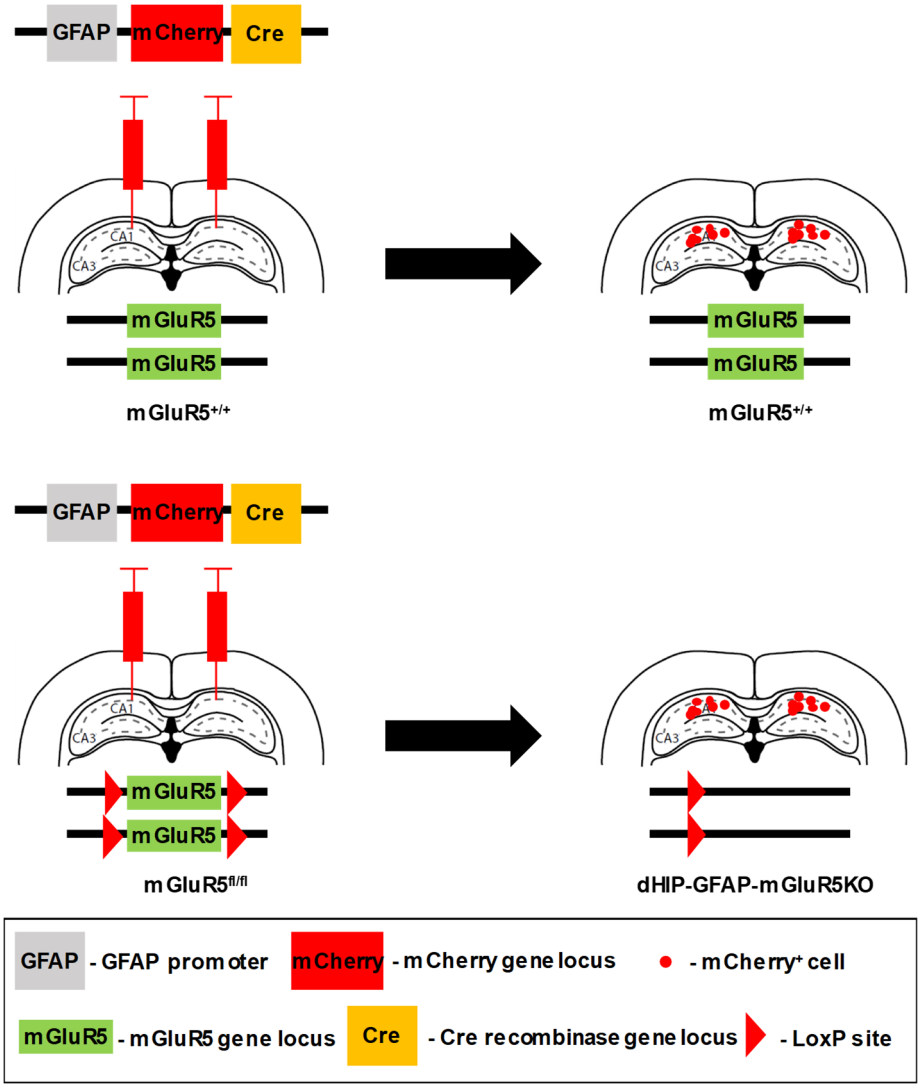

Figure 9 - Scheme of the intracranial bilateral viral injection to delete astrocytic mGluR5 specifically in hippocampal astrocytes

3.2. Behavioral characterization

To study how the deletion of mGluR5 in adulthood affects behavioral activity, the GLAST-mGluR5KO mice and respective littermate controls (mGluR5$^{fl/fl}$) as well as the dHIP-GFAP-mGluR5KO and respective littermate WT (mGluR5$^{+/+}$) performed several behavioral tests. One week prior to the beginning of behavioral characterization, mice were handled for 5 min each day for habituation to the experimenter. Behavior tests such as Open Field (OF) and Elevated Plus Maze (EPM) were performed to evaluate general exploratory behavior of anxious-like phenotype while depressive-like behavior was evaluated by the Tail Suspension Test (TST). Morris Water Maze (MWM), Y-maze Two-Trial Place Recognition Test (2TPR) and Contextual Fear Conditioning (CFC) were used to assess cognition. Mice were placed in the testing room

30 min before each test for habituation to the environment. Mice that did not perform the tests were excluded from the analysis.

3.2.1. Open field

The Open Field (OF) test was performed to assess anxious-like behavior, motor and exploratory activity in an open arena (Seibenhener and Wooten 2015). The OF was performed in a brightly illuminated Plexiglas box (43.2 x 43.2 x 30.5 cm). Mice were placed individually in the center of the arena and left to explore it for 5 min. Their movement was tracked by a system of two 16-beam infrared arrays connected to a computer (Med Associates, Inc). After each trial, the arena was cleaned with 10% ethanol. Time spent in the center, number of rearings and total distance travelled in the arena were measured using the Activity Monitor software (Med Associates, Inc).

3.2.2. Elevated plus maze

To assess anxious-like behavior the Elevated Plus Maze (EPM) test was performed. The EPM apparatus consist in a plus shape structure 72.4 cm above the floor. This structure is composed by two open arms (50.8 x 10.2 cm) and two closed arms (50.8 x 72.4 x 40.6 cm) with an intersection area (hub) of 100 cm^2. Mice were placed individually in the center of the maze, facing one of the open arms, and left to explore the maze for 5 min. Behavioral activity was recorded with a video camera and analyzed using EthoVision XT 13.0 (Noldus Information Technology, Netherlands) to obtain the distance travelled and time spent in the open and closed arms. EPM was performed under white bright light and the maze was cleaned with 10% ethanol between mice. Time spent in open arms was used as a measure of anxious-like behavior since rodents naturally avoid open and lighted spaces (open arms) and prefer dark enclosed spaces (closed arms) (Walf and Frye 2007) .

3.2.3. Tail suspension test

Depressive-like behavior was evaluated by the Tail Suspension Test (TST). This test is used to evaluate learned helplessness since rodents tend to develop an immobile position when placed in an unavoidable stressful situation (Can et al. 2012). In the TST, mice were suspended by their tails using adhesive tape, 80 cm above the floor, for 6 min and behavioral activity was recorded using a video camera. EthoVision XT 13.0 (Noldus Information Technology, Netherlands) was used to obtain, for each mouse, the period of immobility for the final 4 min of test, since the mice had to learn that there is no possible escape.

3.2.4. Morris water maze: reference memory and reversal learning

The Morris Water Maze (MWM) was performed to evaluate spatial reference memory, a hippocampal-dependent task, and behavior flexibility that relies also on the PFC (Vorhees and Williams 2006; Sardinha et al. 2017). The MWM apparatus consists in a dark circular pool (106 cm diameter) filled with water at 23°C, divided in four imaginary quadrants, which were associated with extrinsic visual cues (cross, lines, triangle and square). In one of the imaginary quadrants, a circular escape platform (11 cm diameter, 26 cm height) was placed 1 cm below the water surface. To hide the platform and to increase the contrast to detect the mouse, non-toxic titanium dioxide (Sigma-Aldrich; 250 mg/L) was added to the water. The MWM test was conducted under dim light conditions.

The Reference Memory task is based on the capacity of mice to learn the position of the escape platform, which was kept in the same quadrant during the four days. Each day, mice performed four trials with a maximum duration of 60 s. In each trial, mice were placed in the pool facing the pool wall and oriented to each of the visual cues in a random order. The trial ended when mice reached the hidden platform or when they failed to find the platform within the 60 s. Whenever mice were unable to complete a trial, they were guided to the platform and allowed to stay on it for 20 s. At the fifth day, a probe trial was performed, where the hidden platform was removed from the pool. Mice could explore the pool for 30 s and here the time spent in the previously established platform quadrant was measured. If the mice learned the position of the escape platform, they will spend more time in the quadrant where the platform was hidden before. Escape latencies and distances swum were recorded and further analyzed using EthoVision XT 13.0 (Noldus Information Technology, Netherlands). Swimming patterns were also extracted using Ethovision software and then classified according to Graziano et al. (2003) and as described by Sardinha et al. (2017).

To assess behavior flexibility, a reversal learning task was conducted in the fifth day of the protocol. In this task, the platform was placed in the opposite quadrant as compared to its initial location during the reference memory task. Mice had four trials of 60 s to find the platform in the new quadrant. In the reversal learning task, the time spent, and distance swum in the old and new platform quadrants was measured to evaluate their ability to learn a new rule. All trials were recorded using a video camera and analyzed using EthoVision XT 13.0 (Noldus Information Technology, Netherlands).

3.2.5. Two-trial place recognition task

The Two-Trial Place Recognition (2TPR) task is based on the innate propensity of rodents to explore novel environments and is used to evaluate spatial recognition memory, a form of episodic-like memory (Sardinha et al. 2017). The test was performed in a Y-maze arena composed by three equal arms (33.2 L x 7 W x 15 H cm), made of white Plexiglas, and designated as Start (S), Familiar (F) or Novel (N) arms. At the end of each arm a visual cue was added to allow mice to recognize visited VS. unvisited arms based on their spatial recognition and navigation. In the first trial, mice were placed individually in the S arm and allowed to explore the S and F arms for 5 min. Immediately after, all arms were available and mice were placed again in the S arm and left to explore the maze during 2 min for memory retrieval. If mice retained a memory of the previously explored arms, they will spend more time and travel a higher distance in the novel arm. The test was performed under dim light conditions and the maze was cleaned with 10% ethanol between mice. All trials were recorded using a videocamera and further analyzed using EthoVision XT 13.0 (Noldus Information Technology, Netherlands) software. A Discrimination Index (D.I.) for time and distance in the last third of each arm was calculated using the following equation (1):

$$D.I. = \frac{Novel - \frac{Familiar}{Start}}{Novel + \frac{Familiar}{Start}} \quad (1)$$

Thus, if mice retained memory of previously explored arms and explored more the novel arm, the D.I. will be positive.

3.2.6. Contextual fear conditioning

The Contextual Fear Conditioning (CFC) test was used to evaluate fear memory and associative memory, taking advantage on the ability of rodents to remember and associate an aversive stimulus with a specific environment (Curzon et al. 2009). The CFC test was conducted over 3 days in a sound-attenuated chamber (20 cm x 16 cm x 20.5 cm) (SR-LAB, San Diego Instruments, San Diego, CA, USA) that contained a clear acrylic cylinder with a stainless-steel shock grid and a light bulb mounted above the chamber. In this protocol, apart from the conditioning period, mice were exposed to a context probe and a cue (light) probe, to evaluate freezing behavior (Gu et al. 2012). Freezing is a species-specific response to fear and is defined as a total absence of movement, except for breathing, for a minimum of 1 s. Mice freezing behavior was monitored using a video recording and manually scored using Observador v.2.07 (University of Athens) program.

At day 1, mice were placed in the conditioning white chamber (context A) for 9 min and 30 s. After 2 min and 40 s, the light was turned on and this period co-terminates with a footshock (1 s, ≈ 0.5 mA). These 3 min light-shock pairings were performed for 3 consecutive times. After the last light-shock pairing, mice remained in the chamber for 30 s before being returned to their home cage. The session lasted 9 min and 30 s. To assure that mice presented a fear response, the freezing behavior prior and post-shocks was measured, in the first minute and in the last 30 s of the session, respectively. The acrylic cylinder was cleaned with 10% ethanol between subjects.

At day 2, 24 h after the training period, mice were exposed to a context probe. Mice were placed again in Context A, that mice associate with a light-cued footshock and freezing behavior was measured for 3 min. After this period, mice were returned to their home cage. Two hours later, mice were placed in a novel context (Context B) and freezing behavior was measured for 3 min. The new context had ventilation, a vanilla extract scent and the walls and the floor were covered with black plastic paper. In addition, the experimenter changed his garment to a different pair of gloves and lab coat. Between mice, the cylinder was cleaned with water.

On the last day, corresponding to the cue probe test, mice were placed in the Context B chamber for 3 min. As in day 1, in the last 20 s the light was turned on and mice freezing behavior was measured immediately for 1 min. After 15 s mice were returned to their home cages. At the end of each trial, the cylinder was cleaned with water.

3.3. Molecular analysis

3.3.1. Immunohistochemistry (IHC) analysis

Tissue processing

To confirm that in our mouse model efficient Cre recombination is occurring after the tamoxifen protocol used for administration, in all brain regions and specifically in GLAST-positive (GLAST^{+}) cells, we have used the GLAST-CreER^{T2}-CAG-GFP mice for immunohistological analysis. Here, recombination is also controlled by the GLAST promoter, but the expression of GFP as a reporter gene allows visualization of recombined cells under a fluorescence microscope. Tissue collected from these mice was sectioned and immunoreacted against GFP to strengthen the signal of this protein and allow proper visualization. It is expected that recombination in these mice highly resembles recombination in our GLAST-mGluR5KO, therefore helping to validate the protocol for tamoxifen injection, levels of recombination throughout the

brain. The same way, additional virus-injected mice (dHIPGFAP:mGluR5KO) were used to evaluate effectiveness of the infection in the hippocampus, spreading of the virus within that region and cell specificity. In this case, sections were immunoreacted against the reporter mCherry, therefore allowing proper visualization of infected cells.

For IHC, mice were deeply anesthetized [ketamine (75 mg/kg) and medetomidine (1 mg/kg)] and then perfused with 0.9% saline followed 4% paraformaldehyde (PFA) for tissue fixation. Then, brains were removed and kept in PFA overnight. The following day, tissues were transferred to a solution of 30% sucrose at 4°C, until total impregnation, to avoid water artifacts and to help tissue cryopreservation. Brains from GLAST-CreER^{T2}-CAG-GFP mice were embedded in Neg-50 Frozen Section Medium (ThermoScientific, Thermo Fisher Scientific, Inc., Waltham, MA, USA) and frozen at -20°C, for posterior sectioning in cryostat. Fixed-frozen tissues were cut in 20 μm coronal sections of the entire length of the hippocampus. Sections were collected into different series of 8 sequential slides and maintained at -20°C until the immunohistochemical analysis was performed. Alternatively, fixed brains from dHIP-GFAP-mGluR5KO mice were embedded in agarose 3%, cut in 50 μm sections in a vibratome (Leica CM1900) and collected to 24-well plates for free-floating immunohistochemistry.

IHC assay

Cryostat slides were thawed and dried for 10 min at room temperature (RT) prior to IHC protocol. Both slides and free-floating tissue were firstly washed in PBS and then permeabilized with a 0.3% Triton-X100 (Sigma Aldrich, USA) in PBS (0.3% PBS-T) solution for 10 min. To reduce unspecific bounds, the tissue was incubated with 10% fetal bovine serum (FBS) in 0.3% PBS-T blocking solution for 2 h at RT. Since the tissue was fixed with 4% PFA and to reduce the background, 0.3 M glycine was included in the blocking solution. Glycine will bind to free aldehyde groups that would otherwise bind to the primary and secondary antibodies. This blocking step was followed by the overnight incubation, at 4°C, with the primary antibodies against the reporter proteins goat polyclonal anti-GFP (1:300; Abcam, UK) and chicken polyclonal anti-mCherry, (1:1000; HenBiotech, Portugal) in 2% FBS and 0.3% PBS-T. On the next day, the slices were washed in 0.3% PBS-T and incubated with the respective species-specific secondary antibodies: Alexa Fluor® 488 goat anti-rabbit and Alexa Fluor® 568 goat anti-chicken (1:1000; Invitrogen, ThermoFisher Scientific, USA), in a 0.3% PBS-T solution with 2% FBS, for 1h at RT. After this period, the slices were washed with PBS and the nucleic acids were labeled with 4′,6-diamidino-2-phenylindole (DAPI) (1:2000, Invitrogen, USA) for 10 min at RT. Slices were washed with PBS and then mounted using Immu-mount (ThermoFisher Scientific, USA). All procedures during this day were performed in the dark. Images

were acquired in an Olympus Widefield Upright BX61 microscope (Olympus, Germany) using the 10x and 20x objectives.

3.3.2. Quantitative real-time PCR (qRT-PCR)

Tissue processing

After behavior assessment, GLAST-mGluR5KO and respective littermate controls mice were deeply anesthetized [ketamine (150 mg/kg) and medetomidine (0.3 mg/kg)] for perfusion with 0.9% saline, followed by brain harvesting. Freshly removed tissues were macrodissected to separate the hippocampus from the whole brain, for molecular analysis. The hippocampus was used for Quantitative Real-Time PCR (qRT-PCR) analysis and the remaining brain was used for mGluR5 gene deletion confirmation by PCR.

RNA extraction

Total RNA was extracted from the macrodissected hippocampus by mechanical homogenization, at 4°C, in 1mL of Trizol Reagent (QIAzol Lysis Reagent, Quiagen, Germantown, MD, USA) per 50-100 mg of tissue using a syringe with a 20G needle. After homogenization, the samples were left incubating for 5 min at RT. Then, per 1 mL of Trizol used, 200 µL of chloroform was added to each sample, followed by shacking for 15 s. Next, the samples were centrifuged at 12000 g for 15 min at 4°C to obtain three distinct phases, namely RNA aqueous phase, DNA interphase and organic (DNA and proteins) phase. The aqueous phase was transferred to a new tube and 500 µL of isopropanol were added and left to incubate at RT for 10 min, followed by another centrifugation step at 12000 g and 4°C for 10 min. Subsequently, the supernatant was removed, and the pellet obtained was washed with 1 mL of 75% Ethanol per 1 mL of Trizol used previously. The samples were mixed using a vortex and centrifuged at 7500 g and 4°C for 5 min. Ethanol was removed and the pellet was left to air-dry. Finally, the RNA was dissolved in 20-50 µL of RNase-free water (Sigma) and incubated for 10 min at 60°C, followed by RNA quantification using a nanodrop equipment (NanoDrop ND-1000 Spectrophotometer, ThermoFisher, USA).

cDNA Synthesis

Using a qScript™ cDNA Supermix kit (Quanta Biosciences™, Gaithersburg, Md, USA), 1 µg of RNA was reverse-transcribed into cDNA. For the synthesis of cDNA, 4 µL of qScript cDNA supermix per reaction were used and the volume of RNA for template was normalized with RNase-free water (Sigma) based on

the previous RNA quantification. Reaction mix was performed in a thermal cycler for 5 min at 25°C, 30 min at 42°C and 5 min at 85°C (Table 3).

Table 3 – cDNA mix composition and respective conversion protocol

Reagents	Volume per reaction (µL)	Program
qScript cDNA Supermix	4	25°C – 5 min 42°C – 30 min 85°C – 5 min 4°C – ∞
RNA template	Variable[3]	
RNase-free water	Variable[3]	

[3]Volume of RNA template and RNase-free water used was calculated for each sample depending on total RNA concentration.

qRT-PCR

Quantitative gene expression was assessed by qRT-PCR. Gene expression quantification was performed in an Applied Biosystems 7500 Real-Time PCR System (Applied Biosystems, USA) using a 5x HOT FIREPol® EvaGreen® qPCR Mix Plus, ROX (Solis Biodyne, Estonia). Reaction solution and qRT-PCR protocol used are shown in Table 4. Target gene primers used were designed using PRIMER-BLAST (NCBI, http://www.ncbi.nlm.nih.gov/tools/primer-blast/) and are represented in Table 5.

The housekeeping 18S ribosomal RNA (18S rRNA) gene was used as internal control. The housekeeping 18S ribosomal RNA (*18SrRNA*) gene was used as internal control. The relative gene expression was determined using the $2^{-\Delta\Delta_{Ct}}$ relative quantification method and represented as fold change normalized to the mean of the relative expression for the control group.

Table 4 – qRT-PCR mix composition and respective reaction conditions

Reagent	Volume per reaction (µL)	Program
5x qPCR mix	4	95°C – 15 min 40 cycles of 95°C – 15 s 60°C – 20 s 72°C – 30 s 95°C – 15 s 60°C – 1 min 95°C – 30 s 60°C – 15 s
Primer Forward (20 µM)	0.25	
Primer Reversal (20 µM)	0.25	
H20	14,5	
cDNA	1	

Table 5 – Primers sequences for the genes selected for qRT-PCR

Name	Gene	Primer Sequence 5' – 3'
mGluR5	*Grm5*	F: ATC TGC CTG GGT TAG TTG TG
		R: GCA ATA CGG TTG GTC TTC G
mGluR3	*Grm3*	F: TCG TGG TCT TGG GCT GTT TGT
		R: TGT GCT TGC AGA GGA CTG AGA A
GLAST	*Slc1a3*	F: TGG GCG CCG TGA TCA ACA A
		R: CCA GAC GCG CAT ACC ACA TT
GFAP	*Gfap*	F: AAA CCG CAT CAC CAT TCC TG
		R: TCT GGT GAG CCT GTA TTG GG
IP_3R2	*Itpr2*	F: CTT CCT CTA CAT TGG GGA CAT C
		R: GGG ATA CTT AGC TAT GAG ACG G
18S	*18SrRNA*	F: GGA CCA GAC CGA AAG CAT TTG
		R: TTG CCA GTC GGC ATC GTT TAT

3.4. Statistical analysis

Statistical analysis was performed using the GraphPad Prism software, version 7.04 for Windows (GraphPad software, La Jolla CA, USA), for parametric tests and IBM SPSS Statistics 20 for non-parametric tests. All data passed the Kolmogorov-Smirnov normality test for normal distribution. Statistical outliers were identified using Grubbs' outlier test and excluded from the analysis.

Comparisons between groups ($mGluR5^{fl/fl}$ – GLAST-mGluR5KO and WT – dHIP-GFAP-mGluR5KO) were performed using independent Student's t-test, whereas Two-way analysis of variance (Two-way ANOVA), followed by Sidak *post hoc* analysis was used for multiple comparisons. For the analysis of different strategies used in the MWM, the two-sided Chi-square test was performed. Statistically significant differences were considered when $p<0.05$. Effect size measures (Cohen's d for student's t-test and partial eta squared (η_p^2) for Two-way ANOVA) were calculated. The values are presented as mean ± standard error of the mean (SEM).

4. Results

4.1. The functional impact of astrocytic-specific deletion of mGluR5 in cognitive processing

To study the functional role of astrocytic mGluR5 in cognition, two independent sets of mice (set 1 and set 2) were considered. Mice from set 1, mGluR5$^{fl/fl}$ (n = 14) and GLAST-mGluR5KO (n = 16), were used for behavior characterization, followed by molecular analysis, namely the confirmation of mGluR5 deletion. Mice from set 2, mGluR5$^{fl/fl}$ (n = 10) and GLAST-mGluR5KO (n = 15), were used to confirm the behavioral outcomes previously obtained. To achieve statistically robust data and exclude interference of uncontrolled external factors, behavioral assessment was repeated in different sets of mice, in distinct periods in time. Including more mice is a common strategy to increase data consistency, namely when generating a novel transgenic line.

4.1.1. Validation of the tamoxifen-dependent recombination protocol and confirmation of mGluR5 gene deletion

In order to ablate mGluR5 gene specifically in GLAST^{+} cells of adult mice, a tamoxifen-inducible recombination strategy was used. Hence, tamoxifen was administered to GLAST-CreER^{T2}-mGluR5$^{fl/fl}$ mice, generating the GLAST-mGluR5KO that were used to study the impact of this receptor in behavior (Figure 10A). To validate the efficiency of tamoxifen injections and to assess GLAST-driven expression in the brain, CreER^{T2} mice expressing GFP as a reporter gene under the control of the same promoter (GLAST-CreER^{T2}-CAG-GFP) were also given the drug following the exact same protocol. Briefly, tamoxifen was administered i.p. twice a day for 5 days, followed by an interval of 7 days and then 5 more days of injections (as shown in Figure 10A). Three weeks after the last injection, while GLAST-mGluR5KO mice proceeded for behavioral analysis, GLAST-CreER^{T2}-CAG-GFP mice (n = 2) were sacrificed and brain sections were immunostained against GFP (Figure 10B). Here, we observed a wide expression of GFP throughout the mouse brain (as shown in Figure 10B), which indicates that tamoxifen reached cells efficiently, inducing genetic recombination specifically in astrocytes. Indeed, all GFP-positive cells presented a star-shaped, astrocytic typical morphology while no other cell-specific morphologies were identified.

Finally, to confirm the conditional deletion of the mGluR5 gene in tamoxifen-injected GLAST-mGluR5KO, a tissue-specific genotyping was performed (Figure 10C). Thus, after behavior analysis, both GLAST-mGluR5KO (n = 16) and littermates mGluR5$^{fl/fl}$ (n = 14) mice from set 1 were sacrificed and their brain tissue was processed for the detection of the mGluR5 and CreER^{T2} genes by PCR (Figure 10C). We

observed that all mice presented the unrecombined floxed allele for mGluR5 (270 bp band - Figure 10C1) and that mice that were positive for the CreER^{T2} gene (500 bp band - Figure 10C2) also presented the recombined KO allele where exon 7 from mGluR5 gene is exerted (360 bp band - Figure 10C3). Therefore, these results confirm that only GLAST-mGluR5KO (Figure 10C3) and not their control littermates (Figure 10C1), present the null allele indicating that mGluR5 gene deletion occurred specifically in GLAST-CreER^{T2+} cells, after tamoxifen injection.

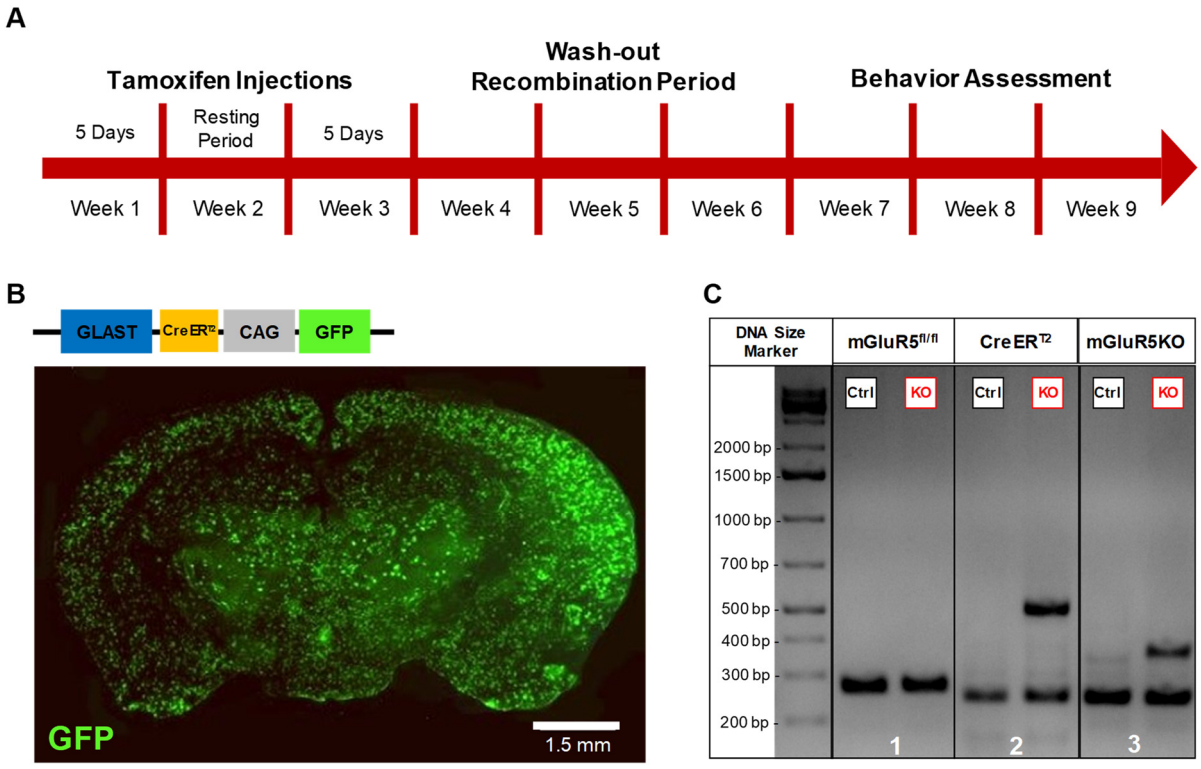

Figure 10 – GLAST promoter-driven expression in the brain and confirmation of mGluR5 gene deletion after tamoxifen injections

(A) Representative timeline used for the *in vivo* study of the role of astrocytic mGluR5 in behavior, from the model induction to behavior assessment. (B) Aligned micrographs (10x objective) of GFP immunostaining in a brain slice from GLAST-CreER^{T2}-CAG-GFP mice previously injected with tamoxifen to induce recombination in GLAST-positive cells, showing GFAP promoter-driven expression throughout the brain. (C) Confirmation of mGluR5 gene deletion after tamoxifen injections using brain tissue from GLAST-mGluR5KO (KO) and mGluR5$^{fl/fl}$ (Control) mice through PCR. (C1) All mice presented the flanked mGluR5 allele (270 bp in C1) and mice that were positive for the CreER^{T2} gene (500 bp band in C2) also exhibited the band for the recombined mGluR5KO allele (without exon 7) at 360 bp (B3), confirming that mGluR5 gene deletion occurred only in GLAST-CreER^{T2}-positive cells. (C2,3) The band at 250 bp (IP$_3$R2 gene) was used as internal control for PCR reaction validation in the case of CreER^{T2}-negative mice. mGluR5$^{fl/fl}$ mice were represented as Ctrl and GLAST-mGluR5KO as KO.

4.1.2. Behavioral characterization of GLAST-mGluR5KO mice

The GLAST-mGluR5KO mice and respective controls performed a battery of tests to assess different behavioral dimensions, such as anxiety, mood and cognition, that could have been affected by the deletion of astrocytic mGluR5. Behavioral assessment was performed in two independent experimental sets (set 1 and set 2) under the same experimental conditions. Thus, mice from both sets were pooled together.

Assessment of anxious- and depressive-like phenotypes upon astrocytic mGluR5 deletion

To understand if the deletion of mGluR5 in astrocytes induces anxious-like phenotypes in adult mice, GLAST-mGluR5KO (n = 31) and control (n = 24) mice were tested in the OF and EPM, that are based in the natural preference of rodents for dark and enclosed places (Figure 11AB). In the OF, we observed that GLAST-mGluR5KO mice and respective controls present a similar percentage of time spent in the center of the arena (t_{53} = 1.20, p = .24, d = .33), number of rearings (t_{53} = 0.026, p = .98, d = .008) and total distance travelled (t_{53} = 0.59, p = .56, d = .16) during the test (Figure 11A). The similarity in the total distance travelled in the arena also show that GLAST-mGluR5KO mice display normal motor function, thus excluding any motor deficits that could compromise their performance in other behavioral tests. Accordingly, the EPM test reveals similar percentages of entries (t_{53} = 0.81, p = 0.42, d = 0.22) and time spent (t_{53} = 1.15, p = .26, d = .32) in open arms between the experimental groups (Figure 11B). Thus, these results indicate that adult mice presenting a deletion of mGluR5 specifically in astrocytes display an exploratory behavior and anxious-like phenotype similar to control littermates.

Furthermore, to assess the impact of mGluR5 deletion in depressive-like behavior, GLAST-mGluR5KO (n = 31) and control (n = 23) mice were tested in the TST (Figure 11C). This test is used to evaluate learned helplessness since rodents tend to stay immobile when exposed to an unavoidable stressful situation. The TST show that mice from both groups stayed immobile for a similar amount of time (t_{52} = 0.91, p = .37, d = .25), during the test. Therefore, ablation of astrocytic mGluR5 does not induce depressive-like behavior.

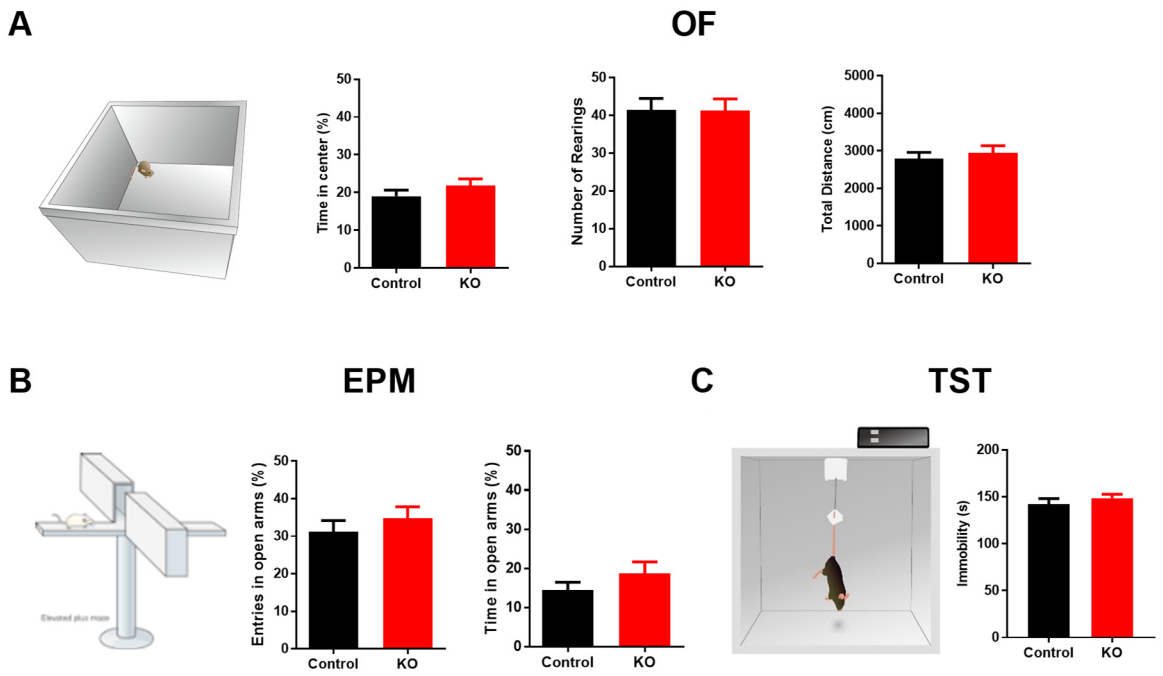

Figure 11 – GLAST-mGluR5KO mice display neither anxious- nor depressive-like behavior

(A) The Open Field (OF) test reveals similar percentage of time spent in the center of the arena, number of rearings and total distance travelled between GLAST-mGluR5KO (n = 31) and mGluR5$^{fl/fl}$ (n = 24) mice. (B) Elevated Plus Maze (EPM) results show that GLAST-mGluR5KO mice (n = 31) display identic percentage of entries and time spent in the open arms when compared to the controls (n = 24). (C) Tail Suspension Test (TST) reveals no differences between groups ($n_{control}$ = 23, $n_{GLAST\text{-}mGluR5KO}$ = 31) regarding immobilization period during the test. Data plotted as mean ± SEM and analyzed using independent t-tests. mGluR5$^{fl/fl}$ mice are plotted in black bars (control) and GLAST-mGluR5KO mice are plotted in red bars (KO).

Assessment of the role of astrocytic mGluR5 for cognitive function

To study if the ablation of mGluR5 in mature astrocytes has an impact in normal cognitive function, GLAST-mGluR5KO mice and respective control littermates were tested in different behavioral paradigms that are highly dependent on the PFC and the hippocampus. For that, we tested mice in spatial reference memory and behavioral flexibility task of the MWM, spatial recognition memory and episodic-like memory task of the Y-Maze 2TPR and contextual fear memory assessed by CFC.

Firstly, GLAST-mGluR5KO (n = 23) and controls (n = 22) were tested in the MWM, which consists of two tasks: one more dependent on the hippocampus (spatial reference memory task) and a second one more dependent on the PFC (reversal learning task) (Figure 12). In the spatial reference memory task, mice had to learn the location of a hidden platform, kept always in the same quadrant, using spatial cues. Our

results show that mice from both experimental groups learned how to find the platform and their performance improved equally [Figure 12A, Escape latency (Interaction: $F_{3, 129} = 0.33$, $p = .81$, $\eta_p^2 = .01$; Days: $F_{3, 129} = 66.2$, $p < .0001$, $\eta_p^2 = .61$; Genotype: $F_{3, 129} = 0.30$, $p = .58$, $\eta_p^2 = .005$), Distance swam (Interaction: $F_{3, 129} = 0.46$, $p = .71$, $\eta_p^2 = .01$); Days: $F_{3, 129} = 40.6$, $p < .0001$, $\eta_p^2 = .49$; Genotype: $F_{3, 129} = 1.27$, $p = .27$, $\eta_p^2 = .02$;]. At the fifth day, mice were submitted to a probe trial when the platform was removed. Here, results reveal that GLAST-mGluR5KO mice spent similar amount of time swimming in the platform quadrant, as compared with their littermate controls ($t_{43} = 0.24$, $p = .81$, d = .07), showing that they equally remember the place where the platform was hidden (Figure 12B). Moreover, analyzing the strategies used to reach the platform during the four days of testing, we observed that mice from both groups used similar percentage of hippocampal-depend strategies (or directed strategies), which is also true for the non-hippocampal-dependent strategies (or random strategies) and failures (no reach) (Figure 12C, $\chi^2(2) = 0.30$, $p = .86$, $\varphi = .08$). Together, these results suggest that deletion of mGluR5 in astrocytes does not seem to affect mice performance in this hippocampal-dependent task, meaning that GLAST-mGluR5KO mice display an intact spatial reference memory. At the fifth day, mice were tested at the reversal learning task, where they had to learn that the platform was placed in a new quadrant, using the same spatial cues. Mice from both groups learned the task, spending more time and swimming higher distances in the new quadrant when compared to the old platform quadrant [Figure 12D, Time spent in the quadrant (Interaction: $F_{1, 43} = 3.51$, $p = .68$, $\eta_p^2 = .08$; Time: $F_{1, 43} = 75.2$, $p < .0001$, $\eta_p^2 = .64$; Genotype: $F_{1, 43} = 4.93$, $p = .032$, $\eta_p^2 = .02$), Distance swum (Interaction: $F_{1, 43} = 2.90$, $p = .096$, $\eta_p^2 = .06$; Distance: $F_{1, 43} = 18.6$, $p < .0001$, $\eta_p^2 = 0.29$; Genotype: $F_{1, 43} = 0.62$, $p = .43$, $\eta_p^2 = .002$)]. Interestingly, GLAST-mGluR5KO mice spent more time in the new quadrant as compared to controls (Figure 12D, $p = .027$), suggesting that the deletion of astrocytic mGluR5 enhanced behavior flexibility. Altogether, these findings show that GLAST-mGluR5KO mice display an intact spatial reference memory, but enhanced behavior flexibility.

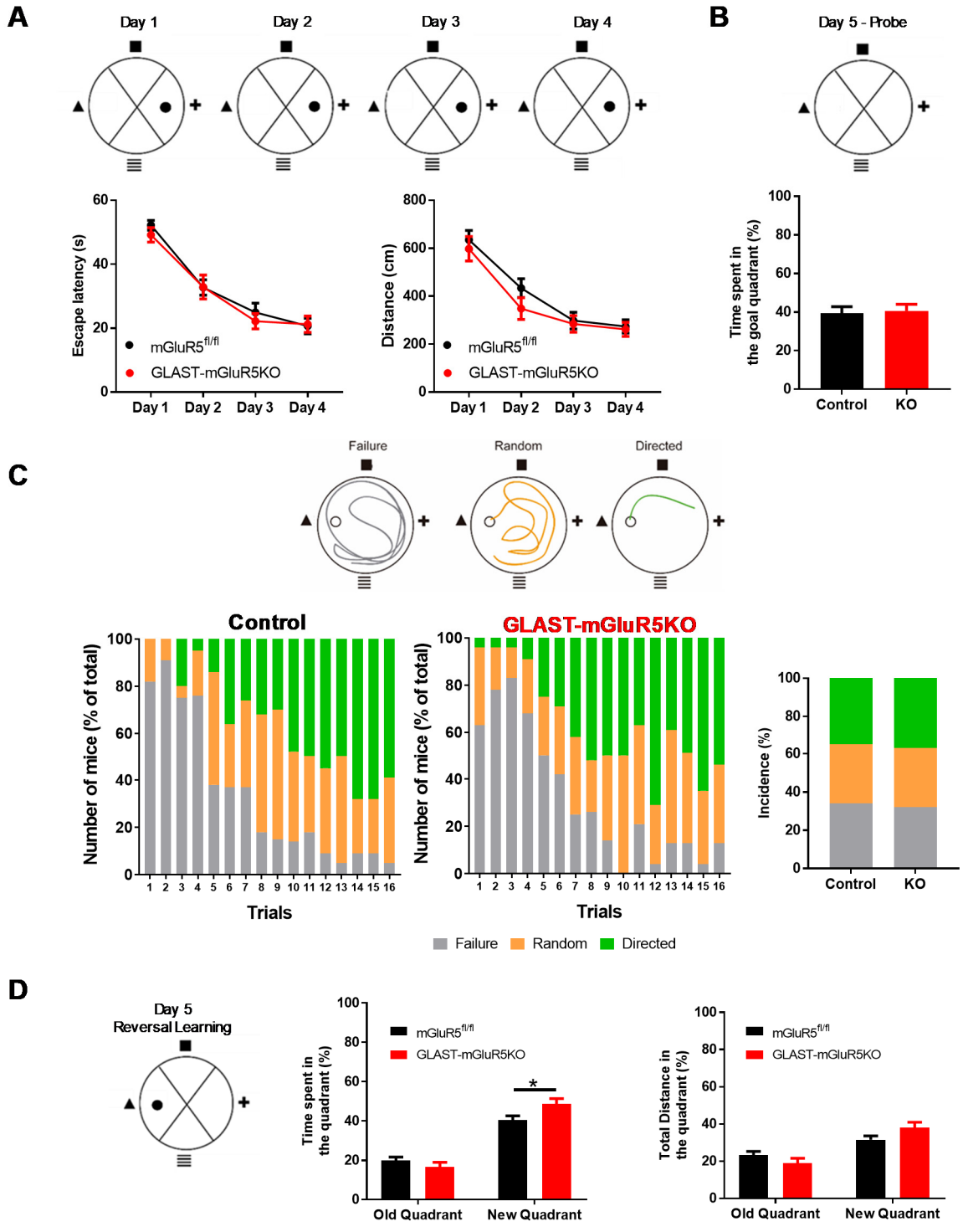

Figure 12 – Ablation of mGluR5 in astrocytes does not affect spatial reference memory, but enhances behavior flexibility in the MWM

(A-C) Spatial reference memory and (D) reversal learning tasks of the Morris Water Maze (MWM) performed by GLAST-mGluR5KO (n = 23) and mGluR5$^{fl/fl}$ (n = 22) mice. (A) Representative task scheme and respective learning curves of escape latency and distance swum showing that mice learned how to find the platform and their performance improved similarly during the four days of test. (B) Probe trial reveals similar percentage of time spent

in the goal quadrant for both experimental groups. (C) Representative scheme of the swim paths. GLAST-mGluR5KO and mGluR5$^{fl/fl}$ mice used similar strategies to reach the platform during the 16 trials of the acquisition task and display a similar proportion of failures, random or directed strategies used to reach the platform for the 4 days of testing. Swimming patterns were classified as failure (gray), random scanning (orange) or directed to the platform (green). (D) Representative scheme for the reversal learning task. GLAST-mGluR5KO mice display higher time spent in the new platform quadrant and similar distance swum when compared to mGluR5$^{fl/fl}$ mice. Data plotted as mean ± SEM and analyzed using (A, D) Two-Way ANOVA, (B) independent t-test and (C) Chi-square test, being * $p < .05$. mGluR5$^{fl/fl}$ mice are plotted in black bars (control in B and D) and GLAST-mGluR5KO mice are plotted in red bars (KO in B and D).

To further explore the role of astrocytic mGluR5 in PFC-dependent tasks, GLAST-mGluR5KO (n = 27) and control (n = 23) mice were tested in the Y-Maze 2TPR test (Figure 13). This test evaluates spatial recognition and episodic-like memory taking advantage on their natural drive to explore novelty. The results obtained show that GLAST-mGluR5KO mice, similarly to the controls, were able to discriminate the novel arm from the previously explored arms, as shown by the D.I. plotted in Figure 13B related to time spent ($t_{48} = 1.21$, $p = .23$, d = .34) and the distance travelled ($t_{48} = 1.32$, $p = .19$, d = .35) exploring the novel arm (Figure 13A,B). Thus, our results show that GLAST-mGluR5KO mice display intact spatial recognition memory and episodic-like memory.

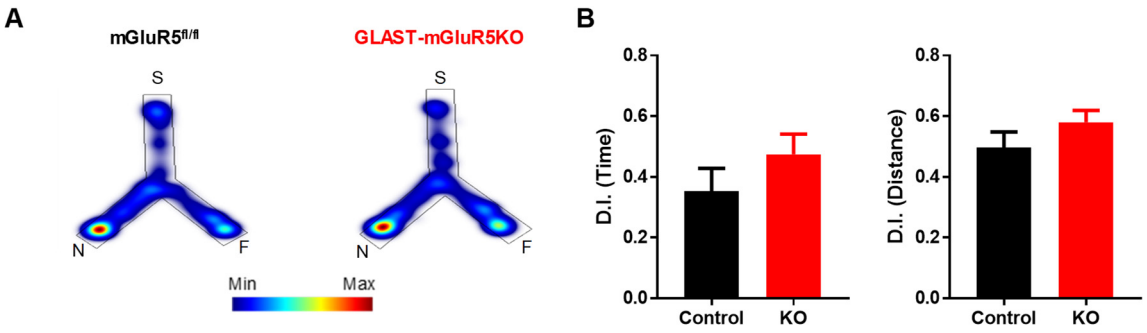

Figure 13 – Deletion of astrocytic mGluR5 does not affect episodic-like spatial recognition memory in a PFC-dependent task

(A) Representative heatmaps of cumulative exploration time in the start (S), familiar (F) and novel (N) arms of the Y-maze for mGluR5$^{fl/fl}$ (n = 23) and GLAST-mGluR5KO (n = 27) mice (cold colors represent less time; warm colors represent more time). (B) Discrimination Index (D.I.) for time spent and distance travelled exploring the novel arm, in comparison to the familiar and start arms, show similar discrimination of the novel arm for mice from both groups. Data plotted as mean ± SEM and analyzed using independent t-tests. mGluR5$^{fl/fl}$ mice are plotted in black bars (control) and GLAST-mGluR5KO mice in red bars (KO).

Finally, GLAST-mGluR5KO (n = 30) and mGluR5$^{fl/fl}$ (n = 24) mice were tested in the CFC test, which evaluates a distinct hippocampal-dependent type of memory, using the ability of mice to remember and associate an aversive stimulus with a specific context. In day 1, after conditioning with 3 light-shock pairings (Figure 14A, Day 1), mice from both genotypes presented a conditioned fear response (Figure 14B). Moreover, a similar baseline activity and freezing response after conditioning was observed in both genotypes (Figure 14B, Interaction: $F_{1, 52} = 0.88$, $p = .35$, $\eta_p^2 = .02$; Time: $F_{1, 52} = 1513$, $p < .0001$, $\eta_p^2 = .97$; Genotype: $F_{1, 52} = 0.73$, $p = .40$, $\eta_p^2 = .02$), discarding any genotype-related alteration in baseline activity. At day 2, mice were exposed again to the same context (Figure 14A, Context A) which showed a significant decrease in the freezing response of GLAST-mGluR5KO mice when compared to their controls (Figure 14C, Context A, $t_{52} = 3.42$, $p = .001$, d = .95). However, when placed in a new context (Figure 14A, Context B), mice from both groups presented similar freezing responses (Figure 14C, Context B,

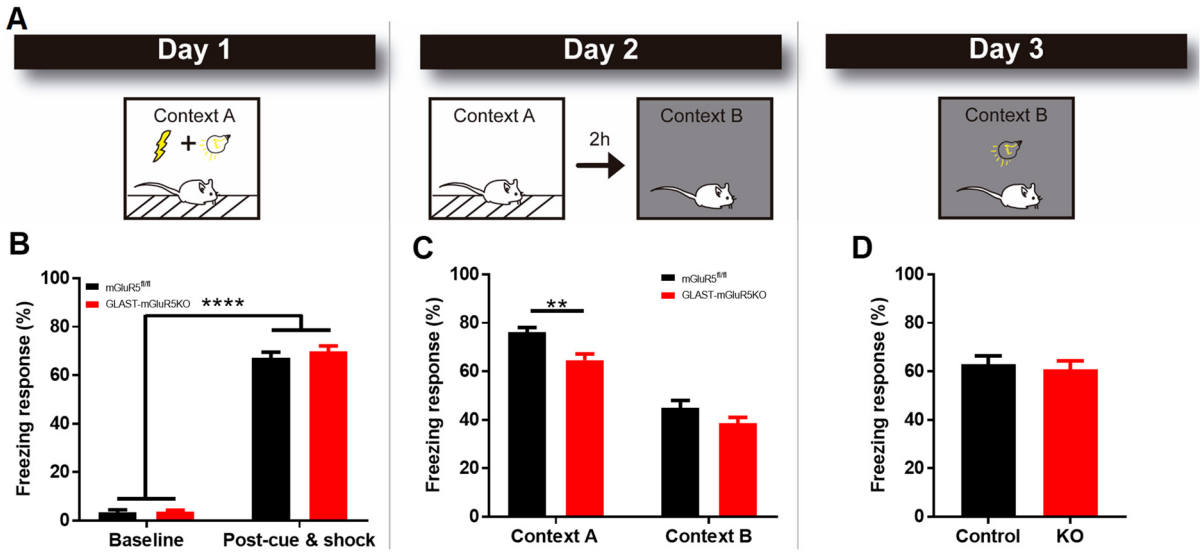

Figure 14 – Deletion of mGluR5 in GLAST-positive cells decreases fear memory

(A) Illustration of the protocol used in the Contextual Fear Conditioning (CFC) to assess fear memory of GLAST-mGluR5KO (n = 30) and mGluR5$^{fl/fl}$ (n = 24) mice (B - D). (B) Freezing response at day 1, before (Baseline) and after conditioning (Post-cue & shock) in context A, showed similar fear conditioning for both genotypes. C) Fear response in Context A showed impaired fear memory in GLAST-mGluR5KO. In Context B, mice from both groups displayed similar percentage of freezing response. (D) Percentage of freezing response in Context B after light stimulus exposure showed similar fear response for GLAST-mGluR5KO mice and littermate controls. Data plotted as mean ± SEM and analyzed using (B) Two-way ANOVA and (C and D) independent t-tests, being * $p < .05$. **** $p < .0001$. mGluR5$^{fl/fl}$ mice are plotted in black bars (control) and GLAST-mGluR5KO mice are plotted in red bars (KO).

t_{52} = 1.12, p = .27, d = .30). At the last day, mice were placed again in the new context, but the light stimulus was turned on (cue probe). Mice from both genotypes displayed similar freezing responses upon light stimulus exposure in a different context (Figure 14D, t_{52} = 0.42, p = .68, d = .12).

4.1.3. Relative expression of specific genes in the hippocampus of GLAST-mGluR5KO mice

Following the behavior assessment, GLAST-mGluR5KO mice and respective littermate controls from set 1 were sacrificed and their brains removed. After macrodissection, the total hippocampus of mice from both groups was used for RNA extraction followed by cDNA synthesis. Then, through a qRT-PCR assay, the relative expression levels of specific genes in GLAST-mGluR5KO (n = 8) and mGluR5$^{fl/fl}$ (n = 14) was assessed. In this assay, we evaluated the expression levels of *Grm5*, our gene of interest (mGluR5), *Grm3*, the other mGluR expressed by astrocytes, *Itpr2* for the IP_3R2 involved in the mGluR5 signaling mechanism in astrocytes, *Slc1a3* that corresponds to the GLAST promoter and important transporter and finally *Gfap* for GFAP, an important structural protein associated with astrocytic morphology (Figure 15). The results show that GLAST-mGluR5KO mice display lower expression levels of *Grm5* (Figure 15A, t_{20} = 3.16, p = .005, d = 1.42) and *Gfap* genes (Figure 15E, t_{20} = 2.78, p = .012, d = 1.17) when compared to mGluR5$^{fl/fl}$ mice. Additionally, similar relative expression levels for the *Grm3* (Figure 15B, t_{20} = 2.05, p = .053, d = .82), *Itpr2* (Figure 15C, t_{20} = 1.81, p = .086, d = .74) and *Slc1a3* (Figure 15D, t_{20} = 3.16, p = .085, d = .77) were observed in both genotypes.

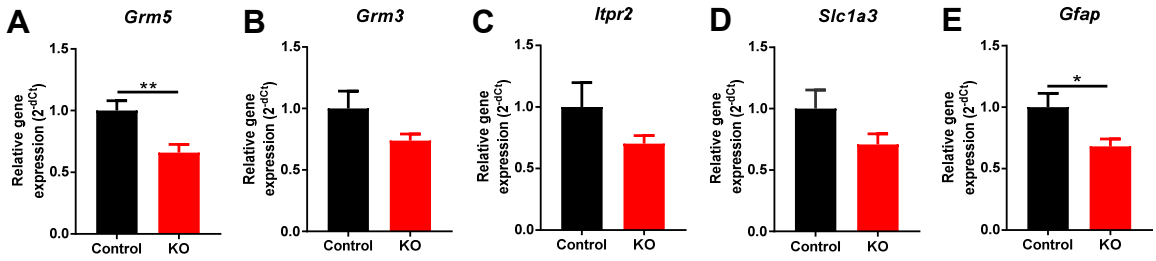

Figure 15 – GLAST-mGluR5 mice display lower expression levels of mGluR5 and GFAP genes

Relative expression of the *Grm5* (mGluR5, A), *Grm3* (mGluR3, B), *Itpr2* (IP_3R2, C), *Slc1a3* (GLAST, D) and *Gfap* (GFAP, E) genes assessed by qRT-PCR. Relative expression levels show a decreased expression of (A) *Grm5* and (E) *Gfap* and similar expression of (B) *Grm3*, (C) *Itpr2* and (D) *Slc1a3* in GLAST-mGluR5KO mice in comparison to mGluR5$^{fl/fl}$ mice. Relative gene expression was calculated using the $2^{-\Delta\Delta Ct}$ relative quantification method and represented as fold change to mGluR5$^{fl/fl}$ control mice. Data plotted as mean ± SEM and analyzed using independent t-tests, being * p < .05. ** p < .01. mGluR5$^{fl/fl}$ mice are plotted in black bars (control) and GLAST-mGluR5KO mice in red bars (KO).

4.2. The functional impact of hippocampus-specific ablation of astrocytic mGluR5 in cognitive function

Using the GLAST-mGluR5KO mice we have shown that deletion of mGluR5 in astrocytes from the whole brain impacts cognitive function. Specifically, these mice displayed impaired fear memory in a hippocampal-dependent task and presented enhanced behavior flexibility in a PFC-dependent test that also integrates a strong spatial memory component, dependent on the dorsal hippocampus. Therefore, we decided to ablate mGluR5 specifically in the hippocampal CA1 region astrocytes of adult mice and characterize their behavior using the same behavioral paradigms and conditions used for the GLAST-mGluR5KO mice.

4.2.1. Validation of the intracranial viral injection in the hippocampus

To study the impact in cognition of mGluR5 ablation specifically in astrocytes of the hippocampus, mGluR5$^{fl/fl}$ mice were bilaterally injected in the dorsal CA1 hippocampal subregion with an AAV5:GFAP-mCherry-Cre (Figure 16A). Three weeks post-injection, dHIP-GFAP-mGluR5KO mice (n = 2) were sacrificed to assess the distribution of infected cells throughout the hippocampus, taking advantage of their particular expression of mCherry reporter protein. After immunostaining against mCherry, to increase the intrinsic fluorescent signal of this reporter, we observed that mCherry-positive (mCherry^{+}) cells were distributed along the CA1 subregion of the hippocampus (Figure 16B,C), confirming the regional cellular infection by the AAV5:GFAP-mCherry-Cre. This labelling was found mostly in the soma of the positive cells, which is in accordance with mCherry cellular compartment location in this Cre-system. Infected cells were distributed mainly throughout CA1 *stratum orients* and *stratum radiatum* layers, however, some infection in the cortex was also observed (Figure 16B,C), namely across the tissue including the needle tract.

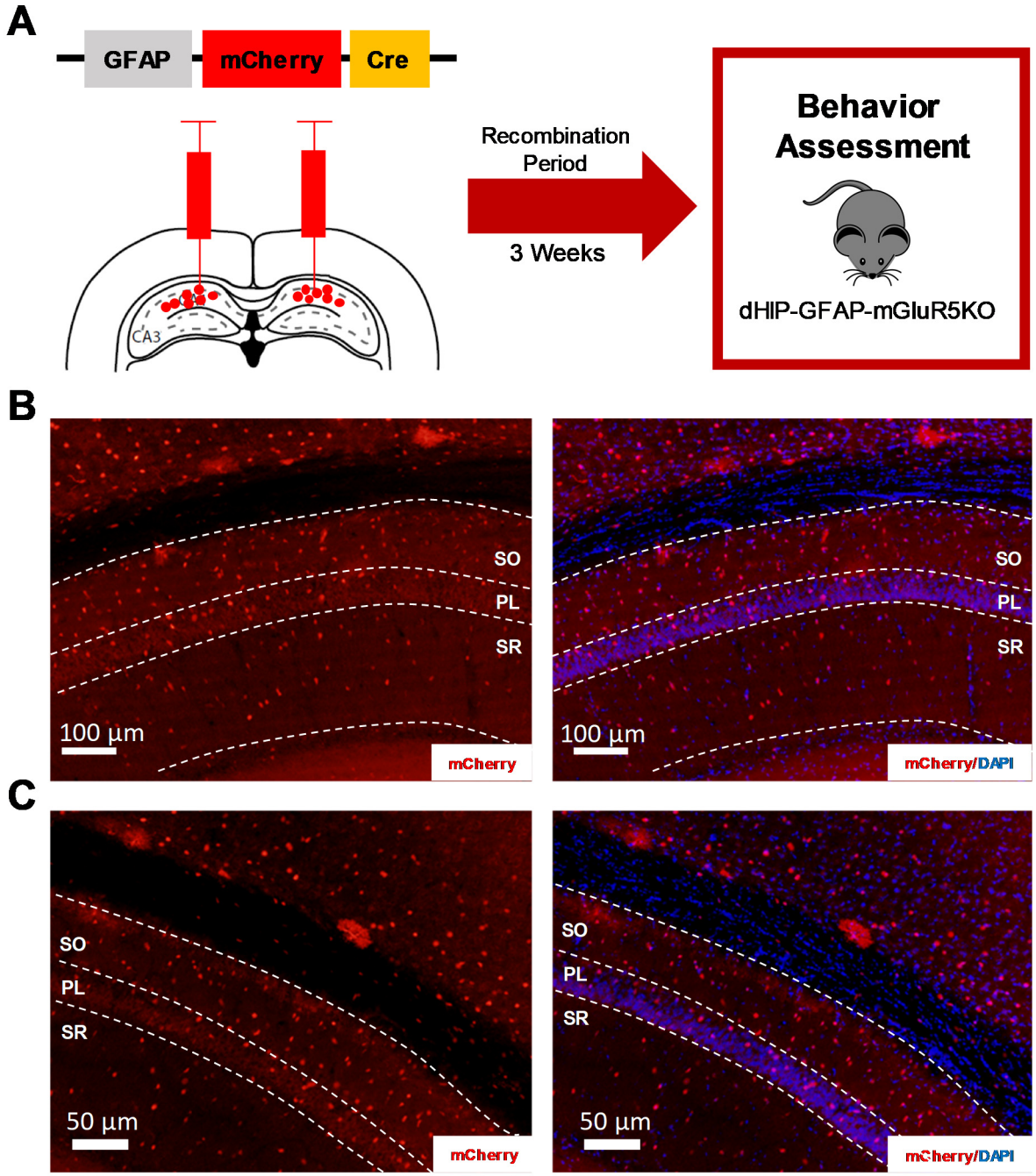

Figure 16 – AAV5:GFAP-mCherry-Cre virus present a well-distributed cellular infection in the CA1 hippocampal subregion

(A) Scheme representing the bilateral stereotaxic injections of AAV5:GFAP-mCherry-Cre virus in the CA1 subregion of the dorsal hippocampus from mGluR5$^{fl/fl}$ and WT mice. (B and C) Anti-mCherry reporter fluorescence (red) and DAPI staining (blue) in the hippocampus, showing the distribution of mCherry-positive cells throughout the CA1 hippocampal subregion, mainly in the *stratum oriens* and *stratum radiatum* layers. Micrographs obtained using the 10x (B) and 20x objectives (C). Scale bars depicted in the images. SO – *stratum oriens*; PL – *stratum pyramidale*; SR – *stratum radiatum*.

4.2.2. Behavioral assessment of dHIP-GFAP-mGluR5 mice

Similarly to the behavior characterization described in 4.1.2, the dHIP-GFAP-mGluR5KO (n = 10) and respective littermate WT (n = 12) mice performed several behavioral tasks to assess the impact of the deletion of mGluR5 in hippocampal astrocytes for anxious- and depressive-like behavior and cognitive function.

Assessment of anxious- and depressive-like behavior after astrocytic mGluR5 ablation in the hippocampus

To assess anxious-like behavior, WT and dHIP-GFAP-mGluR5KO mice were tested in the OF (n_{WT} = 12, $n_{dHIP\text{-}GFAP\text{-}mGluR5KO}$ = 10) and EPM (n_{WT} = 11, $n_{dHIP\text{-}GFAP\text{-}mGluR5KO}$ = 10) tests. The OF results (Figure 17A) showed that mice from both genotypes exhibit identic percentages of time spent in the center (t_{20} = 0.23, p = .82, d = .10), number of rearings (t_{20} = 1.76, p = .094, d = .76) and total distance travelled in the arena (t_{20} = 1.49, p = .15, d = .64). In addition, dHIP-GFAP-mGluR5KO mice also display normal motor function as shown by the total distance travelled (Figure 17A). Moreover, EPM results revealed that the percentage of time spent (t_{19} = 1.35, p = .19, d = .60) and entries (t_{19} = 1.24, p = .23, d = .55) in open arms is similar in mice from both genotypes (Figure 17B). Thus, deletion of astrocytic mGluR5 in the hippocampus neither induced an anxious-like phenotypes in dHIP-GFAP-mGluR5KO mice, nor affected its general exploratory behavior.

Depressive-like behavior in dHIP-GFAP-mGluR5KO (n = 10) and littermate WT (n = 12) mice was assessed by the TST. Our results showed a similar duration of immobility in both groups (Figure 17C, t_{20} = 0.54, p = .59, d = .23), meaning that dHIP-GFAP-mGluR5KO do not display a depressive-like phenotypes.

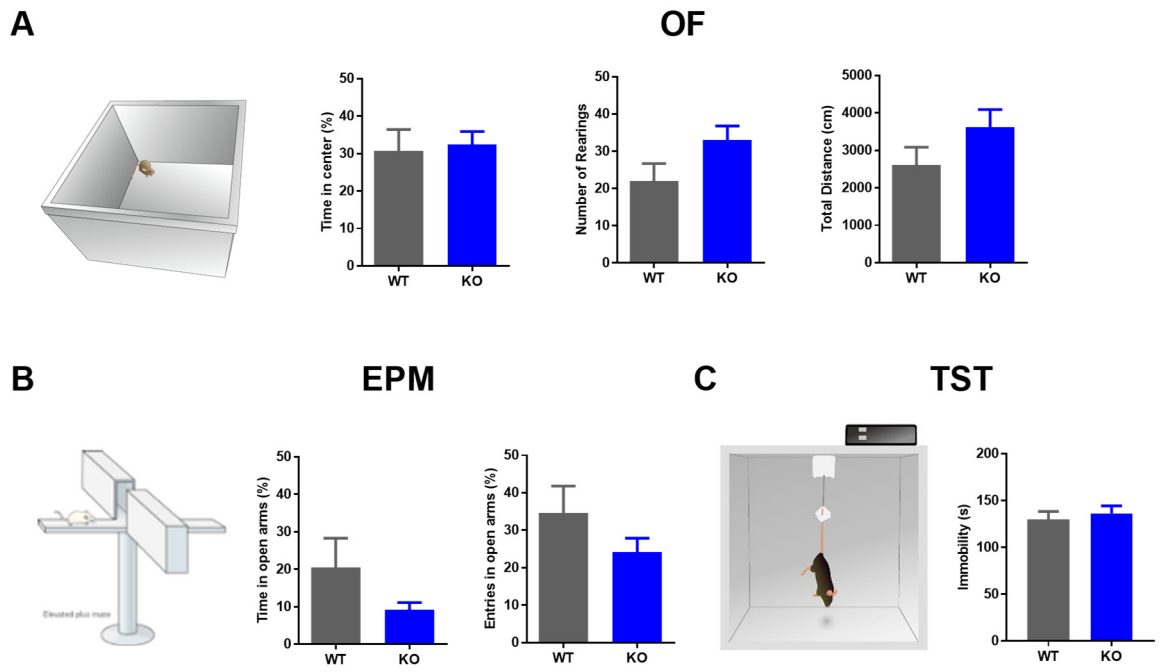

Figure 17 – Ablation of mGluR5 in astrocytes from the hippocampus affects neither anxious- or depressive-like behaviors

(A) Open Field (OF) test showed that WT (n = 12) and dHIP-GFAP-mGluR5KO (n = 10) display similar percentage of time spent in the center of the arena, number of rearings and total distance travelled. (B) Similar percentage of time spent and entries in the open arms of the Elevated Plus Maze (EPM) was observed for WT (n = 11) and dHIP-GFAP-mGluR5KO (n = 10) mice. (C) The Tail Suspension Test (TST) reveals no differences in immobility time between WT (n = 12) and dHIP-GFAP-mGluR5KO (n = 10) mice. Data plotted as mean ± SEM and analyzed using independent t-tests. WT mice are plotted in grey bars and dHIP-GFAP-mGluR5KO mice in blue bars (KO).

Assessment of the impact of astrocytic mGluR5 ablation in the hippocampus for cognition

To assess how the ablation of mGluR5 in hippocampal astrocytes affected cognitive function, dHIP-GFAP-mGluR5KO mice performed the MWM, Y-Maze 2TPR and CFC.

The MWM was used to assess spatial reference memory and behavior flexibility, as previously described for GLAST-mGluR5KO mice. At the spatial reference memory task, our results showed that WT (n = 12) and dHIP-GFAP-mGluR5KO (n = 9) mice learned the task and through the 4 days of testing they exhibited similar performance improvements in finding the platform (Figure 18A, Escape latency (Interaction: $F_{3, 57} = 1.50$, $p = .22$, $\eta_p^2 = .07$; Days: $F_{3, 57} = 58.6$, $p < .0001$, $\eta_p^2 = .76$; Genotype: $F_{3, 57} = 0.47$, $p = .50$, $\eta_p^2 = .003$), Distance swam (Interaction: $F_{3, 57} = 0.59$, $p = .63$, $\eta_p^2 = .03$; Days: $F_{3, 129} = 54.9$, $p < .0001$, $\eta_p^2 = .74$; Genotype: $F_{3, 1.61} = 1.61$, $p = .22$, $\eta_p^2 = .04$)]. At the fifth day, the probe trial confirmed these

results, showing that both experimental groups equally remembered where the platform was hidden as they spent the same amount of time in the goal-quadrant (Figure 18B, $t_{19} = 0.52$, $p = .61$, d = .23). Furthermore, mice of both genotypes displayed similar percentage of directed and random strategies used to reach the platform during the 4 days as well as a similar percentage of failures (Figure 18C, $\chi^2(2) = 0.25$, $p = .88$, $\varphi = .11$). Results from the reversal learning task, performed at the fifth day, show that dHIP-GFAP-mGluR5 mice had more difficulty performing this task when compared to the WT mice [Figure 18D, Time spent in the quadrant: (Interaction: $F_{1, 19} = 8.56$, $p = .009$, $\eta_p^2 = .81$; Time: $F_{1, 19} = 4.88$, $p = .04$, $\eta_p^2 = .20$; Genotype: $F_{1, 19} = 0.42$, $p = .52$, $\eta_p^2 = .01$) Distance swum: (Interaction: $F_{1, 19} = 13.4$, $p = .002$, $\eta_p^2 = .41$; Distance: $F_{1, 19} = 0.089$, $p = .77$, $\eta_p^2 = .005$; Genotype: $F_{1, 19} = 2.43$, $p = .14$, $\eta_p^2 = .04$). In fact, WT mice spent more time ($p = .002$) and swum higher distances ($p < .04$) in the new platform quadrant as compared to the old one, however, dHIP-GFAP-mGluR5 spent the same amount of time swimming in both quadrants ($p = .87$) even though they swum longer distances in the old one ($p = .03$). Moreover, *post-hoc* comparisons between groups show that dHIP-GFAP-mGluR5KO mice have spent less time swimming in the new quadrant when compared to their WT littermates (Figure 18D, $p = .01$). Regarding distance swum (Figure 18D), dHIP-GFAP-mGluR5KO mice travelled larger distances in the old quadrant (p = 0.04) than WT mice and less in the new (p = 0.0006). Thus, dHIP-GFAP-mGluR5 have normal spatial reference memory but display impairments in behavior flexibility in the MWM.

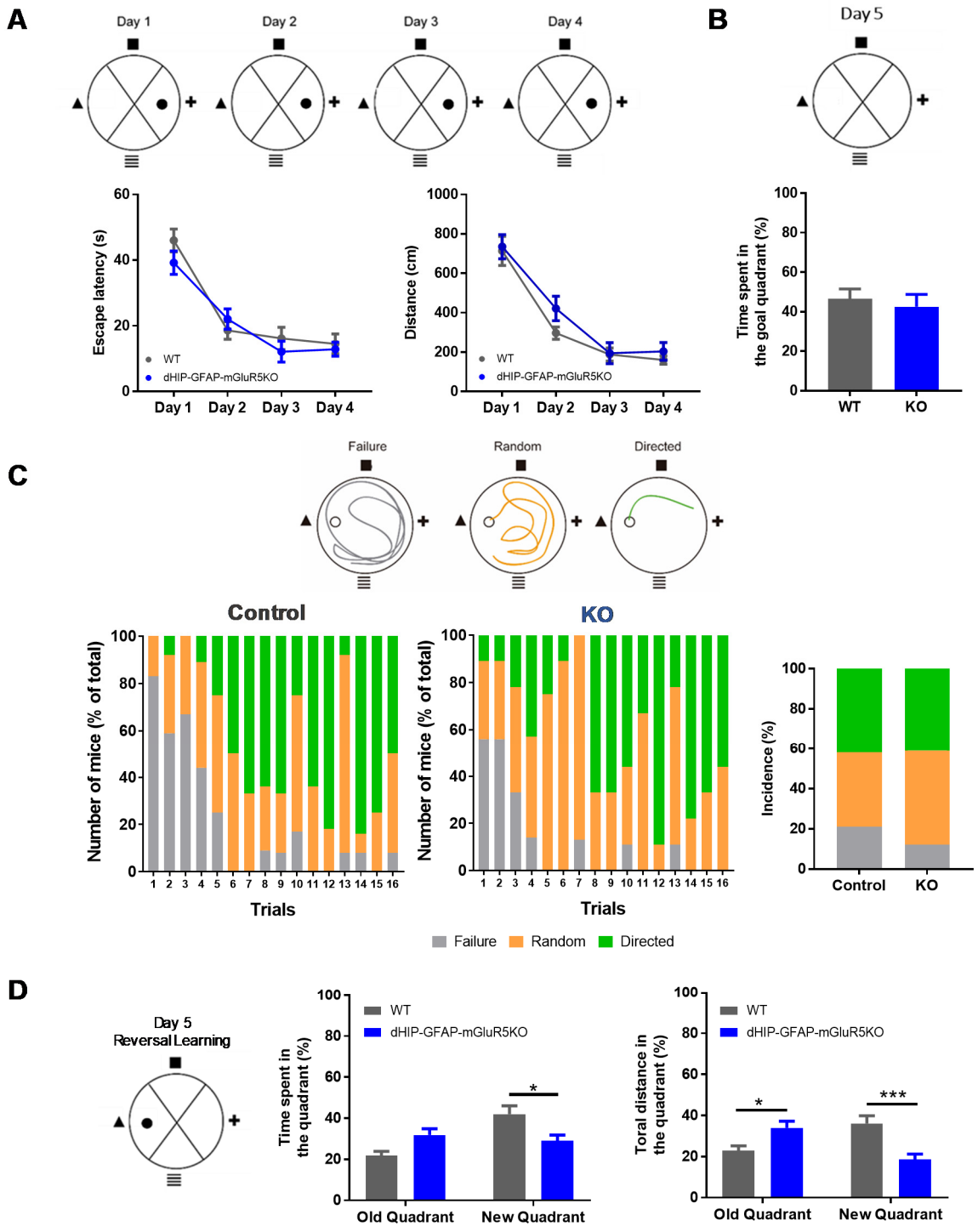

Figure 18 – dHIP-GFAP-mGluR5 mice display normal spatial reference memory, but impaired behavior flexibility in the MWM

(A-C) Spatial reference memory and (D) reversal learning tasks of the Morris Water Maze (MWM) performed by WT (n = 12) and dHIP-GFAP-mGluR5KO (n = 9). (A) Illustrative reference memory task scheme and respective learning curves of escape latency and distance swum showing similar learning patterns during the four days of test for mice

from both experimental groups. (B) Probe trial show that dHIP-GFAP.mGluR5KO and WT mice display similar percentages of time spent in the goal quadrant. (C) Representation of strategies used to reach the platform. A similar proportion of failures, random or directed strategies used to perform the task during the 4 days of testing was observed in both groups. Swimming patterns were classified as failure (gray), random scanning (orange) or directed to the platform (green). (D) Illustration of the reversal learning task. dHIP-GFAP-mGluR5KO mice display less time spent and distance swum in the new platform quadrant and more distance swum in the new quadrant when compared to WT mice. Data plotted as mean ± SEM and analyzed using (A, D) Two-Way ANOVA, (B) independent t-test and (C) Chi-square test, being * $p < .05$ and *** $p < .001$. WT mice are plotted in dark-grey bars (B and D) and dHIP-GFAP-mGluR5KO mice are plotted in blue bars (KO in B and D).

Episodic-like and spatial recognition memory of dHIP-GFAP-mGluR5KO (n = 9) and WT littermates (n = 9) mice was assessed by the Y-Maze 2TPR test (Figure 19). Data revealed that mice from both groups spent similar time ($t_{16} = 0.99$, $p = .33$, d = .49) and travelled similar distances ($t_{16} = 0.82$, $p = .43$, d = .40) in the novel arm when compared to the other arms, as shown by the D.I. (Figure 19B). Thus, dHIP-GFAP-mGluR5KO mice display an intact episodic-like and spatial recognition memory.

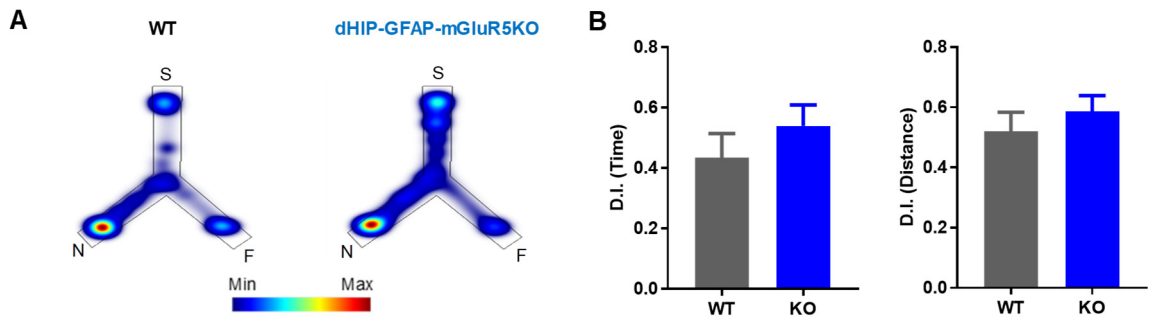

Figure 19 – Ablation of mGluR5 in hippocampal astrocytes does not affect episodic-like and spatial recognition memory

(A) Representative heatmaps of cumulative time exploration in the start (S), familiar (F) and novel (N) arms of the Y-maze for WT (n = 9) and dHIP-GFAP-mGluR5KO (n = 9) mice (cold colors represent less time; warm colors represent more time). (B) Time spent and distance travelled exploring the novel arm, presented as Discrimination Index (D.I.) show similar discrimination of the novel arm for mice from both genotypes. Data plotted as mean ± SEM and analyzed using independent t-tests. WT mice are plotted in grey bars and dHIP-GFAP-mGluR5KO mice in blue bars (KO).

The CFC test was used to assess contextual fear memory of dHIP-GFAP-mGluR5KO (n = 10) and WT (n = 12) mice (Figure 20). At day 1, conditioning day (Figure 20A), mice from both genotypes not only presented similar baseline activity, but they also have shown similar freezing response after conditioning (Figure 20B ,Interaction: $F_{1, 20} = 0.19$, $p = .66$, $\eta_p^2 = .01$; Time: $F_{1, 20} = 760.5$, $p < .0001$, $\eta_p^2 = .97$; Genotype: $F_{1, 20} = 0.73$, $p = .40$, $\eta_p^2 = .02$). At day 2, dHIP-GFAP-mGluR5KO and WT mice presented similar fear responses when placed in the conditioning context (Figure 20C, Context A, $t_{20} = 0.82$, $p = .42$, d = .35) and also when exposed to a new context (Figure 20C, Context B, $t_{20} = 0.30$, $p = .77$, d = .13). Furthermore, in the last day, mice from both groups presented similar freezing percentages in response to the light stimulus presentation in the new context. In summary, ablation of astrocytic mGluR5 in the hippocampus of dHIP-GFAP-mGluR5KO mice did not affect fear memory.

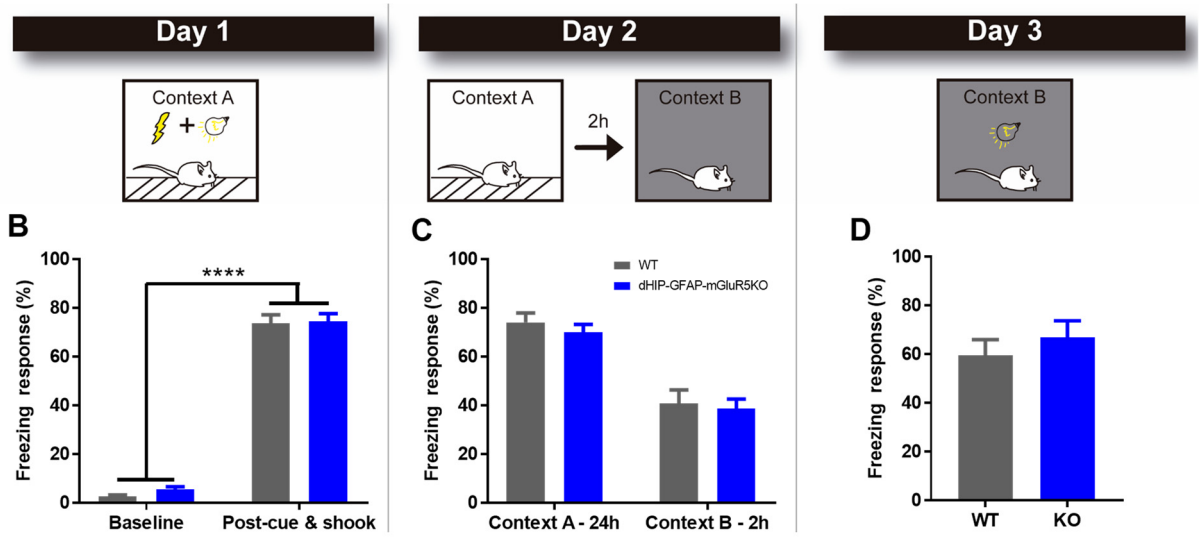

Figure 20 - Contextual fear memory is intact upon astrocytic mGluR5 deletion in the hippocampus

A) Illustrative scheme of the protocol used to study Contextual Fear Conditioning (CFC) in WT (n = 12) and dHIP-GFAP-mGluR5KO (n = 10) mice (B - D). (B) Freezing response at day 1, before (Baseline) and after conditioning (Post-cue & shock) in Context A show similar conditioned fear responses in mice from both groups. C) Fear response in the conditioning Context A and in the new Context B was similar for mice from both groups. (D) dHIP-GFAP-mGluR5KO mice and littermate WT also displayed similar freezing percentages of freezing response in the Context B after light stimulus exposure. Data plotted as mean ± SEM and analyzed using (B) Two-way ANOVA and (C and D) independent t-tests, being **** $p < .0001$. WT mice are plotted in grey bars and dHIP-GFAP-mGluR5KO mice are plotted in blue bars (KO).

5. Discussion

For the past decades, astrocytes have emerged as key players in cognitive processing mainly in learning and memory. These processes are dependent in the PFC and hippocampus, cortico-limbic areas where glutamate is the main excitatory neurotransmitter (Gibbs et al. 2008; Oliveira et al. 2015; Santello et al. 2019). Astrocytes are able to sense glutamate in the synaptic cleft since they express several receptors for this transmitter. Throughout the years, several studies have shown that astrocytic activation by glutamate is mostly mediated by mGluRs, namely mGluR5. Upon mGluR5 activation, astrocytes present intracellular calcium elevations that trigger a cascade of events that will result in gliotransmitters release and ultimately modulate the synaptic activity (Porter and McCarthy 1995, 1996; Latour et al. 2001; Wang et al. 2006; Panatier et al. 2011; Honsek et al. 2012; Panatier and Robitaille 2016). Despite these clear evidences on the importance of mGluR5 in astrocytic functions, the studies focusing on the role of astrocytic mGluR5 in basal conditions were performed mainly in astrocytic cultures or hippocampal brain slices from young rodents. Thus, studies to disclose the role of astrocytic mGluR5 *in vivo*, mainly in adulthood, were needed to understand their role after developmental stages. Therefore, in this dissertation we aimed at exploring the role of astrocytic mGluR5 in behavior of adult mice, mainly in cognition. To achieve our goal, we have successfully generated two mouse models lacking mGluR5 specifically in astrocytes, either in the whole brain (GLAST-mGluR5KO mice) or affecting specifically hippocampal astrocytes (dHIP-GFAP-mGluR5KO). In both models, mGluR5 deletion was temporally controlled to be triggered only in adulthood. A detailed behavior assessment showed that mice from both genotypes display normal locomotor activity, and neither anxious- nor depressive-like behavior. The GLAST-mGluR5KO mice also performed normally in spatial recognition memory and spatial reference memory tasks, but interestingly they presented enhanced behavior flexibility. Curiously, these same mice presented an impairment in fear memory. Molecular analysis on these mice showed decreased levels of expression of the GFAP gene that could be associated with astrocytes atrophy. On the other hand, the dHIP-GFAP-mGluR5KO mice displayed normal spatial recognition memory, spatial reference memory and fear memory but in this case impaired behavior flexibility. All together our results suggest that mGluR5 is important for cognition and its role could be regional specific, as shown by the different results in the same tests for both mouse models. We will now discuss several issues that justify our findings in the existing literature.

Astrocyte promoters and the regional specificity

As explained above, we have generated a mouse model lacking mGluR5 in astrocytes generally in the brain, using a tamoxifen-dependent Cre recombinase form (CreER^{T2}), and a mouse model where mGluR5 deletion was induced only in hippocampal astrocytes, achieved by intracranial injection of a Cre recombinase virus in this region. In both models we took advantage of the Cre-LoxP recombination system which has been considered a powerful tool in studies aiming to elucidate the biological function of specific genes, in specific cell populations as astrocytes. This cell-specificity is guaranteed by the use of promoters, that in this case control the expression of Cre recombinase enzyme. Indeed, the Cre-LoxP system recombination is directly related with the expression of the associated promoter, in specific brain regions (Slezak et al. 2007; Li et al. 2013). Thus, the promoter used should be selected carefully taking that in consideration. Our choice in using two different astrocytic promoters for the control of the Cre recombinase expression was based on the expression of the promoters in the brain, taking also into account the available CreER^{T2} mouse lines and viral constructs. Due to that, for the ablation of mGluR5 in astrocytes from the whole brain, we used the GLAST promoter expressing the CreER^{T2} recombinase (GLAST-mGluR5KO mice). The GLAST-CreER^{T2} was shown by others to be widely expressed in astrocytes throughout the brain, being detected in several brain regions as cortex, hippocampus and cerebellum (Slezak et al. 2007). In fact, we showed that GFP expression, under the control of a similar GLAST-CreER^{T2} promoter (in GLAST-CreER^{T2}-CAG-GFP mice), is expressed in the hippocampus and in the cortex of young adult mice, mostly in cells with typical astrocytic morphology. Since our GLAST-mGluR5KO mouse does not have a fluorescent reporter gene, the same confirmation was not possible for our model. Nevertheless, very similar patterns of expression of Cre recombinase are expected as both experiments were performed using the same GLAST-CreER^{T2} construct. Also due to the lack of a reporter gene in GLAST-mGluR5KO mice, we could not identify recombined cells by immunohistochemistry and use colocalization with different cell markers to assess levels of astrocytic specificity. Indeed, it is true that, during neurogenesis, some GLAST^{+} RG cells from the subventricular zone or DG may give rise to new neurons (Mori et al. 2006). However, by using the tamoxifen-dependent approach, starting injections in young adult mice where neurogenesis is dramatically decreased (Smith and Semënov 2019), we considerably reduce the chance of affecting other cells rather than astrocytes. To note that, in the case of GLAST-CreER^{T2} systems, others have extensively explored the high specify of the promoter for astrocytes, especially in the case of tamoxifen-induction in adult mice. For all these reasons, the GLAST-CreER^{T2} mouse line (already available in our animal facility) appeared as a good choice to tackle the main goal of this dissertation.

For the deletion of mGluR5 specifically in astrocytes from the hippocampus (in dHIP-GFAP-mGluR5KO mice), we have used the commercially available rAAV5:GFAP-mCherry-Cre virus, where Cre recombinase expression is controlled by the GFAP promoter. Almost all astrocytes from the hippocampus express detectable levels of GFAP (Ogata and Kosaka 2002), which is the main reason why several viral approaches targeting the hippocampal astrocytes use this promoter. However, GFAP is also present in RG cells from the DG that, as mentioned for GLAST, may generate either neurons or astrocytes (Mori et al. 2006). In this particular approach tough, differently from the tamoxifen-dependent system, by controlling the site of injection we were able to avoid infection in the DG where RG cells are located, therefore preventing the possibility of genetic recombination in these cells. Moreover, the specific use of rAVV5 serotype also provided an additional cell- and layer-specific tropism in the hippocampus (Aschauer et al. 2013). Indeed, in a pilot experiment we observed recombined cells mainly in CA1 region (local of injection in the dorsal hippocampus), specifically in the *stratum oriens* and *stratum radiatum* layers. Contrarily to GLAST-mGluR5KO mice, here we can also take advantage of the fluorescent mCherry reporter gene, expressed only in recombined cells, to assess astrocyte-specific infection as soon as we proceed for molecular and histological analysis of the brain tissues from dHIP-GFAP-mGluR5KO.

Relevance of astrocytic mGluR5 in adulthood

Besides, the cell and region-specificity discussed above, by using both an inducible form of Cre recombinase and a viral approach, we were also able to temporally control gene recombination and therefore induce deletion of mGluR5 at a very specific moment in the life of the mice (Casper et al. 2007; Slezak et al. 2007; Pfrieger and Slezak 2012; Davila et al. 2013; Li et al. 2013). This temporal control allowed us to avoid any compensatory mechanisms or drastic developmental consequences (Casper et al. 2007; Slezak et al. 2007; Pfrieger and Slezak 2012; Davila et al. 2013; Li et al. 2013), but more importantly, it allowed the deletion of mGluR5 in adult mice when expression of the receptor is already assumed to be low in astrocytes (Sun et al. 2013; Morel et al. 2014). This is extremely important as this represents the novelty of our studies and the main point of this project which is to provide evidence that this low expression in adulthood is still biological relevant, especially in cognition. When we look into the literature, many studies report that astrocytic mGluR5 expression is regulated during development, meaning that mGluR5 is highly expressed by astrocytes during the post-natal development and its expression decreased in adulthood (Schools and Kimelberg 1999; Cai et al. 2000; Sun et al. 2013; Morel et al. 2014). However, the studies reporting these findings are still controversial. Sun and colleagues (2013) showed that 1-week old mice presented highly mGluR5 mRNAs expression levels in cortical and

hippocampal astrocytes, while after the second week levels of astrocytic mGluR5 start to decrease until adulthood when the expression levels are considered to be minimal. In contrast, another study showed that cortical astrocytes present increased mGluR5 expression from P7-21 mice but decreased levels in P40 mice (Morel et al. 2014). The major difference between the approach used in these studies is that Sun and colleagues (2013) used the total mRNA to infer mGluR5 expression, whereas in the study of Morel et al. (2014), they only used the translating mGluR5 mRNA associated with ribosomes, that is the mRNA being actually translated. Thus, despite the decreasing levels of total mRNA of mGluR5 throughout development, mRNA from this receptor is being more translated in later stages of post-natal development. Accordingly, even though expression levels of astrocytic mGluR5 in adulthood point to a minimal expression of these receptor (Sun et al. 2013; Morel et al. 2014), it is still controversial whether the receptor maintains its biological relevance (Panatier and Robitaille 2016), since it is still expressed by astrocytes that cover highly active glutamatergic synapses. Thus, the physiological activity of this receptor in astrocytes should be further explored. Indeed, a good example of a similar scenario is the case of CB1R in astrocytes. These receptors are highly expressed by several types of cells in the brain, but in astrocytes they exhibit lower expression levels. Nevertheless, astrocytic CB1R are still highly involved in modulation of brain functions, as processes of learning and memory (Han et al. 2012; Metna-Laurent and Marsicano 2015; Robin et al. 2018). Hence, we hypothesize that, despite its lower expression in adulthood, astrocytic mGluR5 might also be important for modulation of neuronal activity which might have implications in complex brain functions such as cognition.

Involvement of astrocytic mGluR5 in cognition

In this dissertation, it has been shown that GLAST-mGluR5KO mice display normal spatial reference memory but enhanced behavior flexibility in the MWM. The improved performance in the reversal learning task of the MWM suggests that GLAST-mGluR5KO mice were able to switch faster between the old to new paradigm in the MWM, meaning that they adapted better to the new conditions. This reversal learning task is mainly dependent in the PFC, but the hippocampus is also involved since it is dependent on the spatial cues. Thus, our results suggest that activation of astrocytes by mGluR5 in the PFC and hippocampus is important for the modulation of behavior flexibility during the reversal learning task. It seems that astrocyte activation and further modulation of synaptic activity associated with the performance of this task is important for the maintenance of previously acquired memories. One possible mechanism underlying this effect may be related to changes in synaptic plasticity. In fact, several studies have shown that impairments in hippocampal LTD are associated with deficits in mice performance in

the reversal learning task of the MWM (Nicholls et al. 2008; Dong et al. 2013; Mills et al. 2014). The previously mentioned studies suggest that LTD is involved in the elimination of previously acquired memories when new information is learned, which is important for behavioral flexibility (Nicholls et al. 2008; Dong et al. 2013; Mills et al. 2014). Accordingly, Dong and colleagues (2015) reported that AMPA receptor endocytosis, important for LTD induction, is needed for the decay of LTP and normal loss of long-term memories. Thus, altogether these studies reveal a relation between LTD induction and memory elimination, what is crucial for the performance of mice in the reversal learning task. Furthermore, it has been shown that astrocytes are also involved in the induction of LTP (Henneberger et al. 2010) and LTD (Navarrete et al. 2019; Pinto-Duarte et al. 2019). Therefore, we hypothesize that mGluR5 is required to trigger the astrocytic modulation of synaptic plasticity involved in behavior flexibility.

On the other hand, by assessing fear memory using the CFC, we showed that mGluR5 ablation in astrocytes is important for fear memory as well. Performance in the CFC requires mainly three brain regions, the amygdala, the hippocampus and the PFC. In addition, in fear conditioning the PFC and hippocampus are involved in the formation and regulation of fear memory (Gilmartin et al. 2014). Our results showed that GLAST-mGluR5KO mice display normal fear memory acquisition and when exposed again, 24 h after conditioning, to the context where they were previously shocked, mice display impaired fear memory. However, they were able to distinguish contexts and to associate the light stimulus with an aversive outcome. The results suggest that deletion of mGluR5 in astrocytes of GLAST-mGluR5KO mice results in impaired expression of recently learned fears. The PFC, mainly the mPFC, has risen as a key player in fear memory formation and expression of learned fear (Corcoran and Quirk 2007; Quinn et al. 2008). Corcoran and colleagues (2007) showed that impairments in the mPFC after fear memory acquisition are associated with the prevention of learned fear expression 1 day after the conditioning. Thus, our findings and the literature suggest that astrocytes activation mediated by mGluR5 in the PFC is important for recent memory recall in the CFC. However, when interpreting these results, we should have in mind that mice were able to recall fear memories associated with context and light stimulus. Thus, it is possible that GLAST-mGluR5KO mice have a normal expression of learned fears and other mechanism could be responsible for the decreased freezing response observed. In our CFC protocol, mice were able to associate an aversive outcome with a light stimulus and a context, memories that mice were able to recall. So, when exposed to the conditioning context, it is likely that mice are expecting the light stimulus followed by the foot-shock, what does not happen in the day after conditioning. This might suggest that GLAST-mGluR5KO mice were able to recognize faster that the paradigm was different. Nevertheless, confirmation of this hypothesis would only be possible by performing fear extinction tests,

meaning repetition of these tasks along the following days/weeks. Noteworthy, a study focusing on the role of mGluR5 in neurons, showed that knocking down the mGluR5 gene in these cells induced impairments in fear memory acquisition and presented both mild deficits in the spatial reference memory task of the MWM and impaired behavior flexibility (Xu et al. 2009). As we observed the exact opposite phenotype as a consequence of mGluR5 deletion in astrocytes in GLAST-mGluR5KO mice (intact memory acquisition in CFC and MWM and enhanced behavior flexibility in MWM), we discard the interference of possible non-specific ablation of this receptor in neurons. Indeed, even if a few GLAST^{+} recombined cells generated mGluR5KO neurons during neurogenesis, this was not enough to influence our behavioral readouts. In conclusion, also our results from CFC, showing a decreased freezing response to an aversive context in GLAST-mGluR5KO mice (probably due to higher flexibility/adaptation to new paradigms), strengthens our hypothesizes that LTD might be induced in these mice. In fact, it has been shown that astrocytes are also involved in the modulation of LTD with clear consequences for fear memory (Navarrete et al. 2019; Pinto-Duarte et al. 2019). Navarrete and colleagues (2019) suggest that impairments in hippocampal LTD enhanced long-term memory. The authors showed that impairing LTD by affecting astrocytes normal function in the hippocampus after fear memory acquisition prolongates fear memory retention in the CFC test, 30 days after the conditioning (Navarrete et al. 2019).

The molecular underpinnings of astrocytic mGluR5 involvement in behavior

Following behavior, molecular analysis of the hippocampus from GLAST-mGluR5KO mice, not only confirmed downregulation of mGluR5 but also revealed that GFAP mRNA levels were decreased. To note that, since qPCR analysis was done in the whole hippocampus and neurons have high expression of this receptor, detecting this decrease in mRNA levels of mGluR5 is remarkable. However, in order to confirm that mGluR5 KO occurred exclusively in astrocytes and to quantify levels of know-down for each mouse, cell sorting of both astrocytic and neuronal fractions is planned for a near future. Meanwhile, we have genotyped portions of the brains from these mice to confirm the presence of the null allele form, demonstrating that recombination and deletion of the mGluR5 only occurred in GLAST-mGluR5KO mice. Interestingly, the GLAST-mGluR5KO mice presenting enhancement in behavior flexibility or impairment in fear memory, had lower levels of mGluR5 and GFAP genes. This suggests that levels of mGluR5 are related with the behavioral readouts obtained. Moreover, the decreased GFAP levels also seem to be associated with behavioral data. GFAP is indeed related with astrocytes structure and decreased levels of these protein might be associated with changes in astrocytes morphology, possibly atrophy, that could influence how astrocytes cover/interact and modulate synaptic activity (Heller and Rusakov 2015).

Therefore, it would be interesting to assess if this possible structural alterations in astrocytes are directly associated with deletion of mGluR5 in the cell or if it is a consequence of the deletion for the normal functioning of neural-networks.

Altogether these findings suggest that general ablation of mGluR5 in astrocytes disrupts the normal astrocytic modulation of synaptic strength which seems to have a particular impact in the PFC and hippocampus circuitry. Indeed, according to our findings, astrocytic mGluR5 seems to be particularly important for cognition events dependent on these two brain regions, as proven by the enhanced behavioral flexibility and impaired fear memory found in GLAST-mGluR5KO mice. Therefore, in order to better understand the role of astrocytic mGluR5 in learning and memory, we decided to dissect the impact of this receptor in specific brain regions. Thus, in this work, we have also induced region-specific ablation of astrocytic mGluR5 in the hippocampus, using a viral approach. Our results showed that dHIP-GFAP-mGluR5KO mice display impaired behavior flexibility and normal fear memory. Thus, ablation of mGluR5 only in hippocampal astrocytes was not enough to mimic the results obtained using the GLAST-mGluR5KO mice. In fact, the CFC results showed that dHIP-GFAP-mGluR5KO mice displayed normal fear memory when exposed to the conditioning context, meaning that the astrocytic mGluR5 activation in the hippocampus is not involved in the expression of learned fear. Considering our previous data on GLAST-mGluR5KO mice, where impaired fear memory was observed, this finding seems to support our theory that astrocytic mGluR5 in PFC is playing a key role in learning and memory. Furthermore, we also showed that dHIP-GFAP-mGluR5KO mice display impaired behavior flexibility when tested in the reversal learning task of the MWM. As mentioned before the PFC and the hippocampus are important for the performance of this task. The results obtained using dHIP-GFAP-mGluR5KO mice indicate that affecting only the hippocampus induces different behavioral outcomes then when globally affecting mGluR5 in astrocytes as in GLAST-mGluR5KO mice. Thus, activation of astrocytic mGluR5 in both brain regions seems to be important for the astrocytic modulation of neuronal activity in the PFC and hippocampus and to maintain a normal communication between them during the reversal learning task. However, we do not know how the communication between the hippocampus and PFC is affected by the deletion of mGluR5. For a better integration and correlation of these results, we should assess the impact of mGluR5 in astrocytes specifically from the PFC.

6. Conclusions and future perspectives

In this dissertation, we showed for the first time the involvement of astrocytic mGluR5 in cognitive functions dependent on the PFC and hippocampus, as shown by mice performance in the reversal task of the MWM and in the CFC. Briefly, GLAST-mGluR5KO mice display an enhanced behavioral flexibility and an impaired fear memory, whereas dHIP-GFAP-mGluR5KO exhibit an impaired behavior flexibility and normal fear memory. Therefore, our study suggests that mGluR5 activation is in fact important for cognitive processing in adulthood. Moreover, it also seems that activation of mGluR5 in astrocytes is region specific and its activation in different regions of the cortico-limbic at the same time or in response to one another region might me crucial for a normal function of the circuit in cognitive processing.

Despite these new findings, we are aware that some validations are still needed to confirm our results. Finally, it is crucial to continue exploring the role of astrocytic mGluR5 specially in PFC and hippocampus, using these models or other cutting edge approaches, in order to unravel the role of this receptor and astrocytes in cognitive function. Thus, in the future, we propose to:

1) **Confirm mGluR5 deletion in a pure astrocytic fraction.**

   Our results show that GLAST-mGluR5KO mice had decreased levels of mGluR5 in the hippocampus, however we should isolate a pure astrocytic fraction using fluorescence activated cells sorting in order to obtain mRNA only from astrocytes of GLAST-mGluR5KO (by incubation the tissue with a astrocyte marker, as GLT-1) and dHIP-GFAP-mGluR5KO mice (by using the mCherry reporter). This confirmation in the astrocytic fraction will be crucial to assess levels of knock-down in each mouse and to correlate these with behavioral performance

2) **Assess the expression levels of specific genes of interest in other brain regions, as PFC, of GLAST-mGluR5KO and in the PFC and hippocampus of dHIP-GFAP-mGluR5KO mice.**

   We assessed the relative expression levels of specific genes in the hippocampus of the GLAST-mGluR5KO mice. However, it would be interesting to assess also the expression levels of these genes in the PFC, since the behavioral results showed influence of astrocytic mGluR5 in behavioral tasks dependent on this brain region. Moreover, this molecular analysis should also be performed in the PFC and hippocampus of dHIP-GFAP-mGluR5KO mice and ideally in astrocyte-enriched fractions as mentioned above.

3) **Study morphological alterations that astrocytes might have suffered after mGluR5 ablation**

We found that GLAST-mGluR5KO mice had decrease levels of GFAP, a protein associated with astrocytes structure. Thus, we should assess changes in morphology of these cells using the Simple Neurite Tracer, a Fiji plugin. It is also important to study these possible structural alterations in dHIP-GFAP-mGluR5KO mice. The assessment of astrocytes structure is important to see if mGluR5 deletion induces any alteration in these cells that could be associated with the behavioral results obtained.

4) **Perform electrophysiology in GLAST-mGluR5KO and dHIP-GFAP-mGluR5KO mice.**

We showed that mGluR5 is involved in the regulation of cognitive performance in PFC- and hippocampal-dependent tasks. Therefore, performing electrophysiological recordings to obtain a functional readout of cortico-limbic structures, namely in the hip-PFC regional activity and temporal synchronization, is important to elucidate the link between the role of astrocytic mGluR5 in these different regions.

5) **Evaluate changes in calcium elevations and synaptic plasticity assess functional involvement of astrocytes**

It is crucial to show that astrocytes that underwent recombination do not present Ca^{2+} elevation when stimulated with a mGluR5 specific agonist. Moreover, these types of recording would be also important to study how these mGluR5KO astrocytes are influencing LTP and LTD phenomena.

6) **Use the viral approach to study other brain regions, as the PFC.**

The results obtained using both mouse models showed that modulation mGluR5 expression in the whole brain or in a specific region have distinct behavioral outcomes. Thus, ablating mGluR5 in the PFC is crucial to further explore the role of mGluR5 in specific regions for cognitive processing.

7) **Confirm the observations using the ALDH1L1-CreER^{T2} mouse line.**

In this dissertation we use the GLAST-CreER^{T2} mouse line to target astrocytes, however the GLAST promoter is found in other sub-populations of astrocytes and other cells. Thus, repeating the experiments used for the GLAST-mGluR5KO mice using a different astrocytic promoter is crucial to confirm our results and explore more the role of mGluR5 in astrocytes. Therefore, we should use the ALDH1L1-CreER^{T2} mouse line (recently acquired by our lab), a model that was shown to target specifically mature astrocytes.

7. References

Adamsky A, Kol A, Kreisel T, Doron A, Ozeri-Engelhard N, Melcer T, Refaeli R, Horn H, Regev L, Groysman M, London M, Goshen I. 2018. Astrocytic Activation Generates De Novo Neuronal Potentiation and Memory Enhancement. Cell. 174:59-71.e14.

Allen NJ. 2014. Astrocyte regulation of synaptic behavior. Annu Rev Cell Dev Biol. 30:439–463.

Allen NJ, Barres BA. 2009. Neuroscience: Glia - more than just brain glue. Nature. 457:675–677.

Allen NJ, Eroglu C. 2017. Cell biology of astrocyte-synapse interactions. Neuron. 96:697–708.

Alvarez JI, Katayama T, Prat A. 2013. Glial influence on the blood brain barrier. Glia. 61:1939–1958.

Ango F, Prézeau L, Muller T, Tu JC, Xiao B, Worley PF, Pin JP, Bockaert J, Fagni L. 2001. Agonist-independent activation of metabotropic glutamate receptors by the intracellular protein Homer. Nature. 411:962–965.

Angulo MC, Kozlov AS, Charpak S, Audinat E. 2004. Glutamate released from glial cells synchronizes neuronal activity in the hippocampus. J Neurosci Off J Soc Neurosci. 24:6920–6927.

Anlauf E, Derouiche A. 2013. Glutamine Synthetase as an Astrocytic Marker: Its Cell Type and Vesicle Localization. Front Endocrinol. 4.

Araque A, Carmignoto G, Haydon PG, Oliet SHR, Robitaille R, Volterra A. 2014. Gliotransmitters travel in time and space. Neuron. 81:728–739.

Araque A, Parpura V, Sanzgiri RP, Haydon PG. 1999. Tripartite synapses: glia, the unacknowledged partner. Trends Neurosci. 22:208–215.

Aronica E, Catania MV, Geurts J, Yankaya B, Troost D. 2001. Immunohistochemical localization of group I and II metabotropic glutamate receptors in control and amyotrophic lateral sclerosis human spinal cord: upregulation in reactive astrocytes. Neuroscience. 105:509–520.

Aschauer DF, Kreuz S, Rumpel S. 2013. Analysis of Transduction Efficiency, Tropism and Axonal Transport of AAV Serotypes 1, 2, 5, 6, 8 and 9 in the Mouse Brain. PLoS ONE. 8:e76310.

Bailey CH, Barco A, Hawkins RD, Kandel ER. 2008. 4.02 – Molecular Studies of Learning and Memory in Aplysia and the Hippocampus: A Comparative Analysis of Implicit and Explicit Memory Storage.

Barros CS, Franco SJ, Müller U. 2011. Extracellular Matrix: Functions in the Nervous System. Cold Spring Harb Perspect Biol. 3.

Batiuk MY, Martirosyan A, Voet T, Ponting CP, Belgard TG, Holt MG. 2018. Molecularly distinct astrocyte subpopulations spatially pattern the adult mouse brain. bioRxiv. 317503.

Bayraktar OA, Fuentealba LC, Alvarez-Buylla A, Rowitch DH. 2015. Astrocyte Development and Heterogeneity. Cold Spring Harb Perspect Biol. 7.

Bazargani N, Attwell D. 2016. Astrocyte calcium signaling: the third wave. Nat Neurosci. 19:182–189.

Ben Haim L, Rowitch DH. 2017. Functional diversity of astrocytes in neural circuit regulation. Nat Rev Neurosci. 18:31–41.

Berthele A, Platzer S, Laurie DJ, Weis S, Sommer B, Zieglgänsberger W, Conrad B, Tölle TR. 1999. Expression of metabotropic glutamate receptor subtype mRNA (mGluR1-8) in human cerebellum. Neuroreport. 10:3861–3867.

Bliss TV, Collingridge GL. 1993. A synaptic model of memory: long-term potentiation in the hippocampus. Nature. 361:31–39.

Boury-Jamot B, Carrard A, Martin JL, Halfon O, Magistretti PJ, Boutrel B. 2016. Disrupting astrocyte-neuron lactate transfer persistently reduces conditioned responses to cocaine. Mol Psychiatry. 21:1070–1076.

Bradley SJ, Challiss RAJ. 2012. G protein-coupled receptor signalling in astrocytes in health and disease: A focus on metabotropic glutamate receptors. Biochem Pharmacol. 84:249–259.

Buscemi L, Ginet V, Lopatar J, Montana V, Pucci L, Spagnuolo P, Zehnder T, Grubišić V, Truttman A, Sala C, Hirt L, Parpura V, Puyal J, Bezzi P. 2017. Homer1 Scaffold Proteins Govern Ca2+ Dynamics in Normal and Reactive Astrocytes. Cereb Cortex. 27:2365–2384.

Bushong EA, Martone ME, Ellisman MH. 2004. Maturation of astrocyte morphology and the establishment of astrocyte domains during postnatal hippocampal development. Int J Dev Neurosci Off J Int Soc Dev Neurosci. 22:73–86.

Cabezas R, Avila-Rodriguez M, Vega-Vela NE, Echeverria V, González J, Hidalgo OA, Santos AB, Aliev G, Barreto GE. 2016. Growth Factors and Astrocytes Metabolism: Possible Roles for Platelet Derived Growth Factor. Med Chem Shariqah United Arab Emir. 12:204–210.

Cahoy JD, Emery B, Kaushal A, Foo LC, Zamanian JL, Christopherson KS, Xing Y, Lubischer JL, Krieg PA, Krupenko SA, Thompson WJ, Barres BA. 2008. A transcriptome database for astrocytes, neurons, and oligodendrocytes: a new resource for understanding brain development and function. J Neurosci Off J Soc Neurosci. 28:264–278.

Cai Z, Schools GP, Kimelberg HK. 2000. Metabotropic glutamate receptors in acutely isolated hippocampal astrocytes: developmental changes of mGluR5 mRNA and functional expression. Glia. 29:70–80.

Calì C, Tauffenberger A, Magistretti P. 2019. The Strategic Location of Glycogen and Lactate: From Body Energy Reserve to Brain Plasticity. Front Cell Neurosci. 13.

Can A, Dao DT, Terrillion CE, Piantadosi SC, Bhat S, Gould TD. 2012. The Tail Suspension Test. J Vis Exp JoVE.

Casper KB, Jones K, McCarthy KD. 2007. Characterization of astrocyte-specific conditional knockouts. Genes N Y N 2000. 45:292–299.

Cerqueira JJ, Pêgo JM, Taipa R, Bessa JM, Almeida OFX, Sousa N. 2005. Morphological Correlates of Corticosteroid-Induced Changes in Prefrontal Cortex-Dependent Behaviors. J Neurosci. 25:7792–7800.

Churchwell JC, Morris AM, Musso ND, Kesner RP. 2010. Prefrontal and hippocampal contributions to encoding and retrieval of spatial memory. Neurobiol Learn Mem. 93:415–421.

Ciocchi S, Passecker J, Malagon-Vina H, Mikus N, Klausberger T. 2015. Brain computation. Selective information routing by ventral hippocampal CA1 projection neurons. Science. 348:560–563.

Collingridge GL, Kehl SJ, McLENNAN H. 1983. Excitatory amino acids in synaptic transmission in the Schaffer collateral-commissural pathway of the rat hippocampus. J Physiol. 334:33–46.

Conti F, DeBiasi S, Minelli A, Melone M. 1996. Expression of NR1 and NR2A/B subunits of the NMDA receptor in cortical astrocytes. Glia. 17:254–258.

Corcoran KA, Quirk GJ. 2007. Activity in Prelimbic Cortex Is Necessary for the Expression of Learned, But Not Innate, Fears. J Neurosci. 27:840–844.

Cornell-Bell AH, Finkbeiner SM, Cooper MS, Smith SJ. 1990. Glutamate induces calcium waves in cultured astrocytes: long-range glial signaling. Science. 247:470–473.

Curzon P, Rustay NR, Browman KE. 2009. Cued and Contextual Fear Conditioning for Rodents. In: Buccafusco JJ, editor. Methods of Behavior Analysis in Neuroscience. 2nd ed. Frontiers in Neuroscience. Boca Raton (FL): CRC Press/Taylor & Francis.

Dallérac G, Rouach N. 2016. Astrocytes as new targets to improve cognitive functions. Prog Neurobiol. 144:48–67.

Davila D, Thibault K, Fiacco TA, Agulhon C. 2013. Recent molecular approaches to understanding astrocyte function in vivo. Front Cell Neurosci. 7.

De Pittà M, Brunel N, Volterra A. 2016. Astrocytes: Orchestrating synaptic plasticity? Neuroscience. 323:43–61.

Devaraju P, Sun M-Y, Myers TL, Lauderdale K, Fiacco TA. 2013. Astrocytic group I mGluR-dependent potentiation of astrocytic glutamate and potassium uptake. J Neurophysiol. 109:2404–2414.

Dimou L, Götz M. 2014. Glial cells as progenitors and stem cells: new roles in the healthy and diseased brain. Physiol Rev. 94:709–737.

Djukic B, Casper KB, Philpot BD, Chin L-S, McCarthy KD. 2007. Conditional knock-out of Kir4.1 leads to glial membrane depolarization, inhibition of potassium and glutamate uptake, and enhanced short-term synaptic potentiation. J Neurosci Off J Soc Neurosci. 27:11354–11365.

Donato R, Cannon BR, Sorci G, Riuzzi F, Hsu K, Weber DJ, Geczy CL. 2013. Functions of S100 proteins. Curr Mol Med. 13:24–57.

Dong Z, Bai Y, Wu X, Li H, Gong B, Howland JG, Huang Y, He W, Li T, Wang YT. 2013. Hippocampal long-term depression mediates spatial reversal learning in the Morris water maze. Neuropharmacology. 64:65–73.

Dong Z, Han H, Li H, Bai Y, Wang W, Tu M, Peng Y, Zhou L, He W, Wu X, Tan T, Liu M, Wu X, Zhou W, Jin W, Zhang S, Sacktor TC, Li T, Song W, Wang YT. 2015. Long-term potentiation decay and memory loss are mediated by AMPAR endocytosis. J Clin Invest. 125:234–247.

Emsley JG, Macklis JD. 2006. Astroglial heterogeneity closely reflects the neuronal-defined anatomy of the adult murine CNS. Neuron Glia Biol. 2:175–186.

Feil S, Valtcheva N, Feil R. 2009. Inducible Cre mice. Methods Mol Biol Clifton NJ. 530:343–363.

Fellin T, Pascual O, Gobbo S, Pozzan T, Haydon PG, Carmignoto G. 2004. Neuronal synchrony mediated by astrocytic glutamate through activation of extrasynaptic NMDA receptors. Neuron. 43:729–743.

Fields RD, Araque A, Johansen-Berg H, Lim S-S, Lynch G, Nave K-A, Nedergaard M, Perez R, Sejnowski T, Wake H. 2014. Glial Biology in Learning and Cognition. The Neuroscientist. 20:426–431.

Franklin KBJ, Paxinos G. 2001. The Mouse Brain in Stereotaxic Coordinates. Second Edition. ed. San Diego: Academic Press.

Fuster JM. 2009. The prefrontal cortex. 4. ed., reprint. ed. Amsterdam: Elsevier, Acad. Press.

Gao V, Suzuki A, Magistretti PJ, Lengacher S, Pollonini G, Steinman MQ, Alberini CM. 2016. Astrocytic β2-adrenergic receptors mediate hippocampal long-term memory consolidation. Proc Natl Acad Sci U S A. 113:8526–8531.

Geurts JJG, Wolswijk G, Bö L, van der Valk P, Polman CH, Troost D, Aronica E. 2003. Altered expression patterns of group I and II metabotropic glutamate receptors in multiple sclerosis. Brain J Neurol. 126:1755–1766.

Ghirardini E, Wadle SL, Augustin V, Becker J, Brill S, Hammerich J, Seifert G, Stephan J. 2018. Expression of functional inhibitory neurotransmitter transporters GlyT1, GAT-1, and GAT-3 by astrocytes of inferior colliculus and hippocampus. Mol Brain. 11:4.

Giaume C, Koulakoff A, Roux L, Holcman D, Rouach N. 2010. Astroglial networks: a step further in neuroglial and gliovascular interactions. Nat Rev Neurosci. 11:87–99.

Gibbs ME, Hutchinson D, Hertz L. 2008. Astrocytic involvement in learning and memory consolidation. Neurosci Biobehav Rev. 32:927–944.

Gilmartin MR, Balderston NL, Helmstetter FJ. 2014. Prefrontal cortical regulation of fear learning. Trends Neurosci. 37:455–464.

Graziano A, Petrosini L, Bartoletti A. 2003. Automatic recognition of explorative strategies in the Morris water maze. J Neurosci Methods. 130:33–44.

Gu Y, Arruda-Carvalho M, Wang J, Janoschka SR, Josselyn SA, Frankland PW, Ge S. 2012. Optical controlling reveals time-dependent roles for adult-born dentate granule cells. Nat Neurosci. 15:1700–1706.

Guerra-Gomes S, Sousa N, Pinto L, Oliveira JF. 2018. Functional Roles of Astrocyte Calcium Elevations: From Synapses to Behavior. Front Cell Neurosci. 11.

Guerra-Gomes S, Viana JF, Nascimento DSM, Correia JS, Sardinha VM, Caetano I, Sousa N, Pinto L, Oliveira JF. 2018. The Role of Astrocytic Calcium Signaling in the Aged Prefrontal Cortex. Front Cell Neurosci. 12.

Hadzic M, Jack A, Wahle P. 2017. Ionotropic glutamate receptors: Which ones, when, and where in the mammalian neocortex. J Comp Neurol. 525:976–1033.

Halassa MM, Fellin T, Takano H, Dong J-H, Haydon PG. 2007. Synaptic islands defined by the territory of a single astrocyte. J Neurosci Off J Soc Neurosci. 27:6473–6477.

Han J, Kesner P, Metna-Laurent M, Duan T, Xu L, Georges F, Koehl M, Abrous DN, Mendizabal-Zubiaga J, Grandes P, Liu Q, Bai G, Wang W, Xiong L, Ren W, Marsicano G, Zhang X. 2012. Acute cannabinoids impair working memory through astroglial CB1 receptor modulation of hippocampal LTD. Cell. 148:1039–1050.

Harada K, Kamiya T, Tsuboi T. 2016. Gliotransmitter Release from Astrocytes: Functional, Developmental, and Pathological Implications in the Brain. Front Neurosci. 9.

Heidbreder CA, Groenewegen HJ. 2003. The medial prefrontal cortex in the rat: evidence for a dorso-ventral distinction based upon functional and anatomical characteristics. Neurosci Biobehav Rev. 27:555–579.

Heller JP, Rusakov DA. 2015. Morphological plasticity of astroglia: Understanding synaptic microenvironment. Glia. 63:2133–2151.

Henneberger C, Papouin T, Oliet SHR, Rusakov DA. 2010. Long-term potentiation depends on release of D-serine from astrocytes. Nature. 463:232–236.

Hol EM, Pekny M. 2015. Glial fibrillary acidic protein (GFAP) and the astrocyte intermediate filament system in diseases of the central nervous system. Curr Opin Cell Biol. 32:121–130.

Honsek SD, Walz C, Kafitz KW, Rose CR. 2012. Astrocyte calcium signals at Schaffer collateral to CA1 pyramidal cell synapses correlate with the number of activated synapses but not with synaptic strength. Hippocampus. 22:29–42.

Hoover WB, Vertes RP. 2007. Anatomical analysis of afferent projections to the medial prefrontal cortex in the rat. Brain Struct Funct. 212:149–179.

Iino M, Goto K, Kakegawa W, Okado H, Sudo M, Ishiuchi S, Miwa A, Takayasu Y, Saito I, Tsuzuki K, Ozawa S. 2001. Glia-synapse interaction through Ca2+-permeable AMPA receptors in Bergmann glia. Science. 292:926–929.

Jäkel S, Dimou L. 2017. Glial Cells and Their Function in the Adult Brain: A Journey through the History of Their Ablation. Front Cell Neurosci. 11:24.

Kamphuis W, Mamber C, Moeton M, Kooijman L, Sluijs JA, Jansen AHP, Verveer M, de Groot LR, Smith VD, Rangarajan S, Rodríguez JJ, Orre M, Hol EM. 2012. GFAP isoforms in adult mouse brain with a focus on neurogenic astrocytes and reactive astrogliosis in mouse models of Alzheimer disease. PloS One. 7:e42823.

Kandel ER, Dudai Y, Mayford MR. 2014. The Molecular and Systems Biology of Memory. Cell. 157:163–186.

Kandel ER, Schwartz JH, Jessell TM, Siegelbaum SA, Hudspeth AJ. 2012. Principles of Neural Science, Fifth Edition. McGraw Hill Professional.

Kettenmann H, Verkhratsky A. 2008. Neuroglia: the 150 years after. Trends Neurosci. 31:653–659.

Khakh BS, Sofroniew MV. 2015. Diversity of astrocyte functions and phenotypes in neural circuits. Nat Neurosci. 18:942–952.

Lalo U, Pankratov Y, Kirchhoff F, North RA, Verkhratsky A. 2006. NMDA receptors mediate neuron-to-glia signaling in mouse cortical astrocytes. J Neurosci Off J Soc Neurosci. 26:2673–2683.

Lanjakornsiripan D, Pior B-J, Kawaguchi D, Furutachi S, Tahara T, Katsuyama Y, Suzuki Y, Fukazawa Y, Gotoh Y. 2018. Layer-specific morphological and molecular differences in neocortical astrocytes and their dependence on neuronal layers. Nat Commun. 9:1–15.

Latour I, Gee CE, Robitaille R, Lacaille JC. 2001. Differential mechanisms of Ca2+ responses in glial cells evoked by exogenous and endogenous glutamate in rat hippocampus. Hippocampus. 11:132–145.

Letellier M, Park YK, Chater TE, Chipman PH, Gautam SG, Oshima-Takago T, Goda Y. 2016. Astrocytes regulate heterogeneity of presynaptic strengths in hippocampal networks. Proc Natl Acad Sci U S A. 113:E2685-2694.

Li D, Agulhon C, Schmidt E, Oheim M, Ropert N. 2013. New tools for investigating astrocyte-to-neuron communication. Front Cell Neurosci. 7.

Li K, Li J, Zheng J, Qin S. 2019. Reactive Astrocytes in Neurodegenerative Diseases. Aging Dis. 10:664–675.

Lima A, Sardinha VM, Oliveira AF, Reis M, Mota C, Silva MA, Marques F, Cerqueira JJ, Pinto L, Sousa N, Oliveira JF. 2014. Astrocyte pathology in the prefrontal cortex impairs the cognitive function of rats. Mol Psychiatry. 19:834–841.

López-Bendito G, Shigemoto R, Fairén A, Luján R. 2002. Differential distribution of group I metabotropic glutamate receptors during rat cortical development. Cereb Cortex N Y N 1991. 12:625–638.

Lu YM, Jia Z, Janus C, Henderson JT, Gerlai R, Wojtowicz JM, Roder JC. 1997. Mice lacking metabotropic glutamate receptor 5 show impaired learning and reduced CA1 long-term potentiation (LTP) but normal CA3 LTP. J Neurosci Off J Soc Neurosci. 17:5196–5205.

Malenka RC, Bear MF. 2004. LTP and LTD: an embarrassment of riches. Neuron. 44:5–21.

Mateus-Pinheiro A, Alves ND, Patrício P, Machado-Santos AR, Loureiro-Campos E, Silva JM, Sardinha VM, Reis J, Schorle H, Oliveira JF, Ninkovic J, Sousa N, Pinto L. 2017. AP2γ controls adult hippocampal neurogenesis and modulates cognitive, but not anxiety or depressive-like behavior. Mol Psychiatry. 22:1725–1734.

Matsui K, Jahr CE, Rubio ME. 2005. High-concentration rapid transients of glutamate mediate neural-glial communication via ectopic release. J Neurosci Off J Soc Neurosci. 25:7538–7547.

Matyash V, Kettenmann H. 2010. Heterogeneity in astrocyte morphology and physiology. Brain Res Rev, Synaptic Processes - the role of glial cells. 63:2–10.

Mayford M, Siegelbaum SA, Kandel ER. 2012. Synapses and Memory Storage. Cold Spring Harb Perspect Biol. 4.

McIver SR, Faideau M, Haydon PG. 2013. Astrocyte-Neuron Communications. In: Cui C., Grandison L., Noronha A., editors. Boston: MA: Springer US. p. 31–64.

Mederos S, González-Arias C, Perea G. 2018. Astrocyte-Neuron Networks: A Multilane Highway of Signaling for Homeostatic Brain Function. Front Synaptic Neurosci. 10:45.

Mederos S, Hernández-Vivanco A, Ramírez-Franco J, Martín-Fernández M, Navarrete M, Yang A, Boyden ES, Perea G. 2019. Melanopsin for precise optogenetic activation of astrocyte-neuron networks. Glia. 67:915–934.

Ménard C, Quirion R. 2012. Successful cognitive aging in rats: a role for mGluR5 glutamate receptors, homer 1 proteins and downstream signaling pathways. PloS One. 7:e28666.

Metna-Laurent M, Marsicano G. 2015. Rising stars: modulation of brain functions by astroglial type-1 cannabinoid receptors. Glia. 63:353–364.

Miller EK, Cohen JD. 2001. An integrative theory of prefrontal cortex function. Annu Rev Neurosci. 24:167–202.

Mills F, Bartlett TE, Dissing-Olesen L, Wisniewska MB, Kuznicki J, Macvicar BA, Wang YT, Bamji SX. 2014. Cognitive flexibility and long-term depression (LTD) are impaired following β-catenin stabilization in vivo. Proc Natl Acad Sci. 111:8631–8636.

Molofsky AV, Krencik R, Krenick R, Ullian EM, Ullian E, Tsai H, Deneen B, Richardson WD, Barres BA, Rowitch DH. 2012. Astrocytes and disease: a neurodevelopmental perspective. Genes Dev. 26:891–907.

Morel L, Higashimori H, Tolman M, Yang Y. 2014. VGluT1+ neuronal glutamatergic signaling regulates postnatal developmental maturation of cortical protoplasmic astroglia. J Neurosci Off J Soc Neurosci. 34:10950–10962.

Mori T, Tanaka K, Buffo A, Wurst W, Kühn R, Götz M. 2006. Inducible gene deletion in astroglia and radial glia–a valuable tool for functional and lineage analysis. Glia. 54:21–34.

Nabavi S, Fox R, Proulx CD, Lin JY, Tsien RY, Malinow R. 2014. Engineering a memory with LTD and LTP. Nature. 511:348–352.

Nagelhus EA, Ottersen OP. 2013. Physiological Roles of Aquaporin-4 in Brain. Physiol Rev. 93:1543–1562.

Nagy JI, Patel D, Ochalski PA, Stelmack GL. 1999. Connexin30 in rodent, cat and human brain: selective expression in gray matter astrocytes, co-localization with connexin43 at gap junctions and late developmental appearance. Neuroscience. 88:447–468.

Navarrete M, Araque A. 2008. Endocannabinoids mediate neuron-astrocyte communication. Neuron. 57:883–893.

Navarrete M, Araque A. 2010. Endocannabinoids potentiate synaptic transmission through stimulation of astrocytes. Neuron. 68:113–126.

Navarrete M, Cuartero MI, Palenzuela R, Draffin JE, Konomi A, Serra I, Colié S, Castaño-Castaño S, Hasan MT, Nebreda ÁR, Esteban JA. 2019. Astrocytic p38α MAPK drives NMDA receptor-dependent long-term depression and modulates long-term memory. Nat Commun. 10:1–15.

Nicholls RE, Alarcon JM, Malleret G, Carroll RC, Grody M, Vronskaya S, Kandel ER. 2008. Transgenic Mice Lacking NMDAR-Dependent LTD Exhibit Deficits in Behavioral Flexibility. Neuron. 58:104–117.

Nielsen S, Nagelhus EA, Amiry-Moghaddam M, Bourque C, Agre P, Ottersen OP. 1997. Specialized membrane domains for water transport in glial cells: high-resolution immunogold cytochemistry of aquaporin-4 in rat brain. J Neurosci Off J Soc Neurosci. 17:171–180.

Niswender CM, Conn PJ. 2010. Metabotropic Glutamate Receptors: Physiology, Pharmacology, and Disease. Annu Rev Pharmacol Toxicol. 50:295–322.

Oberheim NA, Goldman SA, Nedergaard M. 2012. Heterogeneity of Astrocytic Form and Function. Methods Mol Biol Clifton NJ. 814:23–45.

Oberheim NA, Takano T, Han X, He W, Lin JHC, Wang F, Xu Q, Wyatt JD, Pilcher W, Ojemann JG, Ransom BR, Goldman SA, Nedergaard M. 2009. Uniquely Hominid Features of Adult Human Astrocytes. J Neurosci. 29:3276–3287.

Ogata K, Kosaka T. 2002. Structural and quantitative analysis of astrocytes in the mouse hippocampus. Neuroscience. 113:221–233.

O'Keefe J, Dostrovsky J. 1971. The hippocampus as a spatial map. Preliminary evidence from unit activity in the freely-moving rat. Brain Res. 34:171–175.

Oliveira J, Sardinha V, Guerra-Gomes S, Araque A, Sousa N. 2015. Do stars govern our actions? Astrocyte involvement in rodent behavior. Trends Neurosci. 38.

Orr AG, Hsiao EC, Wang MM, Ho K, Kim DH, Wang X, Guo W, Kang J, Yu G-Q, Adame A, Devidze N, Dubal DB, Masliah E, Conklin BR, Mucke L. 2015. Astrocytic adenosine receptor A2A and Gs-coupled signaling regulate memory. Nat Neurosci. 18:423–434.

Panatier A, Robitaille R. 2016. Astrocytic mGluR5 and the tripartite synapse. Neuroscience, Dynamic and metabolic astrocyte-neuron interactions in healthy and diseased brain. 323:29–34.

Panatier A, Theodosis DT, Mothet J-P, Touquet B, Pollegioni L, Poulain DA, Oliet SHR. 2006. Glia-derived D-serine controls NMDA receptor activity and synaptic memory. Cell. 125:775–784.

Panatier A, Vallée J, Haber M, Murai KK, Lacaille J-C, Robitaille R. 2011. Astrocytes are endogenous regulators of basal transmission at central synapses. Cell. 146:785–798.

Pannasch U, Freche D, Dallérac G, Ghézali G, Escartin C, Ezan P, Cohen-Salmon M, Benchenane K, Abudara V, Dufour A, Lübke JHR, Déglon N, Knott G, Holcman D, Rouach N. 2014. Connexin 30 sets synaptic strength by controlling astroglial synapse invasion. Nat Neurosci. 17:549–558.

Pannasch U, Rouach N. 2013. Emerging role for astroglial networks in information processing: from synapse to behavior. Trends Neurosci. 36:405–417.

Pannasch U, Vargová L, Reingruber J, Ezan P, Holcman D, Giaume C, Syková E, Rouach N. 2011. Astroglial networks scale synaptic activity and plasticity. Proc Natl Acad Sci U S A. 108:8467–8472.

Parent MA, Wang L, Su J, Netoff T, Yuan L-L. 2010. Identification of the hippocampal input to medial prefrontal cortex in vitro. Cereb Cortex N Y N 1991. 20:393–403.

Parpura V, Verkhratsky A. 2012. Homeostatic function of astrocytes: Ca2+ and Na+ signalling. Transl Neurosci. 3:334–344.

Pascual O, Casper KB, Kubera C, Zhang J, Revilla-Sanchez R, Sul J-Y, Takano H, Moss SJ, McCarthy K, Haydon PG. 2005. Astrocytic purinergic signaling coordinates synaptic networks. Science. 310:113–116.

Pasti L, Volterra A, Pozzan T, Carmignoto G. 1997. Intracellular Calcium Oscillations in Astrocytes: A Highly Plastic, Bidirectional Form of Communication between Neurons and Astrocytes *In Situ*. J Neurosci. 17:7817–7830.

Pekny M, Johansson CB, Eliasson C, Stakeberg J, Wallén A, Perlmann T, Lendahl U, Betsholtz C, Berthold CH, Frisén J. 1999. Abnormal reaction to central nervous system injury in mice lacking glial fibrillary acidic protein and vimentin. J Cell Biol. 145:503–514.

Perea G, Araque A. 2005. Properties of Synaptically Evoked Astrocyte Calcium Signal Reveal Synaptic Information Processing by Astrocytes. J Neurosci. 25:2192–2203.

Perea G, Navarrete M, Araque A. 2009. Tripartite synapses: astrocytes process and control synaptic information. Trends Neurosci. 32:421–431.

Petrelli F, Bezzi P. 2016. Novel insights into gliotransmitters. Curr Opin Pharmacol. 26:138–145.

Pfrieger FW, Slezak M. 2012. Genetic approaches to study glial cells in the rodent brain. Glia. 60:681–701.

Pinto-Duarte A, Roberts A, Ouyang K, Sejnowski T. 2019. Impairments in remote memory caused by the lack of Type 2 IP3 receptors. Glia. 67.

Porter JT, McCarthy KD. 1995. GFAP-positive hippocampal astrocytes in situ respond to glutamatergic neuroligands with increases in [Ca2+]i. Glia. 13:101–112.

Porter JT, McCarthy KD. 1996. Hippocampal astrocytes in situ respond to glutamate released from synaptic terminals. J Neurosci Off J Soc Neurosci. 16:5073–5081.

Quinn JJ, Ma QD, Tinsley MR, Koch C, Fanselow MS. 2008. Inverse temporal contributions of the dorsal hippocampus and medial prefrontal cortex to the expression of long-term fear memories. Learn Mem. 15:368–372.

Rajasethupathy P, Sankaran S, Marshel JH, Kim CK, Ferenczi E, Lee SY, Berndt A, Ramakrishnan C, Jaffe A, Lo M, Liston C, Deisseroth K. 2015. Projections from neocortex mediate top-down control of memory retrieval. Nature. 526:653–659.

Reichenbach N, Delekate A, Breithausen B, Keppler K, Poll S, Schulte T, Peter J, Plescher M, Hansen JN, Blank N, Keller A, Fuhrmann M, Henneberger C, Halle A, Petzold GC. 2018. P2Y1 receptor blockade normalizes network dysfunction and cognition in an Alzheimer's disease model. J Exp Med. 215:1649–1663.

Renzel R, Sadek A-R, Chang C-H, Gray WP, Seifert G, Steinhäuser C. 2013. Polarized distribution of AMPA, but not GABAA , receptors in radial glia-like cells of the adult dentate gyrus. Glia. 61:1146–1154.

Robin LM, Oliveira da Cruz JF, Langlais VC, Martin-Fernandez M, Metna-Laurent M, Busquets-Garcia A, Bellocchio L, Soria-Gomez E, Papouin T, Varilh M, Sherwood MW, Belluomo I, Balcells G, Matias I, Bosier B, Drago F, Van Eeckhaut A, Smolders I, Georges F, Araque A, Panatier A, Oliet SHR, Marsicano G. 2018. Astroglial CB1 Receptors Determine Synaptic D-Serine Availability to Enable Recognition Memory. Neuron. 98:935-944.e5.

Rodrigues SM, Bauer EP, Farb CR, Schafe GE, LeDoux JE. 2002. The group I metabotropic glutamate receptor mGluR5 is required for fear memory formation and long-term potentiation in the lateral amygdala. J Neurosci Off J Soc Neurosci. 22:5219–5229.

Rose CR, Felix L, Zeug A, Dietrich D, Reiner A, Henneberger C. 2018. Astroglial Glutamate Signaling and Uptake in the Hippocampus. Front Mol Neurosci. 10.

Saab AS, Neumeyer A, Jahn HM, Cupido A, Šimek AAM, Boele H-J, Scheller A, Le Meur K, Götz M, Monyer H, Sprengel R, Rubio ME, Deitmer JW, De Zeeuw CI, Kirchhoff F. 2012. Bergmann glial AMPA receptors are required for fine motor coordination. Science. 337:749–753.

Sala C, Roussignol G, Meldolesi J, Fagni L. 2005. Key role of the postsynaptic density scaffold proteins Shank and Homer in the functional architecture of Ca2+ homeostasis at dendritic spines in hippocampal neurons. J Neurosci Off J Soc Neurosci. 25:4587–4592.

Santello M, Toni N, Volterra A. 2019. Astrocyte function from information processing to cognition and cognitive impairment. Nat Neurosci. 22:154–166.

Sardinha VM, Guerra-Gomes S, Caetano I, Tavares G, Martins M, Reis JS, Correia JS, Teixeira-Castro A, Pinto L, Sousa N, Oliveira JF. 2017. Astrocytic signaling supports hippocampal-prefrontal theta synchronization and cognitive function. Glia. 65:1944–1960.

Savchenko VL, McKanna JA, Nikonenko IR, Skibo GG. 2000. Microglia and astrocytes in the adult rat brain: comparative immunocytochemical analysis demonstrates the efficacy of lipocortin 1 immunoreactivity. Neuroscience. 96:195–203.

Schipke CG, Ohlemeyer C, Matyash M, Nolte C, Kettenmann H, Kirchhoff F. 2001. Astrocytes of the mouse neocortex express functional N-methyl-D-aspartate receptors. FASEB J Off Publ Fed Am Soc Exp Biol. 15:1270–1272.

Schools GP, Kimelberg HK. 1999. mGluR3 and mGluR5 are the predominant metabotropic glutamate receptor mRNAs expressed in hippocampal astrocytes acutely isolated from young rats. J Neurosci Res. 58:533–543.

Schulz B, Fendt M, Gasparini F, Lingenhöhl K, Kuhn R, Koch M. 2001. The metabotropic glutamate receptor antagonist 2-methyl-6-(phenylethynyl)-pyridine (MPEP) blocks fear conditioning in rats. Neuropharmacology. 41:1–7.

Seibenhener ML, Wooten MC. 2015. Use of the Open Field Maze to Measure Locomotor and Anxiety-like Behavior in Mice. J Vis Exp JoVE.

Seifert G, Henneberger C, Steinhäuser C. 2018. Diversity of astrocyte potassium channels: An update. Brain Res Bull. 136:26–36.

Serrano A, Robitaille R, Lacaille J-C. 2008. Differential NMDA-dependent activation of glial cells in mouse hippocampus. Glia. 56:1648–1663.

Slezak M, Göritz C, Niemiec A, Frisén J, Chambon P, Metzger D, Pfrieger FW. 2007. Transgenic mice for conditional gene manipulation in astroglial cells. Glia. 55:1565–1576.

Smith K, Semënov MV. 2019. The impact of age on number and distribution of proliferating cells in subgranular zone in adult mouse brain. IBRO Rep. 6:18–30.

Sofroniew MV. 2015. Astrogliosis. Cold Spring Harb Perspect Biol. 7.

Spampinato SF, Copani A, Nicoletti F, Sortino MA, Caraci F. 2018. Metabotropic Glutamate Receptors in Glial Cells: A New Potential Target for Neuroprotection? Front Mol Neurosci. 11.

Spellman T, Rigotti M, Ahmari SE, Fusi S, Gogos JA, Gordon JA. 2015. Hippocampal-prefrontal input supports spatial encoding in working memory. Nature. 522:309–314.

Steiner J, Bernstein H-G, Bielau H, Berndt A, Brisch R, Mawrin C, Keilhoff G, Bogerts B. 2007. Evidence for a wide extra-astrocytic distribution of S100B in human brain. BMC Neurosci. 8:2.

Sun M-Y, Devaraju P, Xie AX, Holman I, Samones E, Murphy TR, Fiacco TA. 2014. Astrocyte calcium microdomains are inhibited by Bafilomycin A1 and cannot be replicated by low-level Schaffer collateral stimulation in situ. Cell Calcium. 55:1–16.

Sun W, McConnell E, Pare J-F, Xu Q, Chen M, Peng W, Lovatt D, Han X, Smith Y, Nedergaard M. 2013. Glutamate-dependent neuroglial calcium signaling differs between young and adult brain. Science. 339:197–200.

Suzuki A, Stern SA, Bozdagi O, Huntley GW, Walker RH, Magistretti PJ, Alberini CM. 2011. Astrocyte-neuron lactate transport is required for long-term memory formation. Cell. 144:810–823.

Szokol K, Heuser K, Tang W, Jensen V, Enger R, Bedner P, SteinhÃ¤user C, TaubÃ¸ll E, Ottersen OP, Nagelhus EA. 2015. Augmentation of Ca2+ signaling in astrocytic endfeet in the latent phase of temporal lobe epilepsy. Front Cell Neurosci. 9.

Tavares G, Martins M, Correia JS, Sardinha VM, Guerra-Gomes S, das Neves SP, Marques F, Sousa N, Oliveira JF. 2017. Employing an open-source tool to assess astrocyte tridimensional structure. Brain Struct Funct. 222:1989–1999.

Tierney PL, Dégenètais E, Thierry A-M, Glowinski J, Gioanni Y. 2004. Influence of the hippocampus on interneurons of the rat prefrontal cortex. Eur J Neurosci. 20:514–524.

Umpierre AD, West PJ, White JA, Wilcox KS. 2019. Conditional Knock-out of mGluR5 from Astrocytes during Epilepsy Development Impairs High-Frequency Glutamate Uptake. J Neurosci. 39:727–742.

Verkhratsky A. 2008. Neurotransmitter Receptors in Astrocytes. In: Astrocytes in (Patho)Physiology of the Nervous System. p. 49–67.

Verkhratsky A, Nedergaard M. 2018. Physiology of Astroglia. Physiol Rev. 98:239–389.

Verkhratsky A, Parpura V. 2014. Introduction to Neuroglia.

Volterra A, Liaudet N, Savtchouk I. 2014. Astrocyte Ca^{2+} signalling: an unexpected complexity. Nat Rev Neurosci. 15:327–335.

Vorhees CV, Williams MT. 2006. Morris water maze: procedures for assessing spatial and related forms of learning and memory. Nat Protoc. 1:848–858.

Walf AA, Frye CA. 2007. The use of the elevated plus maze as an assay of anxiety-related behavior in rodents. Nat Protoc. 2:322–328.

Walz W, Lang MK. 1998. Immunocytochemical evidence for a distinct GFAP-negative subpopulation of astrocytes in the adult rat hippocampus. Neurosci Lett. 257:127–130.

Wang DD, Bordey A. 2008. The astrocyte odyssey. Prog Neurobiol. 86:342–367.

Wang X, Lou N, Xu Q, Tian G-F, Peng WG, Han X, Kang J, Takano T, Nedergaard M. 2006. Astrocytic Ca2+ signaling evoked by sensory stimulation in vivo. Nat Neurosci. 9:816–823.

Wilson CRE, Gaffan D, Browning PGF, Baxter MG. 2010. Functional localization within the prefrontal cortex: missing the forest for the trees? Trends Neurosci. 33:533–540.

Xu J, Zhu Y, Contractor A, Heinemann SF. 2009. mGluR5 has a critical role in inhibitory learning. J Neurosci Off J Soc Neurosci. 29:3676–3684.

Xu J, Zhu Y, Kraniotis S, He Q, Marshall JJ, Nomura T, Stauffer SR, Lindsley CW, Conn PJ, Contractor A. 2013. Potentiating mGluR5 function with a positive allosteric modulator enhances adaptive learning. Learn Mem Cold Spring Harb N. 20:438–445.

Yang Y, Ge W, Chen Y, Zhang Z, Shen W, Wu C, Poo M, Duan S. 2003. Contribution of astrocytes to hippocampal long-term potentiation through release of D-serine. Proc Natl Acad Sci U S A. 100:15194–15199.

Yang Y, Vidensky S, Jin L, Jie C, Lorenzini I, Frankl M, Rothstein JD. 2011. Molecular comparison of GLT1+ and ALDH1L1+ astrocytes in vivo in astroglial reporter mice. Glia. 59:200–207.

Yoon T, Okada J, Jung MW, Kim JJ. 2008. Prefrontal cortex and hippocampus subserve different components of working memory in rats. Learn Mem Cold Spring Harb N. 15:97–105.

Zhang Y, Barres BA. 2010. Astrocyte heterogeneity: an underappreciated topic in neurobiology. Curr Opin Neurobiol. 20:588–594.

Annex

Annex 1 - Local Ethics Committee authorization for experiments with laboratory animals

Órgão Responsável pelo Bem-Estar Animal da EM/ICVS e do I3Bs

Referência do processo: ORBEA EM/ICVS-I3Bs_004/2018

Título do Projeto: Decoding the neuron-astrocyte dialogue that supports cognitive processing

Investigador Principal: João Oliveira

Estabelecimento: Unidade do Biotério do Instituto de Investigação em Ciências da Vida e da Saúde (ICVS) da Escola de Medicina da Universidade do Minho

PARECER

O Órgão Responsável pelo Bem-Estar Animal da Escola de Medicina e seu Instituto de Investigação em Ciências da Vida e Saúde, e do Instituto3Bs (Biomaterials, Biodegradables and Biomimetics) - ORBEA EM/ICVS-I3Bs - analisou o processo relativo ao seu projeto de investigação com recurso a modelos animais intitulado *Decoding the neuron-astrocyte dialogue that supports cognitive processing*.
Os documentos apresentados revelam que o projeto obedece aos requisitos exigidos para as boas práticas na experimentação com recurso à utilização de modelos animais, considerando a aplicação dos 3 Rs de Russel e Burch e a aplicação de limites críticos de sofrimento - *humane endpoints*.

Face ao exposto, o ORBEA EM/ICVS-I3Bs não tem nada a opor à realização do projeto, emitindo o seu parecer favorável.
Salientamos, no entanto, que a autorização legal de projetos de investigação/ experimentação animal é feita pela Direção Geral de Alimentação e Veterinária (DGAV) a quem deverá ser submetido o respetivo formulário do projeto na sua versão final mais completa.

Braga,

MAGDA JOÃO CASTELHANO CARLOS
Assinado de forma digital por MAGDA JOÃO CASTELHANO CARLOS
Dados: 2019.04.03 15:01:14 +01'00'

(Presidente do ORBEA EM/ICVS-I3Bs)